

University of Massachusetts Medical School
eScholarship@UMMS

GSBS Dissertations and Theses

Graduate School of Biomedical Sciences


2011-02-17

Molecular and Functional Properties of Transmitted HIV-1 Envelope Variants: A Dissertation

Michael G. Kishko
University of Massachusetts Medical School

Let us know how access to this document benefits you.

Follow this and additional works at: https://escholarship.umassmed.edu/gsbs_diss

 Part of the [Bacterial Infections and Mycoses Commons](#), [Environmental Public Health Commons](#), [Immunology and Infectious Disease Commons](#), [Investigative Techniques Commons](#), [Therapeutics Commons](#), and the [Viruses Commons](#)

Repository Citation

Kishko MG. (2011). Molecular and Functional Properties of Transmitted HIV-1 Envelope Variants: A Dissertation. GSBS Dissertations and Theses. <https://doi.org/10.13028/1pfn-xa25>. Retrieved from https://escholarship.umassmed.edu/gsbs_diss/519

This material is brought to you by eScholarship@UMMS. It has been accepted for inclusion in GSBS Dissertations and Theses by an authorized administrator of eScholarship@UMMS. For more information, please contact Lisa.Palmer@umassmed.edu.

MOLECULAR AND FUNCTIONAL PROPERTIES OF TRANSMITTED HIV-1
ENVELOPE VARIANTS

A Dissertation Presented

By

Michael Kishko

Submitted to the Faculty of the University of Massachusetts Graduate School of
Biomedical Sciences, Worcester in partial fulfillment of the requirement for the
degree of

DOCTOR OF PHILOSOPHY

February 17, 2011

Immunology and Virology Program

MOLECULAR AND FUNCTIONAL PROPERTIES OF TRANSMITTED HIV-1
ENVELOPE VARIANTS

A Dissertation Presented
By
Michael Kishko

The signatures of the Dissertation Defense Committee signifies
completion and approval as to style and content of the Dissertation

Katherine Luzuriaga, Thesis Advisor

Shan Lu, Member of Committee

Trudy Morrison, Member of Committee

Eva Szomolanyi-Tsuda, Member of Committee

Ronald Desrosiers, Member of Committee

The signature of the Chair of the Committee signifies that the written dissertation
meets the requirements of the Dissertation Committee

Paul Clapham, Chair of Committee

The signature of the Dean of the Graduate School of Biomedical Sciences
signifies that the student has met all graduation requirement of the school.

Anthony Carruthers, Ph.D.
Dean of the Graduate School of Biomedical Sciences

Immunology and Virology Program
February 17, 2011

Acknowledgements

I would like to gratefully acknowledge the people who provided me with help, advice and support during my time at UMass. I would first like to thank Dr. Katherine Luzuriaga for giving the opportunity to pursue this project and supporting my scientific development. I am extremely grateful to Dr. Mohan Somasundaran for his advice and support which helped me navigate the day to day scientific and logistical obstacles inherent in this project. I am indebted to all the members of the Department of Pediatric Immunology both past and present for your support, your assistance with various aspects of the project and for being a great team. It was my privilege to work with you.

I am grateful to Dr. Paul Clapham, the members of his lab, and to Dr. Mark Sharkey for the reagents, techniques, and, most importantly, the intellectual discussions which made parts of this work possible.

I would like to thank the members of my Theses Research Advisory Committee Dr. Paul Clapham, Dr. Shan Lu, Dr. Alan Rothman and Dr. Trudy Morrison. I have enjoyed our interactions and am grateful for your advice and the critiques that have helped make this a stronger body of work. I would also like to acknowledge Dr. Ronald Desrosiers and Dr. Eva Szomolanyi-Tsuda for their service on my Defense Examination Committee.

Lastly I would like to thank my family and the friends I made at UMass for your love, support and patience during my years here. Without you, this accomplishment would not have been possible.

Abstract

In 2008 the Nobel Prize in Physiology or Medicine was awarded to the co-discoverers of the Human Immunodeficiency Virus Type 1 (HIV-1), the causative agent of Acquired Immunodeficiency Syndrome (AIDS). This award acknowledged the enormous worldwide impact of the HIV-1/AIDS pandemic and the importance of research aimed at halting its spread. Since the syndrome was first recognized, 25 million people have succumbed to AIDS and over 33 million are currently infected with HIV-1 (www.unaids.org). The most effective strategy for ending the pandemic is the creation of a prophylactic vaccine. Yet, to date, all efforts at HIV-1 vaccine design have met with very limited success. The consistent failures of vaccine candidates stem in large part from the unprecedented diversity of HIV-1.

Among the novel theories of vaccine design put forward to address this diversity is the targeted vaccine approach. This proposal is based on the finding that mucosal transmission of HIV-1, the most prevalent form, occurs across a selective bottleneck such that typically only a single (or a few) variants of the viral swarm present in a donor are passed to the recipient. While the mechanisms controlling the selection are largely unknown, the targeted vaccine approach postulates that once they are identified, we can utilize this understanding to design vaccines specifically targeted to the characteristics shared by the rare, mucosally transmissible HIV-1 variants.

The studies described in this work were conducted to improve our understanding of the factors influencing viral variant selection during mother-to-child-transmission of HIV-1, a route of mucosal transmission which has globally become the leading cause of child infection. A unique panel was generated, consisting of nearly 300 HIV-1 envelope genes cloned from infected mother-infant pairs. Extensive characterization of the genotypes, phenotypes and phylogeny of these clones was then done to identify attributes differentiating early infant from maternal variants. Low genetic diversity of HIV-1 envelope variants was detected in early infant samples, suggesting a bottleneck and active selection of variants for transmission. Transmitted variants did not differ from non-transmitted variants in CD4 and CCR5 use. Infant isolates replicated poorly in macrophages; a cell subtype hypothesized to be important in the establishment of infection. The sensitivity of infant envelope variants to neutralization by a panel of monoclonal antibodies, heterologous and autologous plasmas and HIV-1 entry inhibitors varied. Most intriguingly, envelopes cloned from infants infected during delivery exhibited a faster entry phenotype than maternal isolates. Together, these findings provide further insight into viral variant selection during mother-to-child transmission. Identification of properties shared by mucosally transmitted viral variants may allow them to be selectively targeted, resulting in improved methods for preventing HIV-1 transmission.

Table of Contents

Signature Page	ii
Acknowledgements	iii
Abstract	iv
Table of Contents	vi
List of Tables	ix
List of Figures	x
List of Third Party Copyrighted Material	xiii
List of Abbreviations	xiv
Preface	xv
Chapter I: Introduction	1
Acquired Immunodeficiency Syndrome	1
Human Immunodeficiency Virus Type 1	2
HIV-1 envelope	5
HIV-1 diversity and subtypes	7
Routes of transmission HIV-1 and the selective bottleneck	12
Mother-To-Child transmission	13
Need for a vaccine	14
Vaccine design approaches	15
HIV-1 envelope correlates of transmission	17
Research framework and objectives	17
Chapter II: Materials and Methods	20

Chapter III: Subtype B cohort and genotype analysis _____	36
Introduction _____	36
Results _____	38
Discussion _____	56
Chapter IV: Subtype B phenotype analysis _____	61
Introduction _____	61
Results _____	63
Discussion _____	80
Chapter V: Subtype C cohort and genotype analysis _____	88
Introduction _____	88
Results _____	91
Discussion _____	103
Chapter VI: Subtype C phenotype analysis _____	106
Introduction _____	106
Results _____	108
Discussion _____	117
Chapter VII: Summary of findings and Future Directions _____	121
Appendix I: Antigenicity of maternal and infant clones _____	128
Introduction _____	128
Results _____	132
Discussion _____	140
Appendix II: Role of endocytosis in HIV-1 entry _____	143

Introduction	143
Results	146
Discussion	149
Bibliography	150

List of Tables

2.1	Primers used for gp160 amplification _____	22
3.1	Subtype B cohort summary _____	39
3.2	Relationship of maternal and infant V1-V5 sequences _____	49
3.3	Genotypic analyses of V1-V5 sequences _____	54
4.1	Maternal and infant viruses replicate well in PBL but poorly in MDM _____	68
5.1	Subtype C cohort summary _____	92
5.2	Relationship of maternal and infant gp120 sequences _____	96
5.3	Co-receptor tropism _____	102
A1.1	Neutralization and inhibition sensitivity of selected <i>env</i> _____	133
A1.2	Rabbit immunization groups _____	134
A1.3	Induction of NAb by the immunization regimens _____	137
A1.4	Frequencies of NAb responses in paired immunization groups _____	139

List of Figures

1.1 HIV-1 life cycle _____	3
1.2 HIV-1 virion and genome organization _____	4
1.3 HIV-1 entry _____	6
1.4 A comparison of evolutionary distances of HIV-1 envelope sequences encoding V2-C5 and influenza HA1 domain of the HA gene through phylogenetic analysis _____	9
1.5 Global distribution of HIV-1 subtypes and recombinant forms as of 2008 _	11
2.1 Detection of very early HIV-1 reverse transcription _____	34
3.1 Flow chart of <i>env</i> clone panel generation _____	40
3.2 Determination of endpoint dilution _____	41
3.3 Screening transformed colonies for full length inserts in correct orientation by PCR _____	42
3.4 Functionality of <i>env</i> clones was determined using cell-cell fusion as the readout _____	43
3.5 Evolutionary relationships of HIV-1 <i>env</i> clones _____	45
3.6 Evolutionary relationship of HIV-1 <i>env</i> clones from subjects M1001 and P1024 _____	47
3.7 Infant quasispecies are more homogeneous than maternal _____	50
3.8 Comparison of gp160 sequences obtained by endpoint dilution and SGA _	52
4.1 Pseudovirus generation _____	64
4.2 Receptor and co-receptor requirements of cloned <i>env</i> _____	65
4.3 Macrophage infectivity _____	66

4.4 Use of β -galactosidase readout for neutralization assays _____	70
4.5 Infant and maternal <i>env</i> are similarly sensitive to neutralization and Inhibition _____	72
4.6 No difference in sensitivity to neutralization by autologous maternal IgG between infant and maternal clones _____	74
4.7 Infant <i>env</i> clones exhibit more rapid entry than maternal _____	76
4.8 Infant <i>env</i> clones escape T20 inhibition more rapidly than maternal _____	77
4.9 Infant <i>env</i> clones proceed through reverse transcription faster than maternal _____	79
5.1 Evolutionary relationships of gp120 sequences from <i>env</i> clones and subtype reference sequences _____	93
5.2 Evolutionary relationships of full length HIV-1 gp160 sequences from 29 <i>env</i> clones _____	95
5.3 Infant quasispecies are more homogeneous than maternal _____	98
5.4 Subject CP2 quasispecies consists of four variants _____	99
5.5 Infant <i>env</i> are shorter and less glycosylated than maternal clones _____	101
6.1 Infant and maternal <i>env</i> are similarly sensitive to 20 μ g/ml of monoclonal neutralizing Abs _____	109
6.2 Infant <i>env</i> may be slightly more resistant to neutralization by pooled seropositive plasma than corresponding maternal clones _____	111
6.3 Infant <i>env</i> may be more sensitive to inhibition by sCD4 than maternal clones _____	113
6.4 <i>Peripartum</i> transmitted <i>env</i> clones exhibit more rapid entry than <i>in-utero</i> transmitted variants _____	116

6.5	<i>Peripartum</i> but not <i>in-utero</i> transmitted infant <i>env</i> exhibit a more rapid entry phenotype than maternal clones _____	114
7.1	Pseudoviruses expressing <i>env</i> cloned from subtype C infected <i>peripartum</i> transmission pairs exhibit a more rapid entry phenotype than those from subtype C <i>in-utero</i> transmission pairs or subtype B infected subjects ____	126
A1.1	Induction of gp120 specific binding antibody responses _____	136
A2.1	Viruses pseudotyped with HIV-1 <i>env</i> and VSV-G exhibit similar sensitivity to Dynasore _____	148

List of Third Party Copyrighted Material

Figure 1.1: Adapted by permission from Macmillan Publishers Ltd: Nature Reviews Microbiology. License number: 2585921082752

Figure 1.3: Adapted by permission from the National Academy of Sciences, USA: Proceedings of the National Academy of Sciences

Figure 1.4: Used by permission from Oxford University Press: British Medical Bulletin. License number: 2585530995506

Figure 1.5: Used by permission from Massachusetts Medical Society: New England Journal of Medicine

List of Abbreviations

Ab	Antibodies
AIDS	Acquired Immunodeficiency Syndrome
ART	Anti-Retroviral Therapy
CPM	Counts per Minute
CTL	Cytotoxic T Lymphocyte
ELISA	Enzyme-Linked Immunosorbent Assay
ELISPOT	Enzyme-Linked Immunosorbent Spot
<i>env</i>	Envelope gene
Env	Envelope protein
HAART	Highly Active Anti-Retroviral Therapy
HIV-1	Human Immunodeficiency Virus Type 1
IC ₅₀	50% Inhibitory Concentration
IgG	Immunoglobulin G
MDM	Monocyte Derived Macrophage
MLV	Murine Leukemia Virus
MOI	Multiplicity of Infection
MPER	Membrane Proximal External Repeat
MTCT	Mother-to-Child Transmission
NAb	Neutralizing Antibodies
NSSS	Negative Strand Strong Stop
PBL	Peripheral Blood Lymphocyte
PNGS	Potential N-Linked Glycosylation Site
RT	Reverse Transcription
sCD4	Soluble CD4
sfu	Spot Forming Units
SGA	Single Genome Amplification
VSV-G	Vesicular Stomatitis Virus Glycoprotein

Preface

Data presented in chapters III and IV was submitted to *PLoS One* as Kishko, M et al “Early Infant HIV-1 Envelopes Exhibit More Rapid Entry than Maternal Variants”.

Macrophage infectivity assays were performed in both our laboratory and the laboratory of Dr. Paul Clapham as part of collaborative study. Data for figure 4.3B were obtained in the Clapham laboratory and are used with their consent.

Rabbit immunizations described in Table A1.2 and the induced antibody response characterization in Table A1.3, Table A1.4 and Figure A1.1 were performed in the laboratory of Dr. Shan Lu. These tables and figures were made by the Lu laboratory as part of a collaborative study and are included with their consent. The neutralization data in Figure A1.1 and Table A1.3 was partially replicated in our laboratory.

I would like to thank Dr. Dennis Burton of The Scripps Research Institute, Roche Palo Alto, for providing an aliquot of the monoclonal neutralizing antibody b12 and Dr. Matthias Dittmar of Barts and The London School of Medicine and Dentistry from whom the fluorescently tagged, replication competent HIV-1 backbone was obtained.

CHAPTER I

Introduction

Acquired Immunodeficiency Syndrome

Acquired Immunodeficiency Syndrome (AIDS) is a disease of the human immune system that progressively reduces its effectiveness, leaving individuals susceptible to opportunistic infections and tumors. AIDS was first recognized by the U.S. Centers for Disease Control and prevention in 1981. Shortly a novel virus, later termed the Human Immunodeficiency Virus Type 1 (HIV-1), was recovered (11) and determined to be the causative agent of AIDS. Since its identification HIV-1 has become a pandemic, with cases reported in every part of the world. Over the last 30 years almost 60 million people are estimated to have been infected and 25 million have succumbed to AIDS. In 2009 33.3 million people were estimated to be living with HIV-1, with 2.6 million new infected that year (83). The tremendous impact of HIV-1 was underlined in 2008 when its co-discoverers, Françoise Barré-Sinoussi and Luc Montagnier, were awarded the Nobel Prize in Physiology or Medicine.

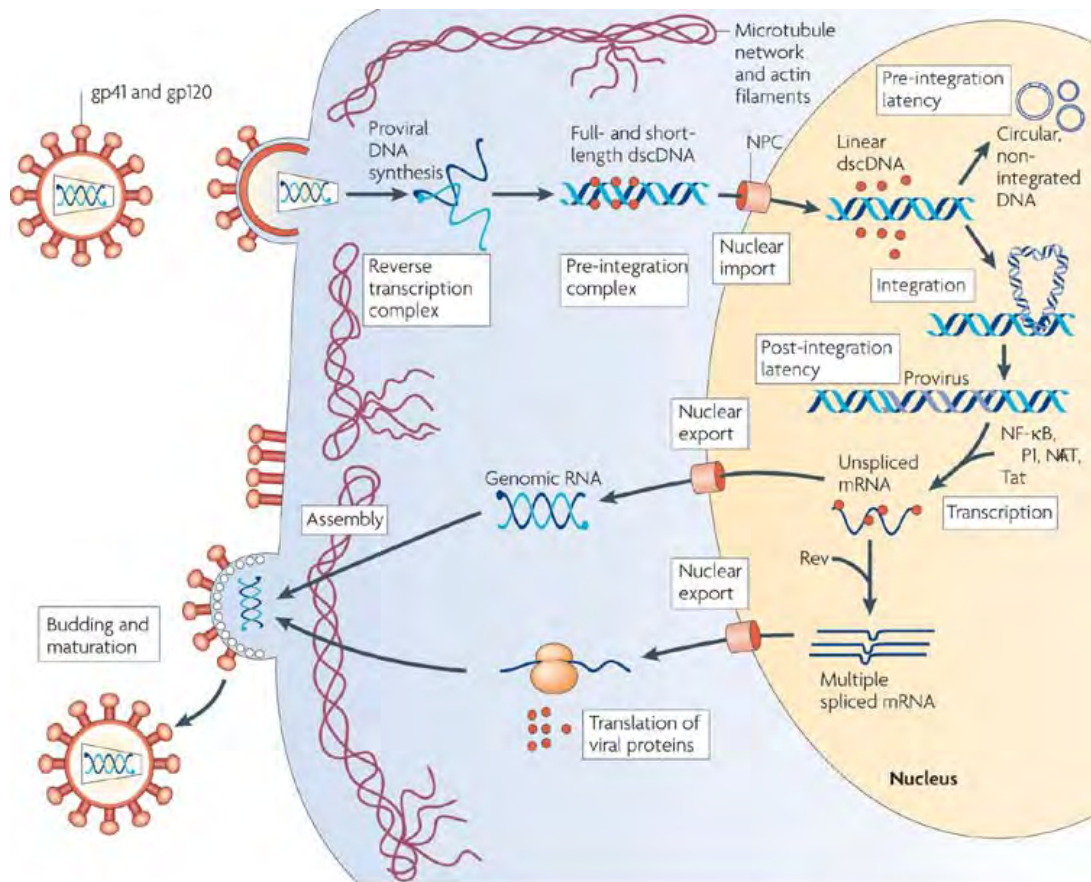
HIV-1 originated in Sub-Saharan Africa, possibly in southern Cameroon (88), early in the 20th century (97, 203) as a zoonotic transmission event from chimpanzees (88). Today the majority of those infected, some 22.5 million, reside in Sub-Saharan Africa, where the adult seroprevalence averages 5%. The Caribbean is the next most heavily affected region, with seroprevalence rates of 1%. Recently, the disease has been spreading rapidly in Eastern Europe and

Central Asia with seroprevalence reaching 0.8% and five countries reporting a greater than 25% increase the incidence of HIV-1 since 2001. With 4.1 million people infected South and South-East Asia have the second largest total number of infections, but the seroprevalence is only 0.3% and the number of new infections is decreasing (83).

Human Immunodeficiency Virus Type 1

HIV-1, the causative agent of AIDS, is a Lentivirus, a genus that typically causes clinical disease following variable periods of infection. Lentiviruses are retroviruses, a family that carries their genetic information as RNA. Following infection, the viral RNA is converted to DNA by a reverse transcriptase enzyme carried in the virus particle. This viral DNA is then integrated into the host cell DNA by a virally encoded integrase (Fig 1.1). Following integration, the virus can proceed along either the lytic or the latent pathway. In the first case the virus becomes active and replicates, killing the host cell and releasing large numbers of new virus particles. In the second case the cell continues to function, but as the integrated viral genome can become activated at any time, latently infected cells serve as a lifelong reservoir of HIV-1.

The mature HIV-1 viral particle consists of a host derived membrane displaying the viral envelope protein and enclosing a protein matrix and capsid core (Fig 1.2A). Within the core are viral proteins and two RNA copies of the genome. The HIV-1 genome consists of nine genes (Fig 1.2B). The *nef*, *vif*, and *vpu* genes are regulatory, as are the transactivators *tat*, *rev*, and *vpr*. The group-



Nature Reviews | Microbiology

Fig 1.1: HIV-1 life cycle. Viral entry requires the binding of gp120 to receptors (CD4) and co-receptors (CCR5 or CXCR4). The viral nucleocapsid enters the cytoplasm and moves toward the nuclear pore complex (NPC). The viral RNA is retrotranscribed into proviral double-stranded cDNA (dscDNA), which forms a pre-integration complex consisting of dscDNA, viral proteins and some host cell proteins. The pre-integration complex is transported into the nucleus through the NPC, and the dscDNA is integrated into a host cell chromosome. After integration, the provirus remains quiescent, existing in a permanent post-integration latent state. On activation, the viral genome is transcribed and translated into regulatory and structural viral proteins. New virions assemble and bud through the cell membrane, maturing through the activity of the viral protease. Adapted by permission from Macmillan Publishers Ltd: Nature Reviews Microbiology, volume 7, 798-812 (November 2009).

<http://www.nature.com/nrmicro/index.html>

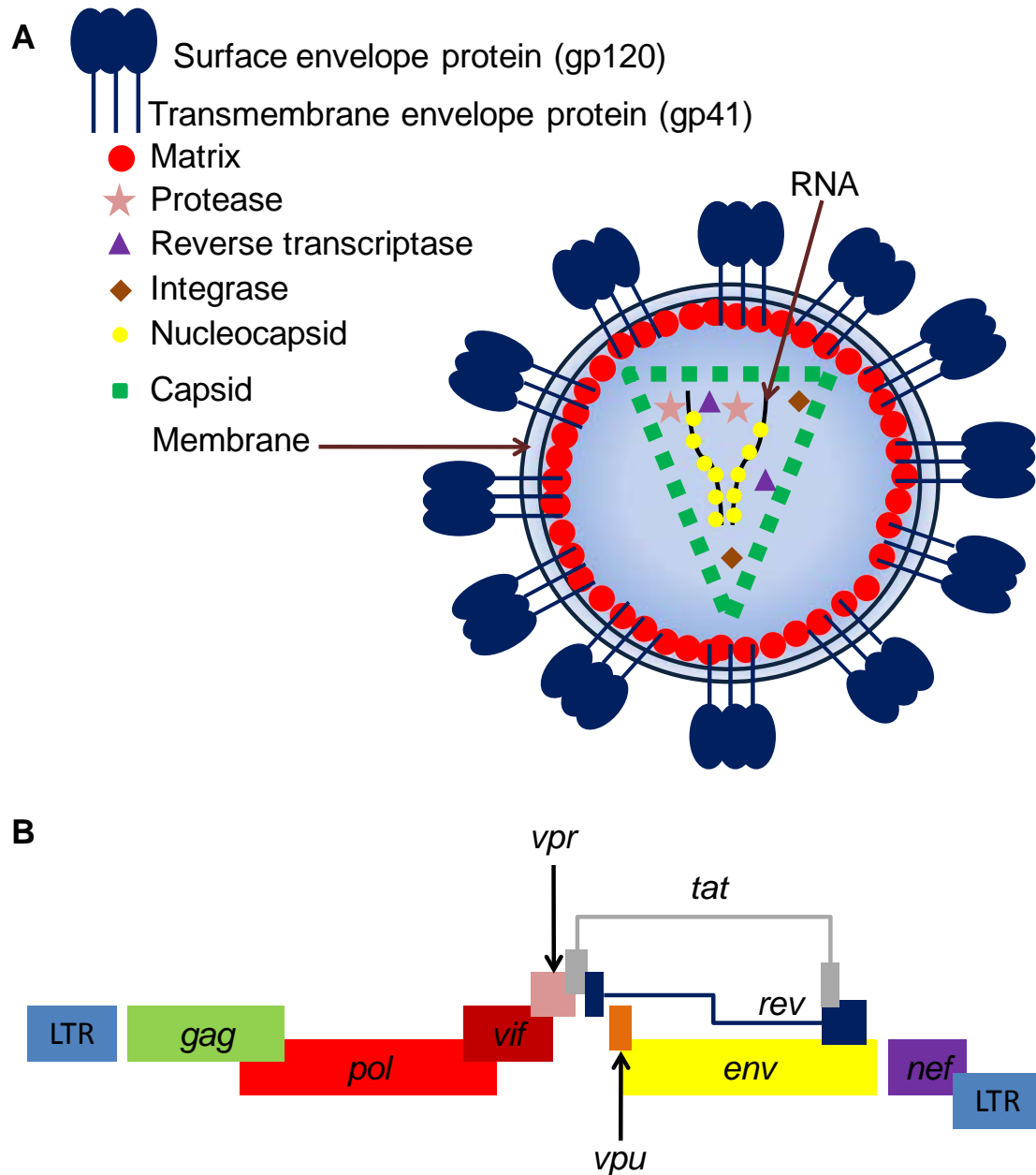


Fig 1.2: HIV-1 virion and genome organization. Each panel uses separate color coding. **(A)** Simplified schematic of an HIV-1 virion. **(B)** Schematic of the HIV-1 genome. Genes are shown only approximately to scale.

specific antigen (*gag*) gene codes for structural proteins including the matrix and capsid. The vital HIV-1 enzymes integrase, protease and reverse transcriptase are encoded by *pol*. The envelope gene (*env*) encodes the envelope glycoprotein, which engages the HIV-1 receptor and co-receptors and mediates virus entry into and fusion with target cells.

HIV-1 Envelope

The HIV-1 envelope is initially expressed as a gp160 glycoprotein precursor which is cleaved into the gp120 and gp41 subunits by host enzymes (45). On mature viruses functional envelope proteins are expressed as trimetric spikes consisting of three gp120/gp41 subunits (73, 198) (Fig 1.3A). The gp120 subunit is exposed on the surface of the viral membrane and binds to the CD4 HIV-1 receptor on a target cell to initiate viral entry (91). This results in a conformation change (172) which exposes the hereto masked co-receptor binding site (184) and allows binding to a co-receptor (4, 49). The gp41 subunit, which is non-covalently bonded to the gp120 (73), is imbedded in the viral membrane. Following co-receptor binding by gp120, gp41 undergoes conformational changes which expose an N-terminal hydrophobic peptide. This peptide inserts into the membrane of the target cell and following subsequent conformational changes causes fusion of cell and viral membranes (199, 200). This fusion is generally thought to occur at the plasma membrane (116), although a recent study reported that HIV-1 fusion occurred only in endosomes (125). Figure 1.3B provides an overview of *env* mediated HIV-1 entry.

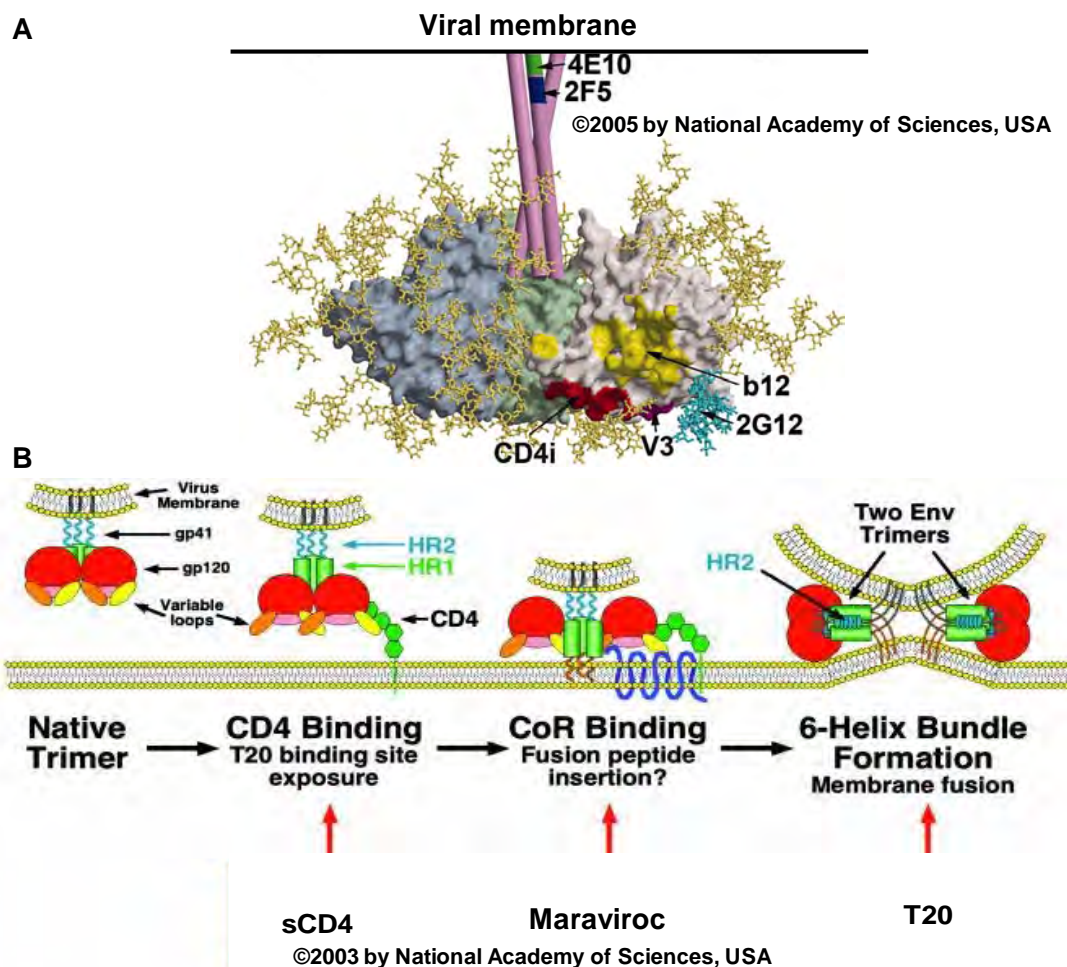


Fig 1.3: HIV-1 entry. **(A)** Model of the Env spike with three gp120 monomers shown in gray, pale green, and pale blue. The gp41 is shown schematically as three pink tubes. Carbohydrate chains are shown in yellow. The approximate locations of epitopes for four broadly neutralizing monoclonal Abs are indicated. Adapted from Burton D R et al. PNAS 2005 Oct 18;102(42):14943-8 with permission of the author. **(B)** The gp120 binds to the CD4 receptor on a target cell to initiate viral entry. This results in a conformational change which exposes the hereto masked co-receptor binding site, allowing binding to a co-receptor. Following co-receptor binding gp41 undergoes conformational changes which expose an N-terminal hydrophobic peptide. This peptide inserts into the membrane of the target cell and following subsequent conformational changes causes fusion of cell and viral membranes. The stages of entry at which three HIV-1 entry inhibitors are believed to act are indicated. Adapted from Moore J P et al. PNAS 2003 Sep 16;100(19):10598-602 with permission of the author.

HIV-1 is an enveloped virus, whose membrane is host derived. The *env* spikes are the only HIV-1 proteins found on the viral surface and are therefore the primary targets for anti-HIV-1 neutralizing antibodies (96, 196). However HIV-1 *env* is heavily glycosylated (Fig 1.3A), making it a difficult target for neutralization. Further, HIV-1 is able to modify the number and location of the glycans on its envelope (196). Most of these glycosylation changes occur in the variable loops of the *env*. These five regions (V1 – V5) are displayed on the surface of the gp120, exhibit a relatively flexible structure and despite being functionally important, are able to accommodate high levels of variability. By changing the lengths and sequences of its variable loops and modifying the number and location of attached glycans over the course of infection, HIV-1 creates an ever evolving glycan shield (196), constantly generating novel *env* variants resistant to the concurrent host antibodies.

HIV-1 diversity and subtypes

HIV-1 and particularly its *env* gene are characterized by marked genetic diversity. The viral population within a single HIV-1 infected individual, termed a quasispecies, can exhibit as much variation in its *env* as is found among all the Influenza virus Hemagglutinin (surface protein) worldwide in a given year (96) (Fig 1.4B, E). Viruses that have altered over 10% of their *env* sequence arise in a single subject over the course of a typical infection (175, 201) (Fig 1.4C). Possibly due to distinct transmission events, the HIV-1 pandemic is composed of four strains; major (M), outlier, N and P, of which M accounts for more than 90%

Fig 1.4: A comparison of evolutionary distances of HIV-1 envelope sequences encoding V2-C5 and influenza HA1 domain of the HA gene through phylogenetic analysis. All panels show maximum likelihood trees using a REV model allowing for rate variation at different sites, following the strategy described in Korber et al Science 2000. The scale bar is the same in a–f for comparisons. (a) Tree based on 20 HA1 domain sequences of A/Sydney-like viruses circulating in Canada during the first half of the 1997–1998 flu season (Osiowy CK, unpublished observations. Accession numbers: AF087700-AF087708 and AF096306-AF096316). (b) Tree based on 96 HA1 domain sequences of human influenza H3N2 viruses. The tree contains all sequences from the Influenza Sequence Database, Los Alamos National Laboratory (<http://www.flu.lanl.gov>), with an isolation year of 1996. (c) Tree based on 9 V2-C5 sequences from a single asymptomatic individual collected at one time point 73 months post-seroconversion – this was a subtype B infection, and is typical of inpatient diversity (Shankarappa et al J Virol 1999). (d) Tree based on HIV-1 subtype CRF03_AB V2-C5 sequences from 26 individuals from Kaliningrad, representing a unique situation where a recombinant form of the virus spread explosively through a population of i.v. drug users, and all viruses were very closely related to a single common ancestor (Liitsola et al AIDS 1998). These samples were collected during 1997–1998, within a year of the introduction of the strain into the population. (e) Tree based on HIV-1 V2-C5 env sequences from a subtype B epidemic, sampled from 23 individuals residing in Amsterdam in 1990–1991 (Lukashov J Virol 1997). (f) Tree based on HIV-1 V2-C5 sequences sampled in 1997 from 193 individuals residing in the Democratic Republic of the Congo (DRC), a remarkably diverse set (Vida et al J Virol 2000).

Figure and legend taken from Korber et al, Evolutionary and immunological implications of contemporary HIV-1 variation. Br Med Bull, 2001;58(1):19-42 by permission of Oxford University Press.

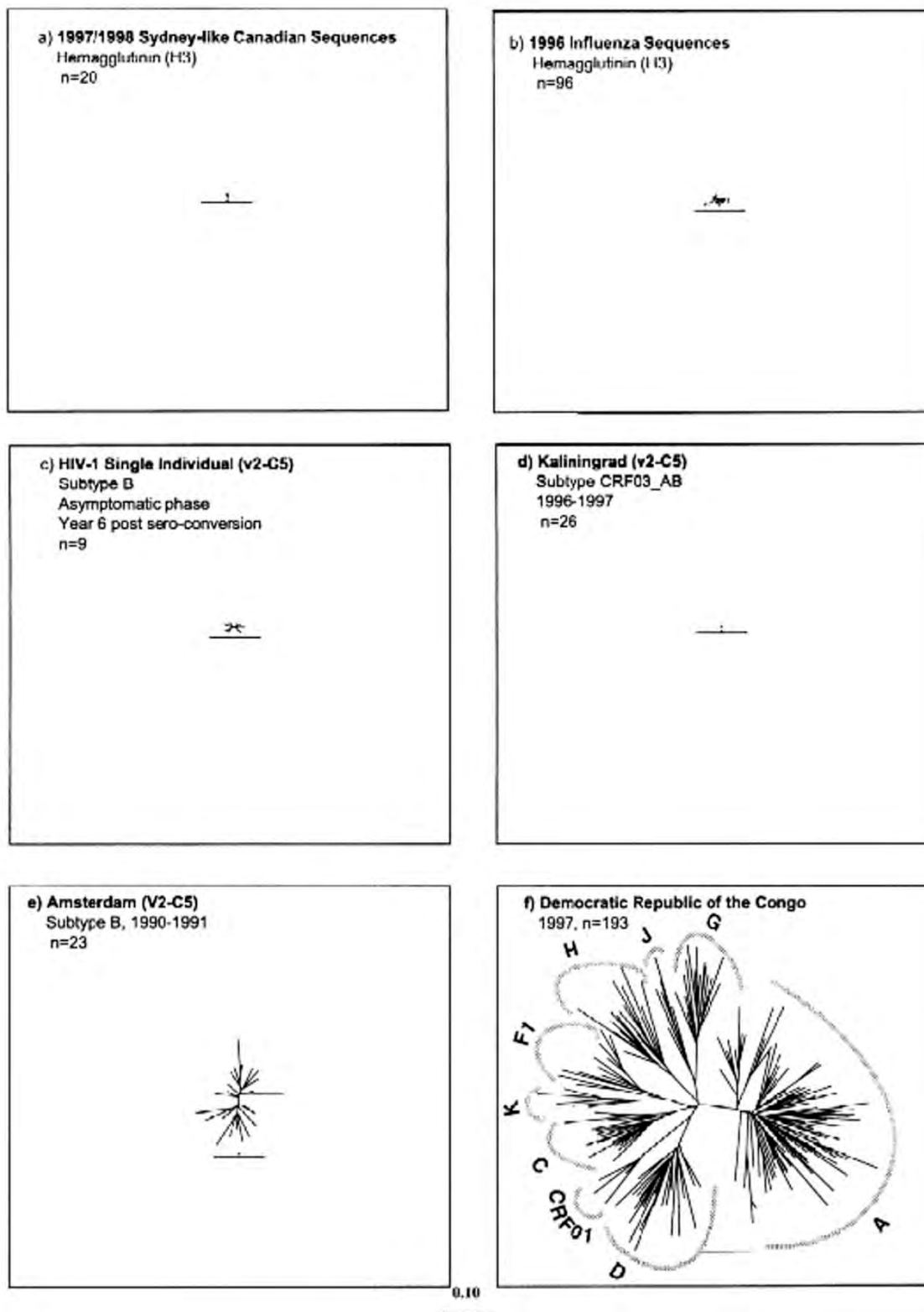


Fig 1.4

of infections (69, 150). Within the M group are 9 distinct subtypes and at least 15 circulating recombinant forms of these subtypes. The genome of HIV-1 can differ by up to 35% between the subtypes (182) (Fig 1.4F). This genetic diversity among subtypes results in phenotypic differences, including transmission rates (14, 161), virulence (9, 85) and reverse transcription rates (79).

Due to founder events, there is a strong enrichment for specific subtypes in different geographic areas (Fig 1.5). Historically most infections in Western Europe and North America were with subtype B (74). Therefore many of the early viral isolates and much of the pathogenesis data were obtained from subjects infected with this subtype. However, worldwide this subtype accounts for approximately 12% of those infected (74). Subtype C, which is most prevalent in Sub-Saharan Africa, is the most rapidly expanding HIV-1 subtype. At least 22 million people are currently infected with subtype C, accounting for almost 60% of all HIV-1 infections (83).

The unprecedented diversity of HIV-1 is thought to be due to the combination of its high replication and turn-over rates (143), lack of proof-reading mechanism of the HIV-1 reverse transcriptase enzyme (153) and high levels of recombination (210). The synergistic effects of these mechanisms could in theory generate every possible mutation in the HIV-1 genome within a single infected individual daily (143). Viruses that survive selective pressures and exhibit enhanced replication fitness generate a complex, constantly evolving and

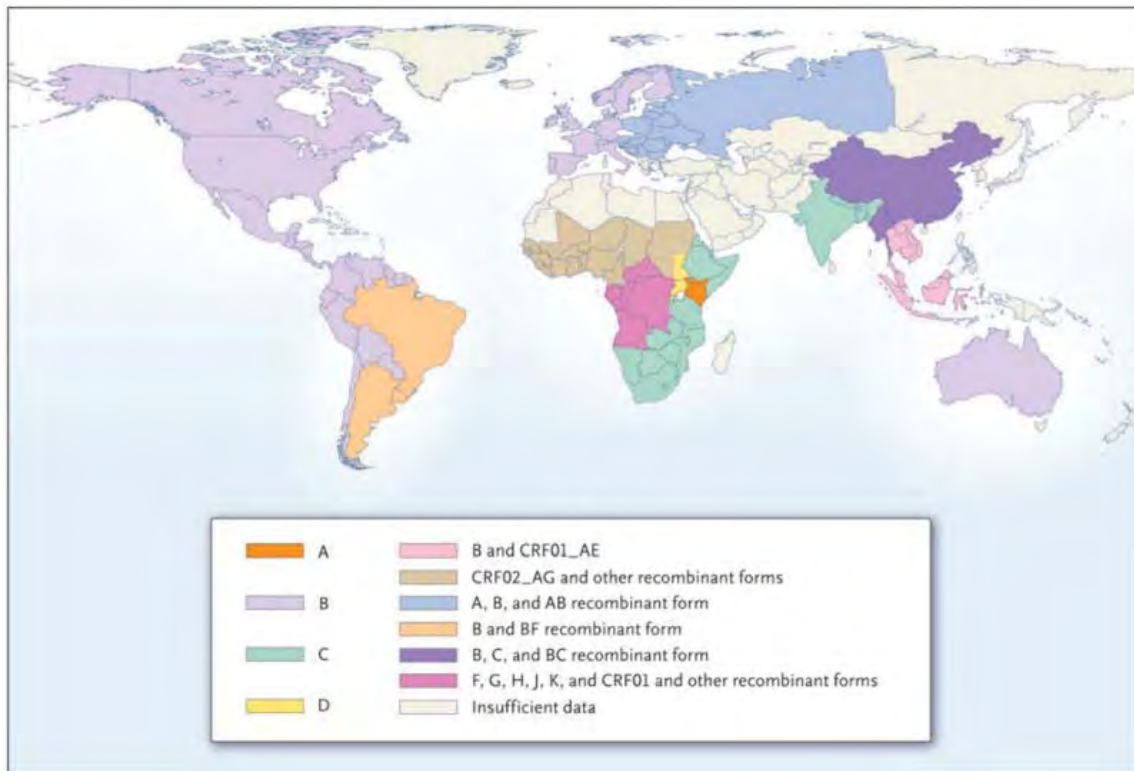


Fig 1.5: Global distribution of HIV-1 subtypes and recombinant forms as of 2008. Image obtained from Taylor et al, *N Engl J Med.* 2008 April 10; 358(15): 1590–1602. ©Massachusetts Medical Society.

increasing distribution of mutant genomes within both individuals and populations (129, 154, 201).

Within an individual this diversification results in the continuous escape of HIV-1 from the host immune response (196) and in the rapid generation of mutants resistant to Anti-Retroviral Therapy (ART) (26, 70, 197) which may greatly complicate treatment. On a population level, transmission of ART resistant viruses has been widely reported and may reduce treatment efficacy (82, 178). More importantly, diversity has greatly complicated vaccine design (16, 188) as, unlike the case with most pathogens, a robust immune response to an existing infection may not prevent super-infection with a different variant of the virus (5, 6).

Routes of HIV-1 transmission and the selective bottleneck

There are three main routes of HIV-1 transmission: sexual, Mother-to-Child (or vertical), and through contaminated needles or un-screened blood products. The first two forms, which occur across mucosal membranes, are collectively termed mucosal transmission and account for the majority HIV-1 infections (140). A hallmark of transmission across an intact mucosa is a marked restriction in the diversity of founder viruses as compared to the quasispecies of a chronically infected subject (1, 40, 58, 87, 168, 202, 204, 206). Large-scale studies utilizing Single Genome Amplification (SGA) and extensive *in-silico* modeling of virus diversification concluded that this genetic bottleneck suggests either the transmission or post-transmission amplification of a single donor

variant in the majority of recipients (58, 87, 168). Further, the majority of transmitted viruses represent rare variants of the donor population (40, 204, 206). This genetic bottleneck may be due to active selection, but the features underlying the selection are largely unknown.

Mother-To-Child Transmission (MTCT)

Initially, HIV-1 patients were predominately male, but the proportion of infected women has been increasing worldwide (83, 156). Today over 50% of those afflicted are young women (83). In Sub-Saharan Africa, a region with historically high rates of MTCT, young women are up to eight times more likely than men to be HIV-1 positive (83). In developed countries access to Highly Active Anti-Retroviral Therapy (HAART), antenatal HIV-1 testing, elective cesarean section and formula feeding have decreased the incidence of MTCT to less than 2% (29, 83, 103). However, in many regions of the world, limited resources and infrastructure continue to restrict treatment options for HIV-1 infected pregnant women (83).

In the absence of intervention, more than a third of the children born to HIV-1 infected mothers will acquire the virus through MTCT (1, 114). In 2009, an estimated 370,000 infants (more than 1000 a day) were infected, accounting for 14% of all new HIV-1 transmission (83). Disease progression in untreated HIV-1 infants is much more rapid than in adults (2), with a 75% mortality rate by the age of 3 (137), accounting for up to 20% of all HIV-1 related deaths (113). In the

most heavily affected areas HIV-1 is now the leading cause of child mortality, responsible for one third of all deaths among children under the age of five (113).

MTCT can occur during gestation (*in utero*), at delivery (*intra partum*) and through breastfeeding (*post partum*), with the latter two routes (collectively termed *peripartum*) accounting for the vast majority of infections (2, 99). Similar to sexual transmission of HIV-1, *peripartum* transmission is thought to occur across a selective bottleneck, with only one or two minor variants of the maternal quasispecies typically transmitted (2, 40, 204, 206). These transmitted variants likely exhibit advantages in crossing mucosal barriers, infecting target cells, or evading immune responses (189). Both virus specific factors (95, 202, 204) and host immune responses (39) have been suggested to play a role in this phenomenon, but the exact features controlling the selective bottleneck are largely unknown.

Need for a vaccine

Despite intense international efforts to slow the spread of the pandemic through education campaigns, testing, needle exchange programs, the distribution of condoms and ART prophylaxis, 2.6 million new HIV-1 infections were reported in 2009 (83). Currently, the only effective treatment for HIV-1 is HAART. In the developed world treatment with combinations of drugs and close monitoring for the rise of resistant variants has greatly improved the life quality and expectancy of those infected. However, in middle and low income countries

only 5.2 out of an estimated 15 million eligible people have access to any form of ART (83).

HIV-1 is most prevalent in Sub-Saharan Africa where, despite international aid, the resources and infrastructure are still unequal to providing HAART to the majority of those afflicted. Of the 1.8 million AIDS related deaths reported worldwide in 2009, 1.3 occurred in Sub-Saharan Africa. The consensus is that the best long term strategy for stopping the spread of HIV-1 is the development of a successful prophylactic vaccine (107, 122, 122). This approach is particularly attractive as, in addition to stopping transmission, it is theorized that such a vaccine, when given to previously infected individuals, could prove therapeutic, lowering their viral burden and perhaps reducing or eliminating the need for HAART (72, 108).

Vaccine design approaches

Traditional vaccine approaches rely largely on the induction of neutralizing antibodies for protection. This approach is particularly relevant to blocking transmission of retroviruses such as HIV-1 that integrate into the genome of the host's cells. In order to be fully protective, a putative vaccine would likely need to elicit sterilizing immunity by inducing an antibody response capable of neutralizing the virus before it could enter cells (20, 118, 122, 130). To date, HIV-1 vaccine candidates have failed to generate broad and effective neutralizing antibody responses in human trials (19, 102, 111, 209).

In the face of this failure, new vaccination models are being explored. One approach is the induction of cell-mediated immunity, particularly the generation of strong cytotoxic T lymphocyte (CTL) responses against the virus. This work is based on the findings that CD8⁺ T cells are absolutely required for control of infection in non-human primate models (10, 173) and that strong and effective CTL responses correlate with control of viremia (163, 181). Unfortunately, the failure of Merck's STEP clinical trial (www.HVTN.org), which sought to prevent infection without generating antibodies, indicates that induction of cell-mediated immunity alone, while beneficial, is insufficient for full protection.

Other approaches focus on overcoming HIV-1's diversity through identification of common neutralization epitopes on the *env* of many different primary isolates (28, 81, 131). A similar approach is to determine consensus or ancestral envelope sequences, synthesize them and use them as vaccine antigens (57). To date, all approaches have failed to provide broad protection. However, vaccine candidates generally utilize envelope antigens from the highly diverse quasispecies of chronically infected patients, yet mucosal transmission, which accounts for the majority of HIV-1 infection, is thought to occur across a strongly selective bottleneck. It is hypothesized that once the factors controlling this selection are identified, they can be used to rationally design vaccines or other therapies targeted to preferentially transmitted variants of the donor quasispecies (1, 113), minimizing the overwhelming diversity of HIV-1. While the factors controlling this selection are largely unknown, they are likely driven by

viral envelope properties that affect cellular tropism, viral entry kinetics, and neutralization sensitivity.

HIV-1 envelope correlates of transmission

Changes in both the genotype and phenotype of *env* between donor and recipient during mucosal transmission have been reported. Shorter, less glycosylated *env* appear to be preferentially transmitted during sexual (25, 166) and vertical transmission (204) of subtypes A and C, although such differences do not occur in subtype B (25). Mucosally transmitted envelopes are almost uniformly CCR5 tropic (8, 35, 174), whereas chronically infected individuals can exhibit a mixture of CCR5, CXCR4, and R5X4 dual tropic *env* clones. During MTCT, HIV-1 specific maternal antibodies (Abs) are present in the infant and it has been reported that envelope variants resistant to neutralization by maternal antibodies are preferentially transmitted (39, 204). Chronic and recently transmitted envelope clones from the same subject differ in their fusion efficiency (48). It has also been reported that the envelopes cloned from recently infected infants confer higher rates of replicative fitness than do those obtained from their mothers (95).

Research framework and objectives

The work reviewed above frames my project. Mucosal HIV-1 transmission does not appear to be simply a random or stochastic process, but likely proceeds across a selective bottleneck. While the factors controlling this selection are largely unknown, they are likely driven by viral envelope properties that affect

cellular tropism, viral entry kinetics and neutralization sensitivity. The following body of work attempts to define the genotypic and phenotypic factors controlling selection during vertical transmission.

I selected MTCT as a model for mucosal transmission because unlike sexual transmission, the donor-recipient relationship is unambiguous and the timing of infection can be accurately determined without requiring prolonged monitoring of uninfected subjects needed in studies that enroll discordant couples. Additionally, while various strategies can potentially decrease the rates of sexual transmission (83), it is currently not logistically feasible to provide effective means to decrease the rates of MTCT to all the infected mothers in parts of the world where they are most urgently needed. A prophylactic vaccine remains the only viable approach for significantly reducing the rates of MTCT. Identification of the factors controlling the selective bottleneck during mucosal transmission may allow rational design of vaccines targeted to preferentially transmitted HIV-1 envelope variants.

To investigate the genotypic and phenotypic correlates of HIV-1 MTCT, I generated two novel panels of HIV-1 *env* from the peripheral blood of subtype B and C infected mother-infant pairs. Using multiple phylogeny analysis techniques I confirmed that all infants in this cohort were infected across a selective bottleneck. I then analyzed the length, glycosylation, and co-receptor tropism of these clones and found that subtype C infant clones were shorter and less glycosylated than maternal. I constructed pseudo and replication competent

viruses expressing these envelopes and determined their ability to infect and replicate in primary cells, finding that enhanced macrophage tropism did not correlate with transmission and that subtype B viruses exhibited very low levels of macrophage infectivity. I investigated the ability of the *env* variants to utilize differing levels of CD4 and CCR5 for infection and found that the ability to utilize lower levels did not correlate with transmission. I compared the sensitivity of pseudoviruses expressing maternal and infant envelope clones to neutralization by a panel of human neutralizing monoclonal antibodies (the binding epitopes of the four antibodies used are shown in Fig 1.3) and heterologous seropositive and autologous plasmas, and did not detect significant differences, which implies that neutralization resistance is unlikely to be a major factor controlling the selective bottleneck. All clones were sensitive to the three HIV-1 entry inhibitors tested (the stages of HIV-1 entry blocked by these inhibitors are shown in Figure 1.3). Infant clone sensitivity to Maraviroc implies that this CCR5 antagonist will make a useful addition to the arsenal of HIV-1 MTCT prevention therapies. Most interestingly, when I compared the entry kinetics of corresponding maternal and infant clones I found that *peripartum* transmitted infant *env* clones exhibited a faster entry phenotype than maternal.

Together, the results presented in the body of this work provide a better understanding of the characteristics of transmitted variants and shed light on the factors controlling the selective bottleneck during vertical transmission of HIV-1, bringing us closer to the rational design of targeted vaccines.

CHAPTER II

Materials and Methods

Study populations

Plasma samples were obtained from 5 HIV-1 subtype B infected women and their infants (Table 3.1). Maternal samples were obtained at or within a month of delivery. None of the infants were breastfed and all were infected during delivery, based on the absence of HIV-1 in cord blood or day of delivery samples (17). Infant samples were obtained within nine weeks of delivery and represent the first time point at which HIV-1 was detected in the infants by viral isolation or the detection of nucleic acids. All women provided individual informed consent according to guidelines of the Human Subjects Committee at the University of Massachusetts Medical School.

PBMC samples were obtained from 5 HIV-1 subtype C infected women and their infants (Table 5.1). Maternal samples were obtained at delivery. Infant samples were obtained within six weeks of delivery and include both *in-utero* and *peripartum* transmission. The Human Research Ethics Committee (Medical) at the University of the Witwatersrand, Johannesburg approved my use of these samples for the current study. This study was exempt from review by the University of Massachusetts Medical School Committee for the Protection of Human Subjects in Research in accordance with federal regulation 45CFR46.101 (b) (4).

PCR amplification of envelope (gp160) clones

Viral RNA was extracted from 50 to 200µl of plasma using the Roche High Pure Viral RNA Kit (Roche Pharmaceuticals, Basel, Switzerland). Eluted RNA was treated with 1µl of RNasin Plus RNase inhibitor (Promega Biosciences, San Luis Obispo, CA), then aliquoted and stored at - 80°C. As plasma was not available for subtype C patients, proviral DNA was extracted from 3×10^5 to 2×10^6 PBMC using the DNeasy Blood & Tissue kit (Qiagen, Valencia, CA), then aliquoted and stored at - 80°C.

Full length HIV-1 gp160 was amplified directly from the viral RNA or proviral DNA by endpoint dilution nested RT-PCR or PCR. The amplicons were approximately 2950 base pairs long (Table 2.1) and contained the 3rd and a portion of the 2nd exon of *tat*, a short piece of *nef*, and full length *vpu* and *rev* genes (Fig. 1.2B). I did this because in *cis* expression of *rev* is vital to the efficient expression of *env* (unpublished observations).

To identify the endpoint dilutions, RT-PCR was performed in octuplet on two fold serial dilutions of each viral RNA extract until a dilution where not more than three of eight wells showed product was reached. For the subtype C panel generation a more stringent cutoff of not more than two of eight wells showing product was used in accordance with the Single Genome Amplification (SGA) protocol developed by Salazar-Gonzalez et al (168).

Subtype B outer and inner primer pairs were the same as reported by Wei, et al (196) and are summarized in Table 2.1. RT-PCR was performed using the Superscript One Step RT-PCR for Long Templates kit (Invitrogen Life

Table 2.1: Primers used for gp160 amplification

Name	Purpose	Binding location^f	Sequence
OS ^a	B outer sense	5852-5876	TAG AGC CCT GGA AGC ATC CAG GAA G
OA ^a	B outer anti-sense	8912-8935	TTG CTA CTT GTG ATT GCT CCA TGT
IS ^a	B inner sense	5957-5982	GAT CAA GCT TTA GGC ATC TCC TAT GGC AGG AAG AAG
IA ^a	B inner anti-sense	8881-8903	AGC TGG ATC CGT CTC GAG ATA CTG CTC CCA CCC
BOM ^c	C outer sense	5852-5875	TAG AGC CCT GGA AYC ATC CAG GAA
env M ^b	C outer anti-sense	9069-9096	TAG CCC TTC CAG TCC CCC CTT TTC TTT TA
BIM ^d	C inner sense	5954-5982	GGC TTA GGC ATT TCC TAT GGC AGG AAG AA
OA ^a	C inner anti-sense	8912-8935	TTG CTA CTT GTG ATT GCT CCA TGT
OFM19 ^e	cDNA generation	9604-9632	GCA CTC AAG GCA AGC TTT ATT GAG GCT TA
Vif1 ^e	SGA outer sense	4900-4923	GGG TTT ATT ACA GGG ACA GCA GAG
OFM19 ^e	SGA outer anti-sense	9604-9632	GCA CTC AAG GCA AGC TTT ATT GAG GCT TA
EnvA ^e	SGA inner sense	5954-5982	GGC TTA GGC ATC TCC TAT GGC AGG AAG AA
EnvN ^e	SGA inner anti-sense	9145-9171	CTG CCA ATC AGG GAA GTA GCC TTG TGT

^aWei et al (195). ^bGao et al (56). ^cModification of OS. ^dModification of IS. ^eSalazar-Gonzalez et al (167). Primer OFM19 used for cDNA generation and as SGA outer anti-sense. ^fLocations are based on the HXB2 sequence.

Technologies, Carlsbad, CA). Conditions for the outer PCR were as follows: 45°C for 30 min, 94°C for 2 min, 40 cycles of 94°C for 15 sec, 52°C for 30 sec, 68°C for 3 min, with a final extension at 72°C for 10 min. Inner PCR was performed using the Platinum Taq DNA Polymerase HighFidelity kit (InvitrogenLife Technologies, Carlsbad, CA). Conditions for the inner PCR were as follows: 94°C for 2 min, 40 cycles of 94°C for 15 sec, 55°C for 30 sec, 68°C for 3 min, with a final extension at 72°C for 10 min.

Subtype C outer primer pair was env M (56) and BOM (TAG AGC CCT GGA AYC ATC CAG GAA) a modification of outer sense primer used by Wei, et al (196). The inner pair was the outer anti-sense used by Wei, et al (196), and BIM (GGC TTA GGC ATT TCC TAT GGC AGG AAG AA) a modification of inner sense primer used by Wei, et al. The sequences, purposes and binding locations of the primers are summarized in Table 2.1. PCR was performed using the Platinum Taq DNA Polymerase HighFidelity kit (Invitrogen Life Technologies, Carlsbad, CA). Conditions for the outer PCR were as follows: 94°C for 2 min, 35 cycles of 94°C for 15 sec, 58°C for 30 sec, 68°C for 3 min, with a final extension at 72°C for 10 min. Inner PCR conditions: 94°C for 2 min, 35 cycles of 94°C for 15 sec, 52°C for 30 sec, 68°C for 3 min, with a final extension at 72°C for 10 min.

The *env* amplicons were sub-cloned into the mammalian expression vector pcDNA3.1/V5-His TOPO TA (Invitrogen Life Technologies, Carlsbad, CA), using the manufacturer's instructions. Colonies containing full length inserts in the correct orientation were identified by a PCR screen using GoTaq Green

Master Mix (Promega Biosciences, San Luis Obispo, CA) and the 5' primer pair T7 and *env*-572 (TAG GCC AGT AGT ATC AAC TCA ACT) and the 3' pair BGH and *env*-587 (AAT CTC CTA CAG TAT TGG AGT CAG) for subtype B, or *env*-581 (CTC TGG AAA ACT CAT TTG CAC CAC) for subtype C. Conditions for both reactions were as follows: 95°C for 5 min, 25 cycles of 95°C for 1 min, 50°C for 1min, 72°C for 1 min, with a final extension at 72°C for 5 min.

Identification of functional clones

The functionality of cloned *env* was determined using an adaptation of a cell-cell fusion assay (145). 293T cells (61) were seeded overnight into 24 well plates and the following morning transfected with plasmids containing the *env* clones. Following an eight hour incubation, HeLa cells expressing high levels of CD4 and CCR5 (TZMBL (37)) were added to the 293T cell monolayers and incubated overnight. Next morning the wells were scored for the presence of syncytia resulting from the interaction of functional *env* expressed by the transfected 293T cells with HIV-1 receptors and co-receptors on the TZMbl cells. 10 to 20 functional *env* clones were obtained from most subjects, with each clone originating from an independent endpoint dilution PCR (Tables 3.1 and 5.1).

Single genome amplification (SGA)

SGA was performed as described by Salazar-Gonzalez et al (168). Briefly, viral RNA extracted as above was reverse transcribed to single-stranded cDNA using primer OFM19. The cDNA was diluted in 96 well plates such that less than 30% of the reactions yielded amplified product. Nested PCR was then

carried out using primers Vif1 and OFM19 for the outer step, and EnvA and EnvN for the inner. The sequences, purposes and binding locations of the primers are summarized in Table 2.1. All correctly sized products were purified and sequenced.

DNA sequencing, phylogenetic analysis and clone selection

The V1-V5 regions of subtype B and the gp120 of subtype C viable molecular *env* clones were sequenced using BigDye Terminator chemistry. Sequences were assembled using the Vector NTI software (Invitrogen Life Technologies, Carlsbad, CA). *Env* sequences from each subject were aligned using ClustalW in the software package in BioEdit (www.mbio.ncsu.edu/BioEdit/BioEdit.html) and trees were constructed using the neighbor joining method (167) implemented in Mega (www.megasoftware.net) using Kimura's correction (90) and 1000 iterations of Bootstrap analysis, and the maximum likelihood method with 500 iterations of Bootstrap analysis implemented in PhyML (www.hiv.lanl.gov). Phylogeny was confirmed using the Highlighter software program (www.hiv.lanl.gov). Potential N-Linked glycosylation sites (PNGS) were identified using the N-Glycosite program (www.hiv.lanl.gov). Frequency of residues at a position was determined in the JProfileGrid application (www.profilegrid.org). The V3 loop charge was determined by comparing the number of positively charged (Aspartic Acid and Glutamic Acid) to negatively charged (Lysine and Arginine) residues.

At least two infant and three to five maternal clones were selected from each transmission pair for in-depth analysis. These included representative clones from each infant variant and at least three maternal variants chosen to sample the breadth of their quasispecies, with clones selected from branches both close to and distant from the infants. Full-length gp160 sequences of both DNA strands were obtained for the selected clones. Additional infant clones were sequenced as necessary to obtain a consensus transmitted sequence for each infant.

Pseudovirus production and titration

Pseudoviruses were made by co-transfecting exponentially dividing 293T cells with a 1:2 ratio of *env* and pSG3 Δ *env* backbone (NIH AIDS Research and Reference Reagent Program (195, 196)) using Polyethylenimine (PEI) (Polysciences, Warrington, PA) as the transfection reagent. PEI is a highly efficient transfection reagent that does not require the addition of cell targeting or membrane-disruption agents (15). It also forms a more stable interaction with DNA than calcium phosphate, resulting in higher transfection efficiency.

Pseudoviral titers were determined using single round infection of TZMbl cells (aka JC53BL (37)) essentially as described (128) except that β -galactosidase staining rather than luminescence was used as the readout. To use this readout, following the final 24-hour incubation step, the plates were fixed with ice-cold gluteraldehyde, washed with PBS and developed with X-gal in yellow PBS. Blue stained cells and cell-clusters were enumerated mechanically

on an ELISPOT reader using the Immunospot 4.0.16 software (Cellular Technologies, Ltd., Cleveland, OH). Titrations were performed at least twice for each pseudovirus and the titers expressed as spot forming units per ml (sfu/ml). Unless otherwise indicated, all experiments were carried out using these pseudoviruses, with 200 sfu as the inoculum dose.

Construction of replication competent fluorescently tagged HIV-1

A fluorescently tagged, replication competent HIV-1 backbone was obtained from Dr. Matthias Dittmar (Centre for Infectious Disease, Institute of Cell and Molecular Science, Barts and The London School of Medicine and Dentistry). Plasmids encoding selected infant and maternal *envs* in this backbone were generated as described (135). Briefly, I used the plasmid TN6G Δ , which encodes the full length NL4.3 HIV-1 clone with the *nef* gene replaced by EGFP, and has unique restriction sites (*Bst* EI and *Nco* I) in the *env* gene available for inserting heterologous *envs*. The complementary restriction sites were introduced into selected infant and maternal *env* clones and used for directional sub-cloning into TN6G Δ . Live, fluorescently tagged virus was produced using essentially the same protocol as for the pseudovirus described above.

Cell line, macrophage and peripheral blood lymphocytes titration and infection

Receptor and co-receptor requirements of pseudoviruses were determined by titration on HeLa cells engineered to express various levels of the

CD4 receptor and CCR5 and CXCR4 co-receptors (151). Titrations were performed as described (145) utilizing anti-p24 immunostaining as the infectivity readout. To determine macrophage infectivity, elutriated monocytes (obtained from the Molecular Virology Core of UMass CFAR) were re-suspended in medium containing macrophage colony stimulating factor and cultured for seven days before use for pseudoviral infections essentially as described (145). Each pseudovirus was tested in duplicate in 3 independent assays. To normalize between different pseudoviral preparations, all titers were expressed as a ratio of the titer on the cell line or macrophage culture divided by the titer on TZMbl cells.

For infection of peripheral blood lymphocytes (PBLs), fresh PBLs were maintained in RPMI 1640 medium supplemented with 10% FBS, stimulated with phytohemagglutinin (5 μ g/ml) for 2 days and interleukin-2 (10U/ml) for a further 2 days prior to infection. Infections with live virus (consisting of my *env* sub-cloned into TN6G Δ) were performed at an MOI of 0.01 or 0.001 as indicated (based on TZMbl or PBL titers as appropriate) and carried for seven days before being read for HIV-1 positive cells by anti-p24 immunostaining.

Neutralization assays

Neutralization assays using human monoclonal antibodies, pooled HIV-1 positive patient plasma, autologous maternal plasma, or entry inhibitors were performed as previously described (109, 110, 117, 128, 176) using 200 sfu of pseudovirus to infect TZMbl cells and measuring residual infection using the β -galactosidase readout. To determine the activity of CCR5 antagonists, the assay

was modified such that cell monolayers were incubated with serial dilutions of the inhibitors for one hour before the addition of virus. Following the addition of virus, plates were incubated overnight and the media was replaced with fresh un-supplemented media. Pseudoviral stocks expressing well-characterized *env* from the NIH AIDS Research and Reference Reagent Program Standard Reference Panels of Subtype B or C HIV-1 *Env* Clones (109, 110, 117, 128, 176) were used in every experiment and showed low intra-assay variation and values similar to those reported (109, 110) (Fig 4.4). Monoclonal neutralizing Abs (NAbs) b12, 2G12, 4E5 and 2F5 were obtained from the NIH AIDS Research and Reference Reagent Program; an additional aliquot of b12 was generously provided by Dr. Dennis Burton of The Scripps Research Institute. The maximum b12 and 2G12 antibody concentration used in neutralization assays was 20µg/ml, while 4E10 and 2F5 were used at 50µg/ml in subtype B neutralization assays and at 20µg/ml in subtype C assays. HIV-1 entry inhibitors soluble CD4 (sCD4, Progenics Pharmaceuticals, Tarrytown, NY), Enfuvirtide (T20, generously provided by Roche, Palo Alto, CA), and Maraviroc (obtained through the NIH AIDS Research and Reference Reagent Program) were also evaluated in these assays. All plasma was heat inactivated at 56°C for 30 minutes before use. Sero-negative plasma was used as a negative control and showed no neutralization activity at a 1:15 dilution. Pseudovirus expressing murine leukemia virus (MLV) *env* was used as a non-specific neutralization control (152, 186) and generally failed to be inhibited by the highest concentration of plasma used.

Autologous maternal plasmas exhibited significant levels of non-specific activity. Therefore the autologous neutralization assays were performed using purified Immunoglobulin G.

For all antibodies and inhibitors, the 50% inhibitory concentration (IC₅₀) relative to untreated control infections was determined by subtracting the background foci counts of un-infected wells from both the averaged counts of triplicate antibody dilution wells and the averaged counts from octuplet cell-only and uninhibited-virus control wells. Percentage inhibition values were then calculated using the formula:

$$\left(1 - \left[\frac{(AntibodyDilution) - (CellOnly)}{(UninhibitedVirus) - (CellOnly)} \right] \right) \times 100$$

Graphs were prepared by plotting log₁₀ Antibody Concentration vs. Percentage Inhibition for each antibody/virus combination using the sigmoid fit function of the OriginPro 7.5 SRO v7 software package (139). EC₅₀ values calculated by the OriginPro software were used as final IC₅₀ determinations.

Autologous neutralization using purified Immunoglobulin G

Immunoglobulin G (IgG) was purified from plasmas showing high non-specific activity using the NAb Protein Spin Kit (Thermo Scientific, Rockford, IL) according to the manufacturer's protocol. Elution fractions one and two were pooled and dialyzed in culture media using the Slide-A-Lyzer Dialysis Kit, 10K MWCO (Pierce Biotechnology, Rockford, IL). The amount of IgG in the dialyzed extracts and the original maternal plasma was quantified using the Human IgG

ELISA Kit (ZeptoMetrix Corporation, Buffalo, NY). Autologous neutralizations were set up at an initial IgG concentration of 0.5mg/ml.

Measuring entry by determining the ratio of viral titers at 24 and 48 hours

TZMbl titrations of pseudoviruses expressing *env* clones comprising a mother-infant pair were set up in duplicate plates. The plates were developed at 24 and 48 hours post-infection using the β -galactosidase readout and counted on an automated ELISPOT reader. The natural *log* of the difference between the 24 and 48-hour titers was determined for each clone.

Measuring T20 escape kinetics

This assay was used to examine the entire entry process. To preserve possible differences in rates of entry due to variability in the interactions of the *env* with receptors and co-receptors virus was not pre-bound to the cells. TZMbl monolayers were pre-seeded overnight in 96 well plates. Next morning the culture medium was removed and monolayers were infected with 200 sfu of pseudovirus. At 30 minutes post infection a set of triplicate wells received 50 μ l of 20 μ g/ml T20 fusion inhibitor and was incubated for a further 48 hours. Similarly, additional triplicate wells were treated with T20 at 60, 90, 120 and 240 minutes. Infections were allowed to continue un-inhibited in two additional wells per time point to serve as maximal infection controls. Care was taken to maintain 37°C throughout the assay so as to avoid any inhibitions due to temperature fluctuation. The plates were developed using the β -galactosidase readout. For

each virus the percentage of the mean of each test triplicate relative to the mean of the untreated control from the same time point was calculated.

Measuring HIV-1 entry in PBL

Clones from mother-infant pairs M1003-P1189, M1002-P1031 and M1001-P1024, where transmission occurred in the absence of anti-retroviral therapy (Table 3.1), were selected for further analysis of their entry phenotype. I examined all infant clones from P1189 and P1024, and one clone from each variant of P1031. From each of these pairs, I chose the maternal clone with the highest and lowest 24 to 48-hour titer ratio. Pseudoviral stocks expressing these clones were treated with deoxyribonuclease I to remove carryover plasmid DNA from the transfection process, aliquoted and frozen. Because subsequent infections were performed in PBL instead of TZMbl, the reverse transcription (RT) activity of the treated viral aliquots in counts per minute (CPM) was determined using an exogenous RT assay and used to calculate the viral dose.

1×10^5 PBL stimulated with phytohemagglutinin and interleukin-2 as above, were infected with 1×10^6 CPM of pseudovirus in a total volume of 100 μ l of ice-cold culture media supplemented with 30 μ g/ml DEAE-Dextran (Sigma-Aldrich, St. Louis, Missouri). The virus was pre-bound to the cells by centrifugation at 2,500 RPM for 90 minutes at 4°C. Unbound virus was then removed, the cells washed in ice-cold media, infection synchronized by addition 100 μ l of 37°C culture media and the plates put into a 37°C incubator. At desired time points, infected cells were removed from the wells, lysed, and total DNA extracted using

the DNAzol reagent (Invitrogen, Carlsbad, California) according to the manufacturer's instructions.

To compare rates of entry the number of copies of the HIV-1 negative strand strong stop (NSSS) cDNA in 5µl of extracted DNA was quantified by TaqMan real time PCR. NSSS is the earliest HIV-1 reverse transcription product. An overview of HIV-1 reverse transcription and the locations of the primers and probe for detecting the NSSS are show in Figure 2.1. NSSS was amplified using HIV-1 LTR specific primers C1/f (TAG ACC AGA TCT GAG CCT GGG A) and AA55 (CTG CTA GAG ATT TTC CAC ACT GAC). Amplification was performed in 20µl reactions containing 10µl TaqMan Fast Universal PCR Mix (2X) No AmpErase UNG (Applied Biosystems, Foster City, CA), 20µM primer mix, 100µM fluorogenic probe 2nr4nr (5' 6-FAM 3' TAMRA, AGC CTC AAT AAA GCT TGC CTT GAG TGC) and 5µl of cellular DNA extract. The reactions were conducted using the 7500 Fast Real Time PCR System (Applied Biosystems, Foster City, CA) (provided as a service by the Molecular Biology Core of UMass CFAR), utilizing the default cycling parameters of 95°C for 20 sec followed by 45 cycles 95°C for 3 sec and 60°C for 30 sec. Samples were run in duplicate and concurrently run CCR5 housekeeping gene values were used to normalize between extractions. For each viral stock tested, background levels were determined in parallel infection with heat-inactivated virus and subtracted from the live infection signal.

Statistical analyses

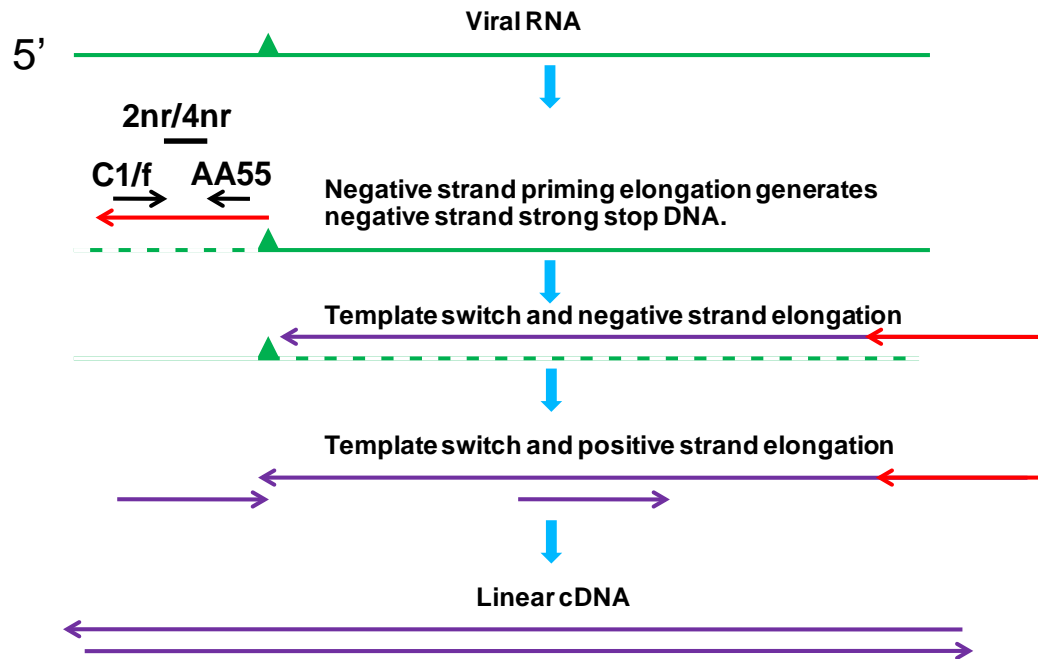


Fig 2.1: Detection of very early HIV-1 reverse transcription products. A simplified schematic of HIV-1 reverse transcription. Green line = viral RNA. Green triangle = primer binding site for cellular tRNA. Red line = negative strand strong stop cDNA. Purple line = cDNA. Dashed green line represents degradation of the RNA strand of the RNA:DNA duplex. Binding locations of the primers and probe designed to detect the negative strand strong stop cDNA are indicated by black arrows and a black line respectively.

Pairwise differences between maternal and infant values were evaluated using the Mixed Model ANOVA (177) with mother-infant pairs included as random effects. The analyses were performed using the Proc Mixed procedure (171) in the SAS statistical Software package (SAS Inc, NC, USA). The ratios of 24 to 48 hour titers did not follow a Gaussian distribution. Therefore, for statistical analysis, I *log* transformed the data for better conformation to normality.

To analyze T20 escape kinetics, curves characterizing the viral titer as a function of time were developed by fitting second order polynomial regressions using General Linear Mixed Models (121), and pairwise comparisons of infant and maternal slopes were performed using Mixed Model ANOVA with mother-infant pairs included as random effects. Goodness of fit for the models was evaluated using the deviance (-2 times log likelihood of the model). Differences in model parameters between generations were evaluated using the pseudo F tests for the model term. The distributional characteristics of the outcome (percent infected) were evaluated two ways, graphically by visual inspection of frequency histograms and by the Kolmogorov-Smirnov goodness of fit test for normality (32), both using residuals from fitted models.

Significance was reported when $p \leq 0.05$.

Nucleotide sequence accession numbers

Nucleotide sequences of gp160 clones are available under GenBank accession numbers HM368224 - HM368258 for the subtype B panel.

CHAPTER III

Subtype B cohort and genotype analysis

Introduction

Studies in multiple cohorts, across several subtypes, have demonstrated that a marked restriction in the diversity of founder viruses in blood and plasma occurs during mucosal HIV-1 transmission across both sexual (87, 168) and vertical (2, 40, 202) routes. This restricted diversity suggests either the transmission or post-transmission amplification of a single donor variant in the majority of recipients (2, 40, 67, 204). Identification of properties shared by mucosally transmitted viral variants may guide the development of improved methods to prevent transmission of HIV-1.

While the mucosal sites of initial viral replication are not easily accessible, early infection of CD4⁺ T cells and rapid systemic dissemination of the virus allows identification of founder viruses using blood samples (58, 87, 168). In this chapter, I describe a cohort of subtype B infected mother-infant pairs from whose peripheral blood I generated a panel of vertically transmitted and non-transmitted full-length *env* clones. In order to test the hypothesis that transmission of viral variants is not simply a random or stochastic process, but is driven by viral envelope properties that affect neutralization sensitivity, cellular tropism and viral entry kinetics, I examine the genotypes and phylogeny of this panel, and select a subset of representative *env* clones for expression on pseudotyped and live viruses.

I found that the infant quasispecies were more homogeneous than maternal and genetically most similar to minor variants of the maternal blood quasispecies, suggesting they were indeed transmitted across a selective bottleneck. In the following chapter I describe my extensive characterization of the phenotypes of the selected clones and identify functional correlates of HIV-1 subtype B vertical transmission.

Results

Envelope panel generation

To begin investigating the mechanisms influencing viral variant selection during MTCT, I amplified full-length *env* genes from the plasma RNA samples of mothers who transmitted HIV-1 to their infants. Infant samples were collected within two months and maternal samples within one month of transmission (Table 3.1). I generated at least ten functional *env* clones from each infant and a minimum of twelve from each mother. Figure 3.1 provides a flow chart overview of how the panel of *env* clones was generated. Each clone was obtained from an independent, limiting dilution RT-PCR reaction (Fig 3.2), transformed into a mammalian expression vector and colonies containing full length inserts in the correct orientation identified by a PCR screen (Fig 3.3).

Development of a viability screening assay

To facilitate testing the *env* clones for functionality, I developed a high-throughput screen by adapting the cell-cell fusion assay used by Peters et al (145). In this assay, transfection of 293T cells with functional *env* clones results in formation of distinct syncytia after TZMbl cells are added to the 293T cell cultures. Figure 3.4 shows representative wells 18 hours after the addition of TZMbl cells to mock transfected 293T cells (Fig 3.4A and C) and to 293T cells transfected with a functional *env* (Fig 3.4B and D). This assay can screen up to 48 *env* clones with less than three hours of total setup time, eliminating non-functional clones prior to sequencing. Over 87% of clones tested proved viable.

Table 3.1: Subtype B cohort summary

Subject ^a	Sample Timing ^b	Plasma Viral Load (copies/ml)	CD4	CD8	CD4:CD8	No. of <i>env</i> clones	No. of pseudo viruses	ART status
M1003	0	14,158	466	932	0.50	12	4	None
P1189	31	311,538	2872	1975	1.45	10	2	None
M1002	28	ND	872	1225	0.71	25	5	None
P1031	54	685,169	2147	927	2.32	11	3	None
M1001	2	26,000	534	726	0.74	19	4	None
P1024	51	750,000	3312	4504	0.74	11	2	None
M1007	-8	ND	870	1176	0.74	22	4	ZDV
P1046	66	1,229,730	2573	1693	1.52	22	4	ZDV
M1006	-33	260,541	134	403	0.33	20	5	ZDV
P1049	30	647,919	ND	ND	ND	10	2	ZDV

^aM, Mother; P, Infant. ZDV, Zidovudine. ND, No data. ^bTiming of samples used for cloning in days after delivery; negative numbers indicate days before delivery.

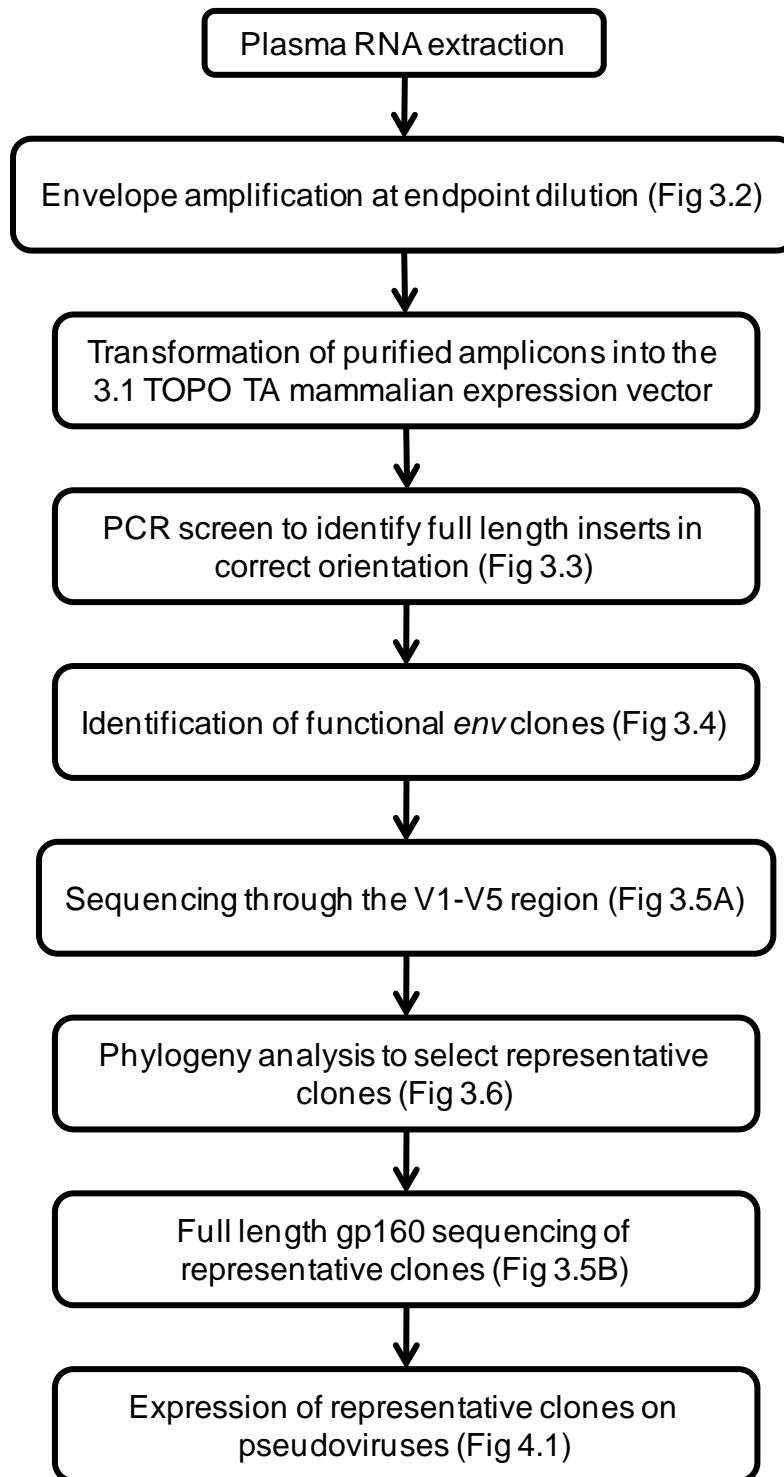


Fig 3.1: Flow chart of *env* clone panel generation.

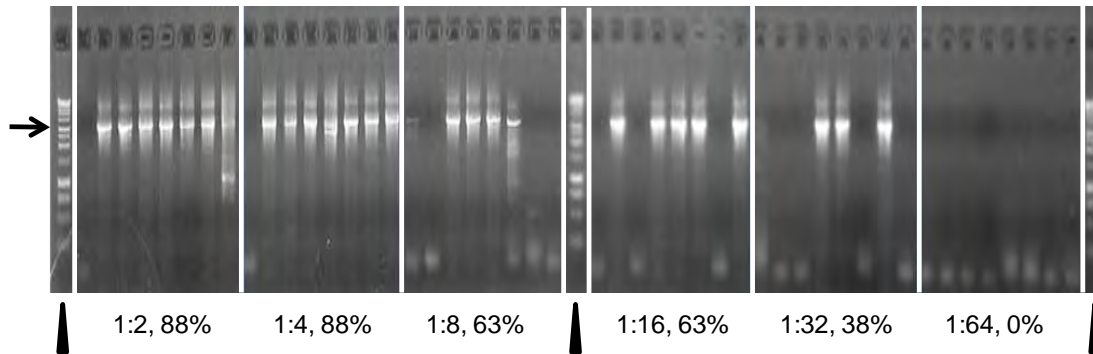


Fig 3.2: Determination of endpoint dilution. A representative gel of the inner products of nested RT-PCR run in octuplet on serial two fold dilutions of plasma RNA. Triangles indicate one kilobase ladders, arrow indicates expected location of 3 kilobase gp160 products. Octuplets are separated by white lines, with the template dilution and percent of successful amplifications given below. Endpoint dilutions are those at which not more than three of eight wells show product. In the above gel a 1:32 dilution achieved the endpoint.

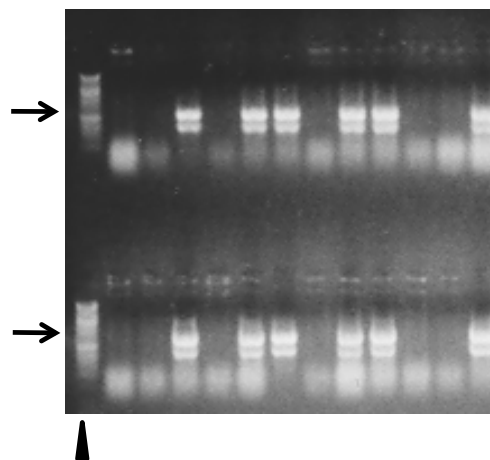


Fig 3.3: Screening transformed colonies for full length inserts in correct orientation by PCR. Each column is an individual colony from a transformation plate. Triangle indicates one kilobase ladder. Upper arrow indicates expected size of product from a reaction utilizing a forward primer binding in the vector and a reverse primer in the insert. Lower arrow indicates expected size of product from a reaction utilizing a reverse primer binding in the vector and a forward primer in the insert. Products in both the upper and lower rows indicate that a full-length insert in the correct orientation is present in that colony.

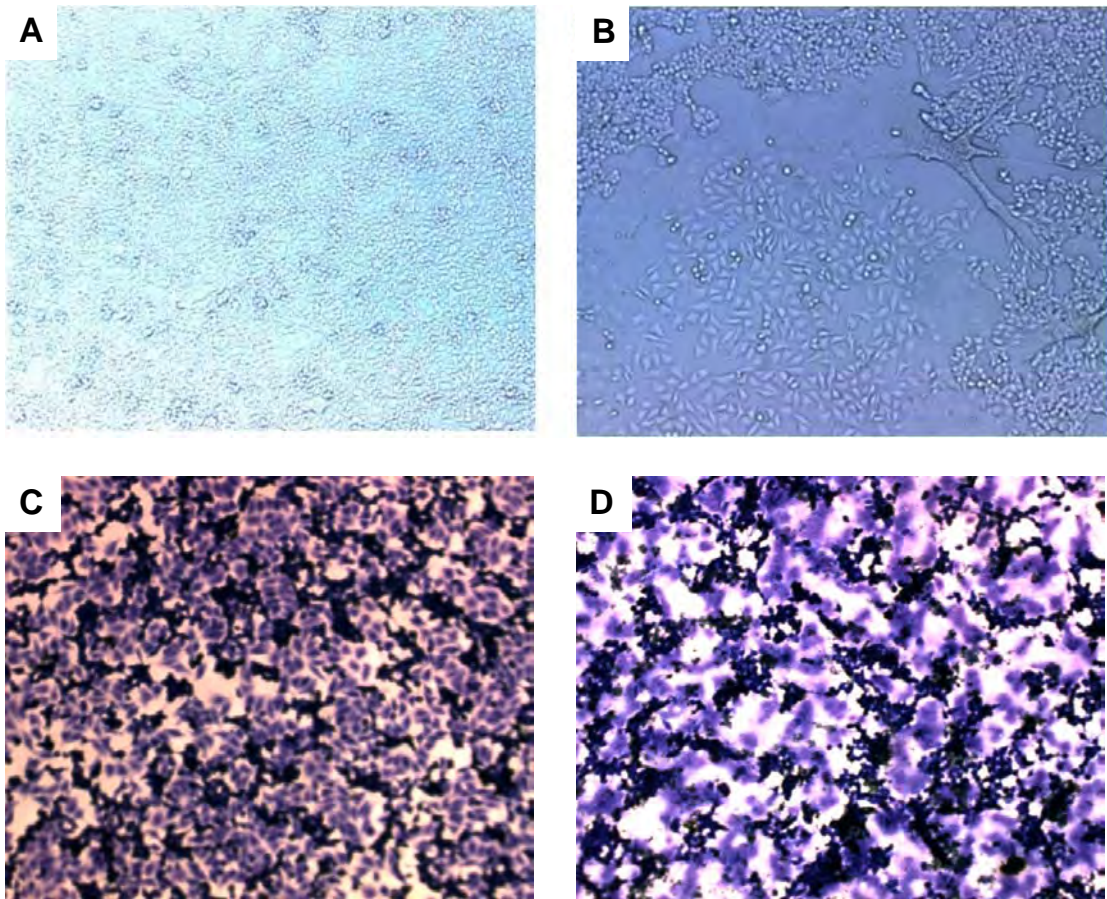


Fig 3.4: Functionality of *env* clones was determined using cell-cell fusion as the readout. HeLa cells expressing high levels of CD4 and CCR5 were added to monolayers of 293T cells mock-transfected (**A, C**) or transfected with functional *env* (**B, D**). Wells in (**C**) and (**D**) were stained to enhance the appearance of syncytia.

Clone sequencing and phylogeny analysis

Utilizing the above assay, I identified 162 functional maternal and infant *env* clones. I sequenced these clones from the start of the first to the end of the fifth variable loop (V1-V5), thus encompassing most of the expected diversity of the clones and constructed a neighbor-joining tree based on their alignment (Fig 3.5A). For one patient (P1031) three clones were sequenced through V1-V3 only and are not included in the tree. The resulting tree revealed clear epidemiological linkages within each mother-infant pair, with no evidence of cross-pair or other contamination. Comparison to subtype reference sequences (Fig 3.5A) confirmed that all subjects were infected with subtype B.

To determine why some full-length clones were non-functional, I determined the V1-V5 sequences of 14 *env* clones that failed to induce syncytia during viability screening. Five of these clones exhibited mutations within V1-V5 consistent with loss of function. Two clones exhibited deletions of over 200 nucleotides, both resulting in a frame shift. A third clone exhibited a similarly large deletion with no frame shift. Two other clones were non-viable due to single nucleotide insertions causing frame shifts. The V1-V5 region spans approximately 1/3 of the HIV-1 gp160. Provided that deleterious mutations occur randomly throughout the *env*, approximately 1/3 of the non-viable clones examined would be expected to exhibit such mutations within V1-V5, as was the case.

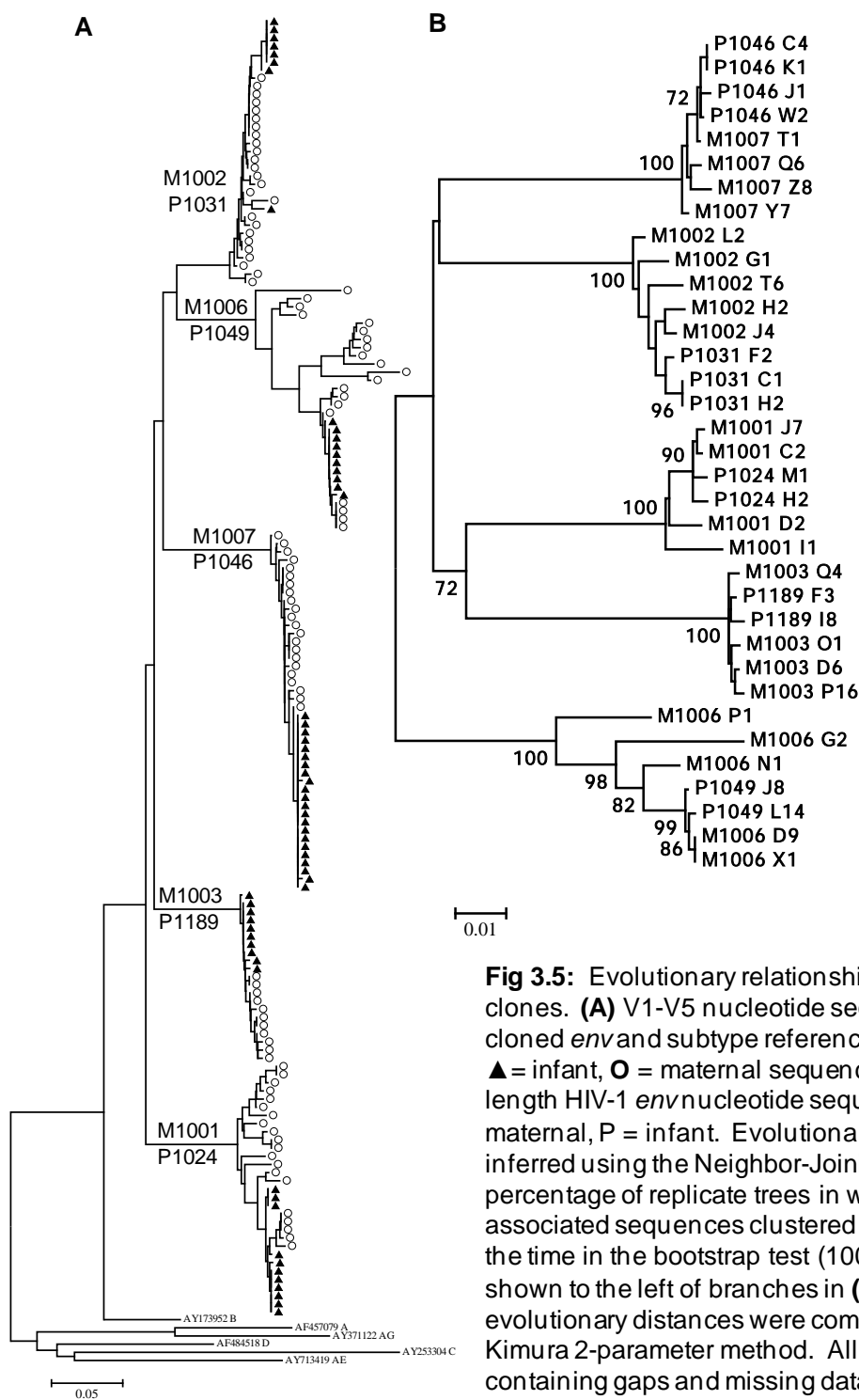
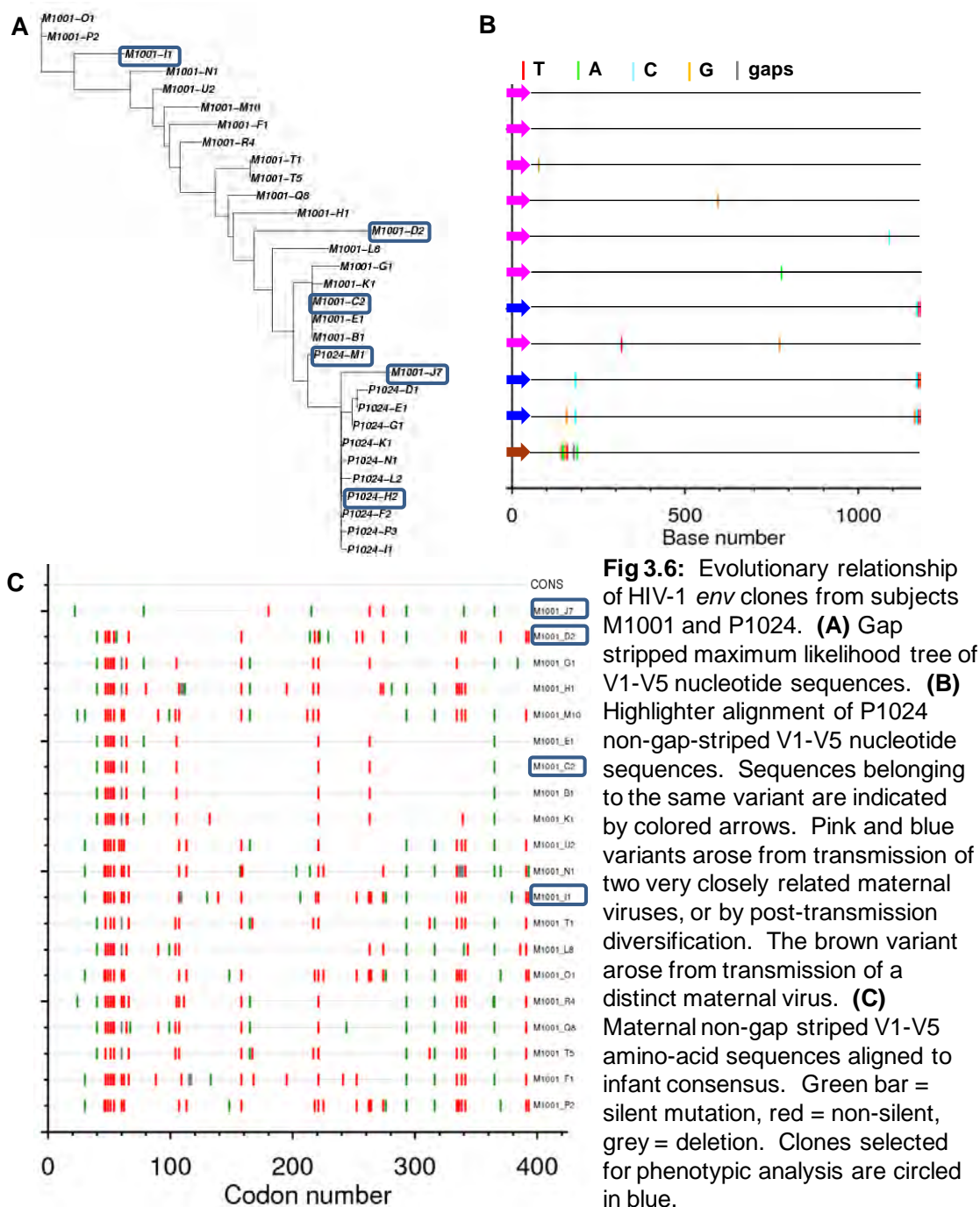


Fig 3.5: Evolutionary relationships of HIV-1 *env* clones. **(A)** V1-V5 nucleotide sequences of cloned *env* and subtype reference sequences. ▲ = infant, ○ = maternal sequence. **(B)** Full length HIV-1 *env* nucleotide sequences. M = maternal, P = infant. Evolutionary history was inferred using the Neighbor-Joining method. The percentage of replicate trees in which the associated sequences clustered together >70% of the time in the bootstrap test (1000 replicates) are shown to the left of branches in **(B)**. The evolutionary distances were computed using the Kimura 2-parameter method. All positions containing gaps and missing data were eliminated from the dataset. Horizontal scale bars represent **(A)** 5%, or **(B)** 1% genetic distance.

The phylogeny of each mother-infant pair was extensively analyzed and the information used to determine the number of maternal variants transmitted to the infants and to select representative clones for phenotype analysis. Single maternal variants were transmitted to infants P1189, P1049 and P1046, two variants to infant P1031 and two or three to infant P1024 (Fig 3.5A). Of the three variants detected in P1024, two arose from very closely related viruses, or through post-transmission diversification (Fig 3.6A and B). From each of the two distantly related infant variants a clone was selected for in-depth analysis (Fig 3.6A). The four maternal clones selected for phenotypic analysis from M1001 were chosen to sample the breadth of the subject's quasispecies, with two clones taken from variants similar to those found in the infant and two from more distantly related variants (Fig 3.6A and C).

Following this criteria, at least two infant and four maternal clones were selected from each pair. A total of 35 *env* clones were chosen for in-depth analysis. Full-length envelope sequences were obtained for the selected clones (Fig 3.5B). Additional sequences were obtained as necessary to determine the consensus gp160 sequence for each infant. The consensus sequence of clones amplified shortly following transmission from a subject infected with a single donor variant represents the sequence of the transmitted virus (67). Of the 13 infant clones selected, four were identical to their infant's gp160 consensus. Eight clones differed from the consensus by two amino acids or less, one differed



by three, and one (P1024 H2) differed by six. Thus the selected infant clones were very similar or identical to the presumed sequence of the maternal transmitted variant.

The relationship between maternal and infant quasispecies was further analyzed utilizing an adaptation of the algorithm described by Haaland et al (67). The number of amino acids differing between each infant V1-V5 sequence and the most closely related maternal sequence were determined, as were the number of maternal sequences differing from an infant variant by less than three amino acids in V1-V5 (Table 3.2). A maternal sequence differing from an infant variant by less than three amino acids likely gave rise to that variant. If such sequences represent less than 5% of the maternal quasispecies, a minor maternal variant was likely transmitted to the infant (67). Infant P1024 was apparently infected with two or three minor variants of the maternal quasispecies, infant P1049 with a single major variant, infant P1031 with two minor variants, while infants P1189 and P1046 each received a single minor variant. The infant quasispecies were more homogeneous than maternal, with the mean diversity, measured by number of base substitutions per site within each subject ranging from 0.1 to 0.3% among infants and 0.6 to 4.6% among mothers (Fig 3.7).

I compared maternal gp160 sequences to their infant's consensus to determine how closely clones selected for their similarity to infant *env* approached the transmitted sequence. Clones most closely related to the infants were; M1003 P16 which differed from the infant consensus by three amino acids,

Table 3.2: Relationship of maternal and infant V1- V5 sequences

Infant	Sequences analyzed ^a	Differences ^b	Less than 3 differences ^c	Variant transmitted
P1189	12	1	1	Minor
P1031	25	3	0	Minor
		11	0	Minor
P1024	19	5	0	Minor
		3	0	Minor
		3	0	Minor
P1046	22	1	1	Minor
P1049	20	2	4	Major

^aNumber of maternal sequences analyzed.

^bNumber of amino acids that differ between an infant variant consensus sequence and the most closely related maternal sequence.

^cNumber of maternal sequences differing from the infant variant consensus by less than 3 amino acids.

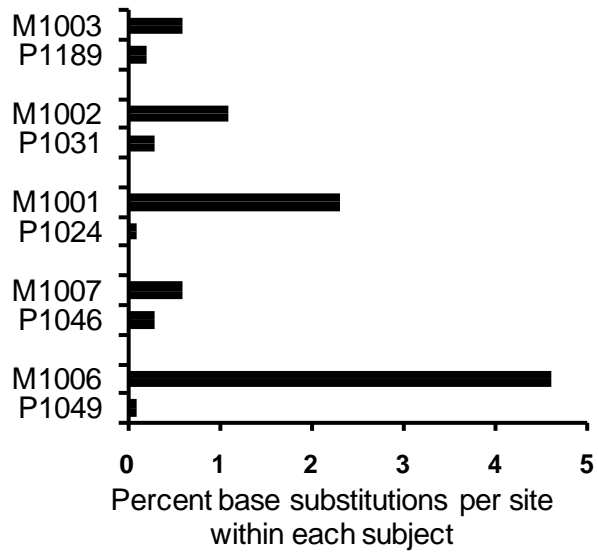


Fig 3.7: Infant quasispecies are more homogeneous than maternal. The percent of base substitutions per site over the V1-V5 region for each subject was computed using the Kimura 2-parameter method in the MEGA4 software program.

M1001 J7 which differed by four amino acids, M1007 T1 which differed by three amino acids, M1006 X1 which differed by three amino acids, and M1002 J4 which differed by 15 amino acids. This list excludes silent mutations. No maternal sequence was identical to the consensus of an infant variant. I also compared each maternal sequence to each sequence amplified from her infant. I did not detect any maternal sequence identical to any infant sequence.

Single Genome Amplification (SGA)

SGA is becoming the standard for quasispecies analysis in HIV-1 infected subjects (168). This technique differs from endpoint dilution in that amplicons are directly sequenced without first being cloned into bacteria. This avoids occasional point mutations that may arise due to the relatively low fidelity of bacterial Taq. SGA thus results in a slightly more accurate representation of a subject's quasispecies than endpoint dilution. However, as un-transformed *env* can't be tested for functionality, numerous non-viable clones are sequenced when SGA is utilized. Further, if SGA generated clones are to be used in phenotypic assays, they must be transformed into bacteria and re-sequenced to confirm that they are identical to the original sequences. Thus, there are more practical limitations to large-scale SGA as compared to endpoint dilution when generating clone panels for functional assays. To compare the accuracy of these two techniques, for two randomly selected infants (P1189 and P1049) 10 to 20 additional clones were amplified using SGA. When the consensus gp160 sequences generated by SGA were compared to those obtained by endpoint

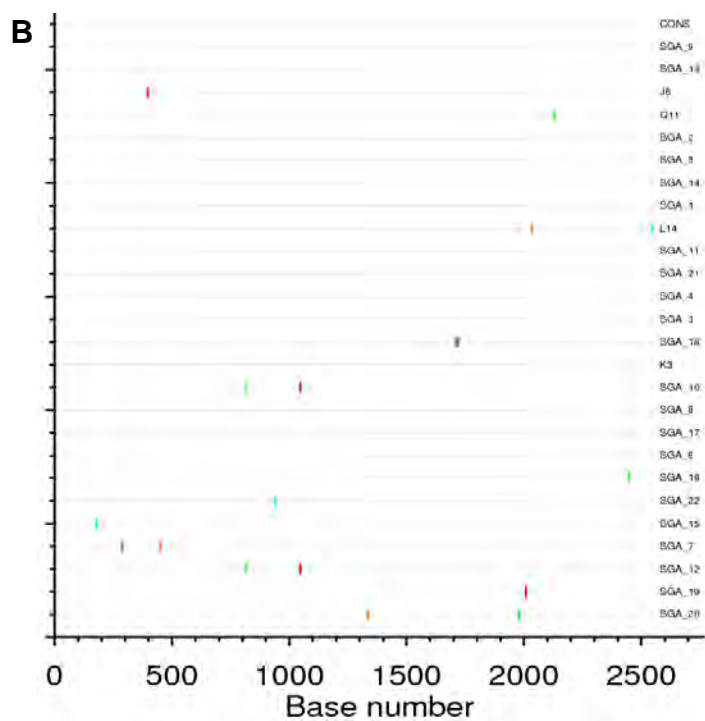
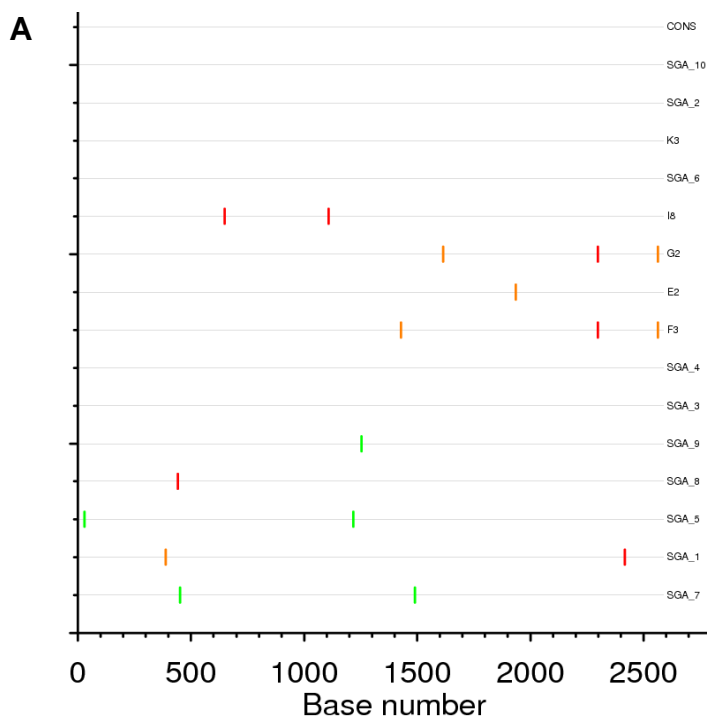


Fig 3.8: Comparison of gp160 nucleotide sequences obtained by endpoint dilution and SGA. All gp160 sequences obtained for infants **(A)** P1189 and **(B)** P1049 were aligned against their respective SGA consensus sequences. Sequences obtained by SGA are named SGA_#. Color bars indicate differences from consensus. A:Green, T:Red, G:Orange, C:Light blue, Gaps:Grey.

dilution PCR they proved identical (Fig 3.8).

V1-V5 length and glycosylation

Changes in envelope length and glycosylation levels are reported to correlate with mucosal transmission of some subtypes of HIV-1 (25, 166, 204). I did not find such correlations in my panel. In pairs M1001-P1024 and M1007-P1046 the median V1-V5 length of infant sequences was greater than maternal, while in pairs M1002-P1031, M1006-P1049 and M1003-P1189 the medians were similar (Table 3.3). The median number of V1-V5 PNGS was smaller in the infant sequences than in the maternal in pair M1002-P1031, greater in pair M1001-P1024, and equal in pairs M1007-P1046, M1006-P1049 and M1003-P1189 (Table 3.3).

Co-receptor tropism

The V3 loop charge and glycosylation are predictive of co-receptor tropism (12, 27). Examination of these factors did not reveal any CXCR4 tropic variants in my panel and only one mother (M1006) was predicted to harbor CCR5/CXCR4 dual tropic variants. Only CCR5 (R5) tropic maternal variants were transmitted to the infants (Table 3.3). *In vitro* co-receptor tropism analysis, using the HIJ HeLa cell line which expresses CD4 and CXCR4 but no CCR5 (151), confirmed these predictions (Table 3.3).

Search for genotypic correlates of transmission

I next examined both the V1-V5 and full-length gp160 sequence alignments of clones from each mother-infant pair for genetic correlates of

Table 3.3: Genotypic analyses of V1-V5 sequences

Subject ^a	V1-V5 length ^b	V1-V5 PNGS ^c	V3 charge	V3 glycan	V3 crown motif ^d	Tropism ^e
M1003	335	24(23-25)	+3	Yes	APGR	CCR5
P1189	335	25(25-25)	+3	Yes	APGR	CCR5
M1002	329(329-333)	21(20-24)	+3	Yes	GPGR	CCR5
P1031	329(329-330)	19(19-20)	+3	Yes	GPGR	CCR5
M1001	345(342-347)	23(22-25)	+2	Yes	GPGR, GPGR	CCR5
P1024	346(345-346)	24(23-24)	+2	Yes	GPGR	CCR5
M1007	328(328-335)	23(22-24)	+4	Yes	GPGR	CCR5
P1046	335	23(21-23)	+4	Yes	GPGR	CCR5
M1006	332(320-349)	24(17-26)	+3 +4 +5	Yes, No	QPGR, QPGR	CCR5, CCR5/CXCR4
P1049	332	24(24-24)	+3	Yes	QPGR	CCR5

^aM, Mother; P, Infant. ^bMedian length of the *env* V1-V5 region as median (min-max).

^cMedian number of potential N-linked glycosylation sites in the V1-V5 region as median (min-max). ^dDominant variant presented first. ^eTropism determined *in-vitro*.

transmission. I performed the comparisons both visually using Highlighter and statistically, comparing the frequencies of amino acids expressed at each position. Within each transmission pair, I found mutations unique to the infants. However, these differences appeared subject specific as other infants did not exhibit similar mutations at the same positions. A search of the Los Alamos HIV-1 sequence database failed to find enrichment for these mutations among recently infected infants from other mother-infant cohorts. These mutations were also not detected in my subtype C mother-infant cohort described in chapter V.

Discussion

Studies in multiple cohorts, across several subtypes and routes of transmission have reported a marked restriction in the diversity of founder viruses following mucosal HIV-1 infection (1, 40, 58, 87, 168, 202, 204, 206). This restricted diversity suggests either the transmission or post-transmission amplification of a single donor variant in the majority of recipients (2). It is widely suggested that this genetic bottleneck is due to active selection, including both virus specific factors (95, 202, 204) and host immune responses (39), although purely stochastic transmission has also been reported (22, 187). If the genetic bottleneck is indeed selective, identification of the mechanisms underlying the selection could inform design of therapies for blocking mucosal transmission of HIV-1.

In agreement with most previous studies, I determined that a genetic bottleneck occurred during MTCT of HIV-1 in my cohort. Phylogenetic analyses of V1-V5 sequences from 162 full-length viable *env* clones amplified from 5 mother-infant pairs showed that infant quasispecies were more homogeneous than maternal. The highest sequence diversity seen in the infants, 0.3%, fits well with the model of Keele et al (87), which indicates that the maximum diversity expected within an individual shortly after infection with a single virus is 0.6%. Indeed, three of five infants were likely infected with single variants of the maternal blood quasispecies and one with two maternal variants. The final infant harbored three variants of which two were very closely related. These closely

related variants could have arisen through post-transmission diversification following a single transmission event.

To investigate whether the genetic bottleneck was selective, I determined what portion of each maternal quasispecies was closely related to the V1-V5 consensus of each variant identified in her infant. As, on average, I amplified 20 maternal *env* clones from each transmission pair, a unique maternal sequence represent approximately 5% of the maternal quasispecies. Thus, if 20 unique maternal sequences are amplified, stochastically each represents a major variant of an extremely diverse quasispecies. Of the seven or eight infant variants identified in my cohort, one was very similar to four identical maternal sequences, and thus likely arose from the transmission of that major maternal variant. The remaining infant variants were not closely related to any of, on average, 13 (range 8 to 16) unique variants identified in the corresponding mothers, and thus likely arose through the transmission of minor variants of the maternal quasispecies. This enrichment for infant sequences different from those most prevalent in mother is unlikely to be due simply to a random, stochastic process. My data are therefore in agreement with studies reporting a selective bottleneck during MTCT of HIV-1 (40, 92, 202).

A limitation of this analysis is that half or more of each maternal quasispecies consisted of unique sequences and that generally identical sequences are not detected in a mother and her infant. This is most likely due to the breadth of maternal quasispecies and can only be addressed by greatly

increased sampling. However, the generation and Sanger sequencing of sufficient clones to fully characterize the quasispecies of a chronically infected subject is not practical. More accurate exploration of the relationships between maternal and infant quasispecies will require Deep Sequencing approaches.

To investigate the viral envelope properties underlying this phenomenon, I selected 35 representative clones and further examined their genotypes. I did not identify any maternal gp160 sequence that was identical to any amplified from the corresponding infant's quasispecies, nor to that infant's consensus. The most closely related maternal sequences differed from the infant consensus by at least 3 non-silent mutations. In this work, I looked for *env* dependent correlates of viral variant selection during MTCT. There are several reports of single amino acid changes in *env* sequences causing considerable phenotypic differences. These include the correlation of asparagine at 283 with enhanced macrophage tropism (41, 43, 148) and the natural polymorphism F673L providing intrinsic resistance to neutralization by the monoclonal NAb 4E10 (62, 133). Additionally, linear sequences may not be predictive of the *env* conformation. As no maternal gp160 sequence was identical to her infant's consensus, I did not consider any to be representative of the transmitted virus. Therefore, both in this and all subsequent chapters I compare infant and maternal genotypes and phenotypes without further segregating the maternal clones into those that are closely and distantly related to the infants'.

Several groups have reported selection for shorter, less glycosylated *env* during mucosal transmission of non-B HIV-1 subtypes (25, 166, 204).

Phylogenetic analysis determined that all subjects in my cohort were infected with subtype B, the dominant subtype in the USA (74), where my subjects were recruited. In agreement with a previous report (74) my data indicate that *env* length and glycosylation heterogeneity do not play a major role in viral variant selection during mucosal transmission of HIV-1 subtype B.

The great majority of *env* sampled shortly following mucosal transmission exclusively utilize the CCR5 co-receptor for entry (8, 35, 174). My finding that all infant clones in my panel exhibited CCR5 tropism is in agreement with co-receptor tropism being a selective factor during MTCT. I performed exhaustive comparisons of my maternal and infant sequences for additional genetic correlates of selection during MTCT. Within each mother-infant pair, I found numerous positions at which all infant clones differed from the majority, or often all, of the maternal sequences, but these mutations were subject specific. Aside from enrichment for CCR5 tropism, genotypic correlates of selection during subtype B MTCT have not been reported.

To confirm the accuracy of the infant consensus sequences, which, when sampled shortly following transmission, represent the sequence of the transmitter-founder virus (67), SGA was performed on two randomly selected infants. Using SGA, I amplified at least 10 clones de novo from each infant and found that the consensus gp160 SGA and endpoint dilution generated

sequences were identical. This fits with a recent report that standard PCR and SGA provide similar measures of viral diversity provided a sufficient number of templates is analyzed (84). If the primary interest is in the consensus transmitted sequence very shortly following infection, accurate results can be obtained by endpoint dilution more cost-effectively than by SGA.

During the construction of my *env* panel I adapted an assay developed to monitor cell fusion into a rapid, high-throughput screen to determine the functionality of cloned *env*. Sequencing of non-functional *env* identified mutations underlying the loss of functionality, while no functional clone ever exhibited frame-shifts or large deletions or insertions. Thus, the assay allows rapid, inexpensive identification of functional *env* without requiring sequencing or pseudoviral production. This allowed me to considerably streamline my *env* panel generation.

In summary, in this chapter I described the creation of a unique panel of vertically transmitted and non-transmitted *env* clones and determined that aside from CCR5 tropism there are no obvious genetic correlates of subtype B MTCT.

CHAPTER IV

Subtype B phenotype analysis

Introduction

In chapter III I described the generation of a panel of envelope clones from a subtype B infected mother-infant cohort. I determined that vertical transmission in my cohort occurred across a selective bottleneck. Such selection is frequently reported, but its genotypic correlates have not been identified. I likewise failed to detect mutations enriched for in the infants compared to their mothers that were not subject specific. I therefore proceeded to investigate the phenotypes of my selected *env* clones in order to identify functional differences between maternal and infant isolates.

I was encouraged in this approach by reports that infant *env* clones are more viable than maternal in competition assays (95), and have been reported as more resistant to neutralization by autologous maternal plasma (39, 204). However, no mechanisms or genetic correlates underlying the enhanced viability of infant clones have been reported, rendering this information of limited utility to informing the design of therapies for preventing transmission. The enhanced resistance of infant clones to neutralization by maternal plasma is due to subject specific mutations, is not seen in every mother-infant pair tested (204), and does not appear to play a selective role during sexual transmission (36), implying that it is not the sole factor controlling selection during mucosal transmission. I therefore investigated the receptor and co-receptor levels required for infection

by my maternal and infant viruses, their ability to replicate in T cells and macrophages, their sensitivity to neutralization by a panel of human monoclonal neutralizing antibodies, pooled heterologous seropositive and autologous maternal plasmas, their sensitivity to inhibition by three HIV-1 entry inhibitors, and their entry kinetics.

Results

Pseudovirus generation

To investigate the phenotypes of the cloned *env* they were expressed on pseudoviruses. These pseudoviral particles have no functional genomic copy of *env*, rendering them capable of only one round of infection. Figure 4.1 provides a graphical overview of the pseudoviral generation process. The pseudoviruses were titered on TZMbl cells (aka JC53BL, Fig 4.2B), a HeLa line expressing HIV-1 Tat inducible β -galactosidase and Luciferase genes. In assays utilizing non-TZMbl HeLa cell lines or primary cells, anti-p24 immunostaining was used as the infectivity readout (Fig 4.2A, Fig 4.3A).

Receptor and co-receptor requirements

The HIV-1 receptor (CD4) and co-receptor (CCR5) requirements of the selected *env* clones were analyzed by titrating pseudoviruses on cell lines expressing varying levels of CD4 and CCR5 (Fig 4.2). All viruses infected each cell line and there was no significant pairwise difference between the infant and maternal titers on any cell line. All clones achieved largest titers on TZMbl cells, which express the highest levels of CD4 and CCR5. Titers decreased with decreasing levels of CD4 or CCR5, but were more sensitive to changes in CD4.

Replication in primary macrophages and PBL

I used two different approaches to evaluate whether macrophage infectivity plays a role in viral variant selection during MTCT. First, I investigated the ability of pseudoviruses expressing the *env* clones to mediate infection of

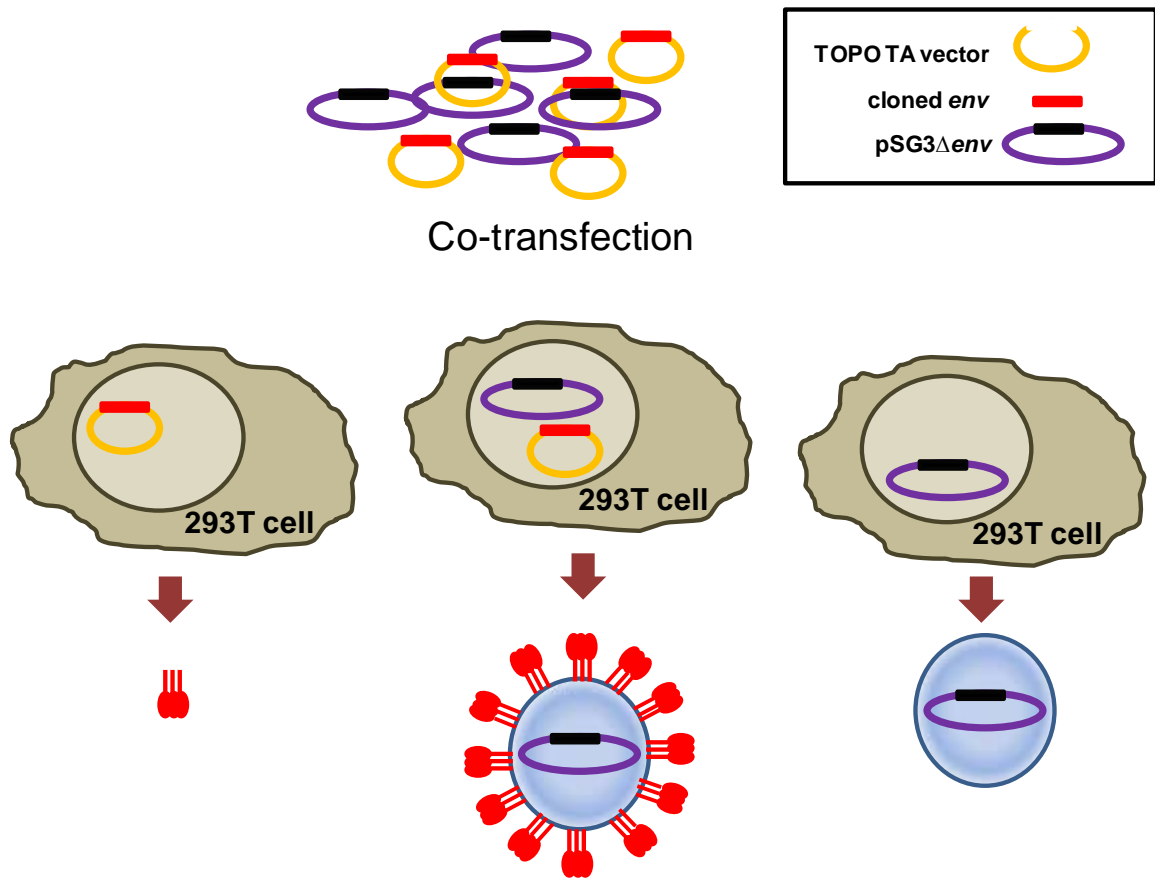


Fig 4.1: Pseudovirus generation. Cloned *env* in a mammalian expression vector lacking an HIV-1 packaging signal and plasmids encoding the full length HIV-1 genome containing a non-functional copy of the *env* gene are co-transfected into 293T cells. Following expression of both plasmids, pseudovirus displaying the cloned *env* and containing no functional genomic copy of *env* are released.

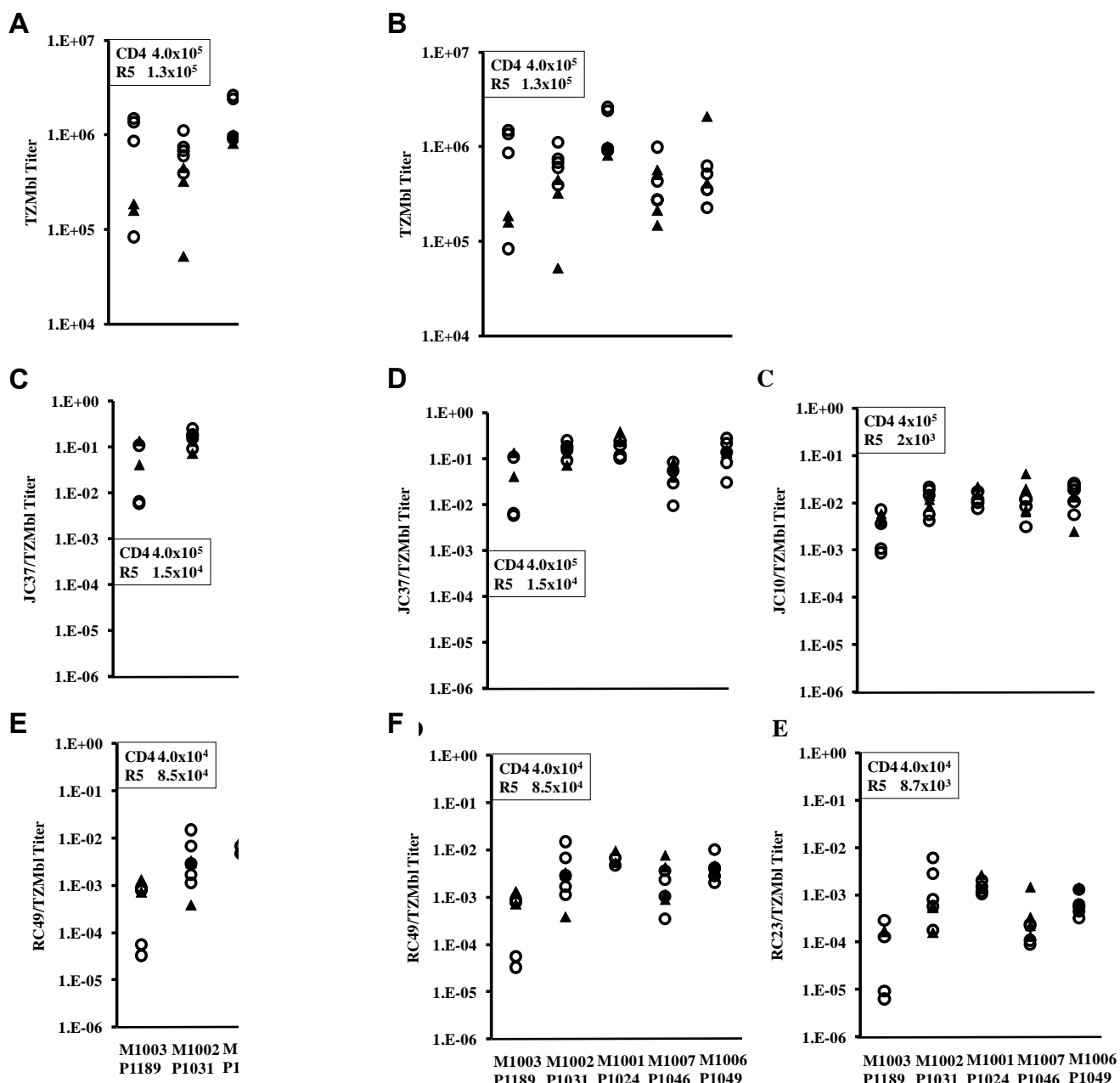


Fig 4.2: Receptor and Pseudoviruses express engineered to express immunostaining of the To normalize between expressed as a ratio o cells. **(B)** TZMbl, **(C)** average of 3 independent number of receptor and co-receptor molecules per cell as reported by Platt et al (150) is inset in the charts. \blacktriangle = infant, \circ = maternal.

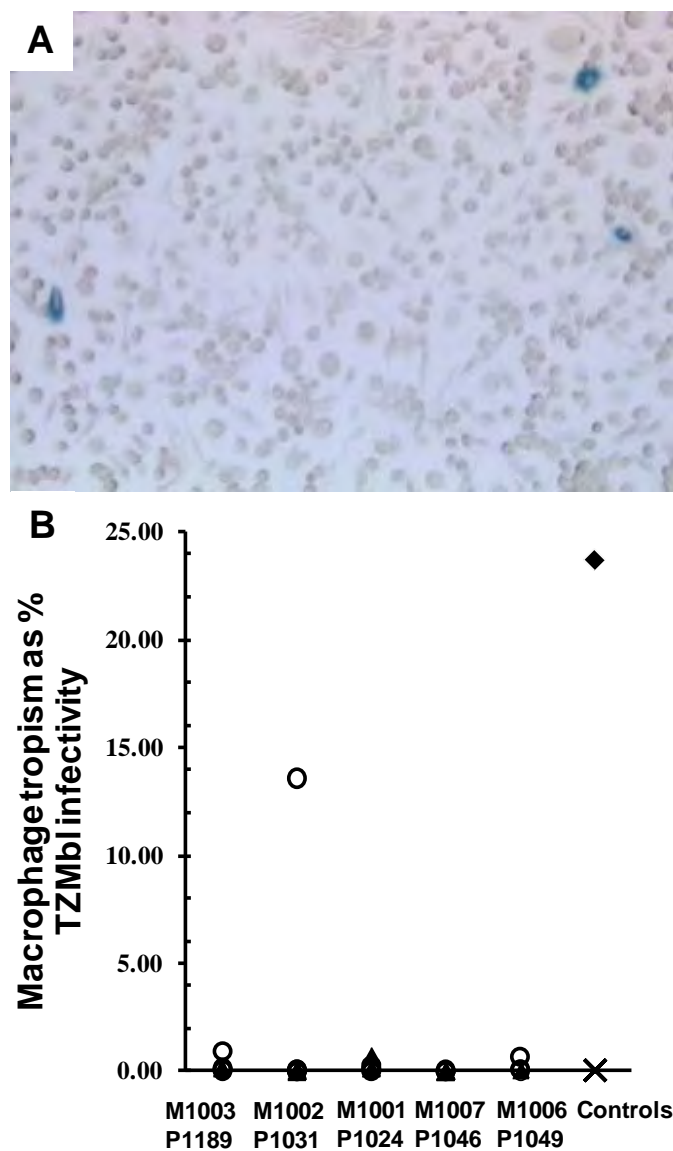


Fig 4.3: Macrophage infectivity. Pseudoviruses expressing cloned *env* were titrated on primary macrophage cultures. **(A)** Anti-p24 immunostaining of infected macrophages. Infected cells appear blue. **(B)** Macrophage infectivity is expressed as the percentage of the TZMbl titer achieved on macrophages. Data is representative of three independent assays performed in duplicate. ▲ = infant, ○ = maternal. Controls: ◆ = JRFL (macrophage tropic), ✕ = JRCSF (non-macrophage tropic).

primary macrophage cultures in a single round infection (Fig 4.3). All infant viruses exhibited low or no infectivity in monocyte derived macrophages (MDM), and only a single maternal clone (M1002 G1) attained a high level of infection as compared to the JRCSF (non-macrophage tropic) and JRFL (macrophage tropic) controls (Fig 4.3B).

Macrophage infectivity was further investigated by infecting matched donor MDM and peripheral blood lymphocytes (PBL) with green fluorescent protein tagged recombinant *env* clones from two randomly selected mother-infant pairs. No fluorescence was detected in macrophage cultures throughout two weeks of infection while high levels of fluorescence were detected in each PBL infection (Table 4.1). Measurement of HIV-1 p24 in the supernatants collected from cultures over the course of infection showed a steady decline from the input levels of p24 in macrophage infections, while PBL infections showed an increase (Table 4.1). Altogether, these data demonstrate robust replication in PBL but uniformly poor replication in macrophages.

Adaptation of neutralization assays to utilize β -galactosidase as the readout

The TZMbl cell line used in standardized neutralization assays (109, 110, 117, 128, 176) contains β -galactosidase and Luciferase readout genes. The β -galactosidase readout is typically used when viral stocks are titered, with infected cells counted manually through a microscope. Using this method allows direct visualization of infected cells rather than detecting RLUs in the supernatant of a

Table 4.1: Maternal and infant viruses replicate well in PBL but poorly in MDM

Clone ID	Fluorescence ^a		p24 ELISA					
	MDM	PBL	MDM			PBL		
			Increase ^b	Day 3 ^c	Day 6 ^c	Increase ^b	Day 3 ^c	Day 6 ^c
M1003 P16	+/-	++	No	172	89	Yes	1,295	5,397
M1003 D6	+/-	+	No	109	44	Yes	1,510	3,057
M1003 O1	+/-	+++	No	200	187	Yes	6,978	30,000
M1003 Q4	+/-	+	No	200	105	Yes	4,627	22,105
P1189 F3	+/-	+	No	200	178	No	4,395	3,511
M1007 Z8	+/-	+	No	3	4	Yes	309	1,114
M1007 Q8	+/-	+	No	0	0	Yes	246	1,991
M1007 Y7	+/-	+	No	3	0	Yes	460	2,269
P1046 W2	+/-	++	No	2	0	Yes	417	6,744
P1046 C4	+/-	+	No	17	5	Yes	655	1,302
P1046 J1	+/-	++	No	14	0	Yes	593	2,495
P1046 K1	+/-	+	No	11	0	Yes	586	1,325

^aQualitative readout: +/- = background fluorescence levels similar to that in a mock-infected cultures, +++ = fluorescence levels similar to those in cultures infected with the TN6GΔ (NL4.3 delta nef EGFP) positive control, ++ = fluorescence levels approximately 50% of that in positive control cultures, + = fluorescence levels approximately 25% of that in positive control cultures. ^bIncrease in p24 antigen levels above input over the course of the experiment. ^cp24 in pg/ml on days 3 and 6 post-infection. Infections with clones from the M1003-P1189 transmission pair (above dashed line) were carried out at an MIO of 0.01, while those from the transmission pair M1007-P1046 (below dashed line) were done at an MOI of 0.001.

lysed monolayer. The β -galactosidase readout leaves the TZMbl monolayers intact making trouble shooting easier, and allows long-term storage and re-reading of plates. X-gal and yellow PBS (which comprise the β -galactosidase substrate) are also significantly less expensive than luminometer substrates. These reasons make the β -galactosidase readout an attractive alternative to Luciferase in standardized neutralization assays, but manually counting infected cells in hundreds of wells is not feasible. I determined that following development with β -galactosidase, the infected cells can be detected and accurately counted using an automated ELISOPT reader (Fig 4.4). In several side-by-side neutralization assays I found the IC_{50} values obtained utilizing the Luciferase readout were similar to those determined when using β -galactosidase (Fig 4.4C). The difference in IC_{50} between the two readouts was of the same magnitude as that between repeat assays using the same readout out.

Sensitivity of envelope clones to neutralization by monoclonal antibodies

Using the β -galactosidase readout, I tested the neutralization sensitivity profile of my pseudoviruses to a panel of well-established human monoclonal NAbs to determine the frequency of resistance conferring mutations in naïve subjects. The NAbs tested were b12 (CD4 binding site), 2G12 (carbohydrate-dependent) and the gp41 Membrane Proximal External Repeat (MPER) specific NAbs 2F5 and 4E10. Figure 1.3A shows the locations of the binding sites of these antibodies on the *env* spike.

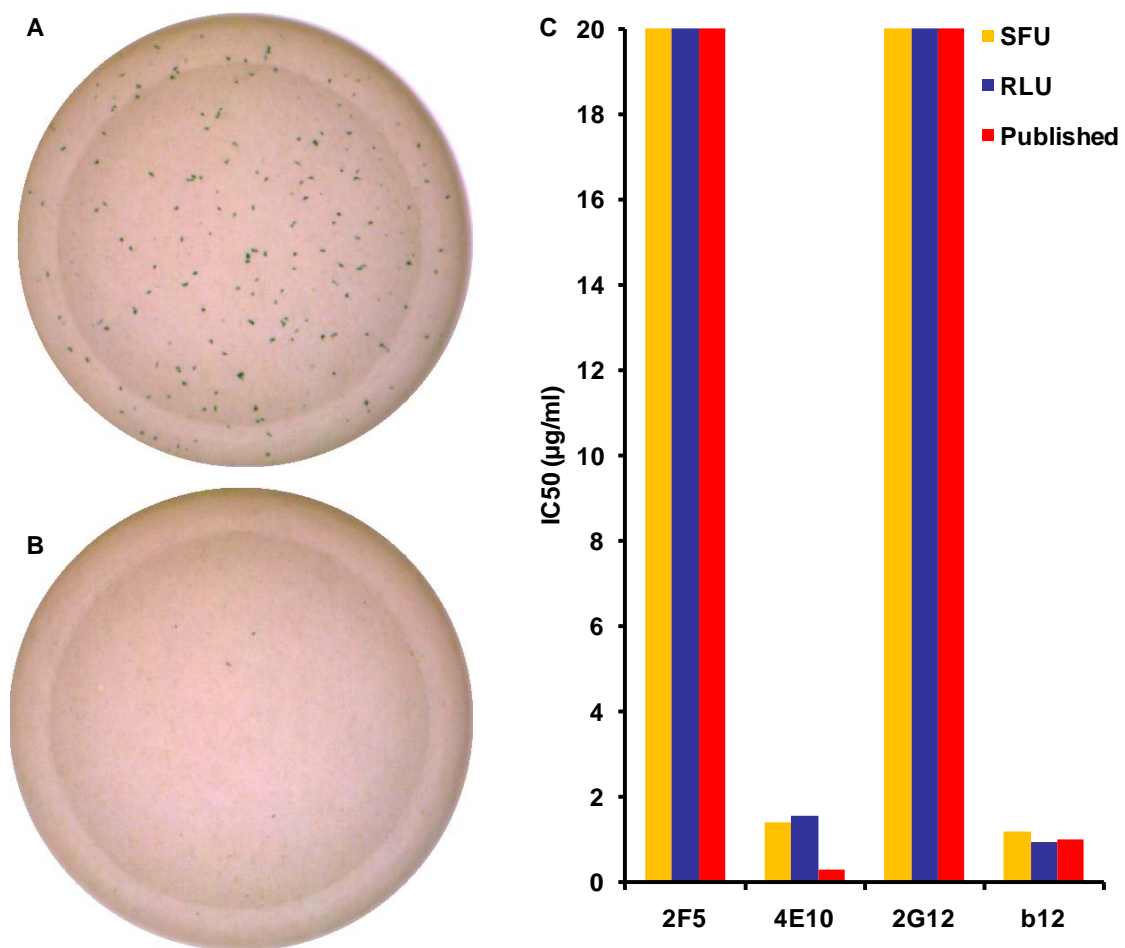


Fig 4.4: Use of β -galactosidase readout for neutralization assays. **(A)** Representative picture of an infected and **(B)** mock infected TZMbl monolayer obtained by an automated ELISPOT reader. **(C)** Comparison of neutralization readouts. The sensitivity of a pseudovirus expressing the SVPC3 *env* clone to neutralization by four broadly neutralizing monoclonal antibodies was determined using both readouts. The IC₅₀ reported by Li et al (109) for this clone is included for comparison.

No infant or maternal clone was resistant to 2F5 (Fig 4.5A). The only clone resistant to 4E10 (P1046 J1, Fig 4.5A) exhibited the rare, natural polymorphism, F673L, associated with resistance (63, 133). All clones from three of five infants were resistant to 20 μ g of 2G12 (Fig 4.5A) and exhibited mutations eliminating one of 5 PNGS implicated in 2G12 binding (170). In infant P1024, the mutation was N386D, in P1049 it was N392K, and in P1046 it was T292I. Most maternal clones from these pairs exhibited similar levels of 2G12 resistance and displayed the corresponding mutations. Infants P1031, P1046, and P1049 had some clones resistant to 20 μ g of 2G12, but each had one sensitive clone (Fig 4.5A). A similar pattern of sensitive and resistant clones was seen in the corresponding mothers. When pairwise analyses were performed, I did not detect any trends for differential neutralization sensitivity between infant and maternal variants.

Sensitivity of envelope clones to neutralization by pooled seropositive plasma

The neutralization sensitivity profile of the pseudoviruses to pooled heterologous plasma with high NAb activity was next determined (Fig 4.5B). Sensitivity varied over a 4-fold range within transmission pairs, but all infant and maternal viruses were sensitive to neutralization at plasma reciprocal dilutions ranging from 109 to 1588. When a pairwise analysis was performed, no trends for differential neutralization sensitivity between infant and maternal variants were detected across the five pairs.

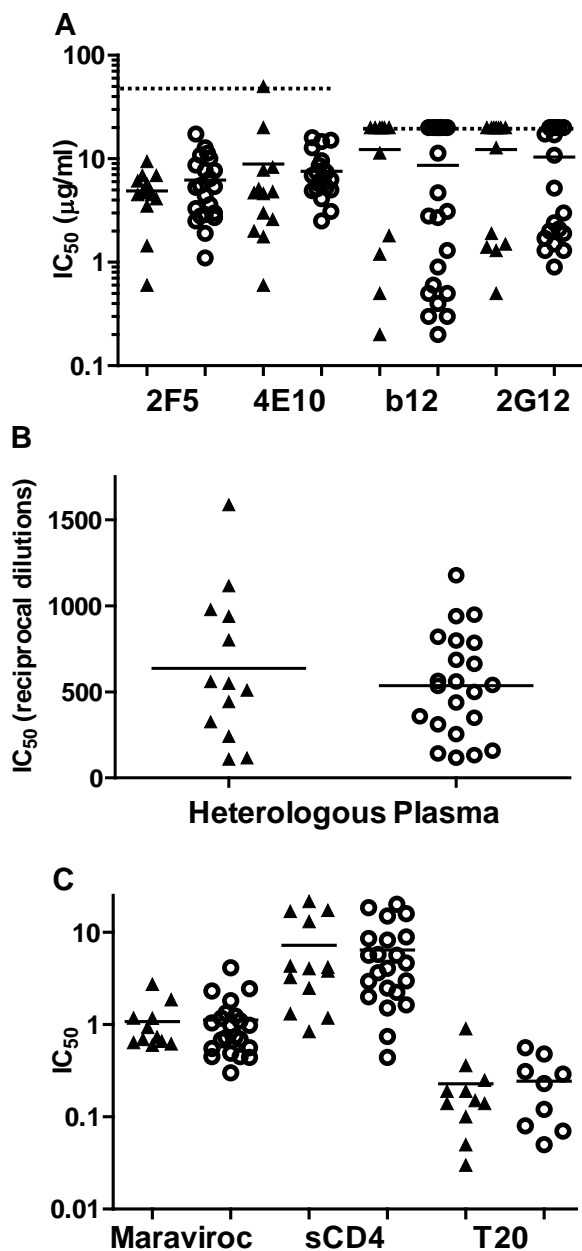


Fig 4.5: Infant and maternal *env* are similarly sensitive to neutralization and inhibition. Sensitivity of infant and maternal clones to **(A)** NABs, **(B)** pooled seropositive plasma, **(C)** entry inhibitors was determined using 200 sfu of pseudovirus to infect TZMbl cells. Values are an average of two different pseudovirus stocks run in triplicate in the same experiment. Dotted lines in **(A)** indicate maximum concentration of NAb used. Solid lines indicate infant and maternal means. Maraviroc IC_{50} is in ng/ml, sCD4 in $\mu\text{g/ml}$ and T20 in $\mu\text{g/ml}$. \blacktriangle = infant, \bigcirc = maternal.

Sensitivity of infant envelope clones to entry inhibitors

The sensitivity of infant clones to three HIV-1 entry inhibitors was evaluated (Fig 4.5C). The inhibitors used were sCD4, T20 (fusion inhibitor) and Maraviroc (CCR5 antagonist). The stages of entry at which these inhibitors act are indicated in Figure 1.3B. No clone was resistant to any inhibitor and infant *env* exhibited IC₅₀ ranges similar to the maternal. No significant within-pair differences in sensitivity to these inhibitors were observed between maternal and infant viruses.

Sensitivity of envelope clones to neutralization by autologous IgG

Preliminary experiments indicated that maternal plasmas exhibited high levels of non-specific activity. Therefore, I used purified IgG in autologous neutralization assays. None of the purified IgG showed non-specific activity against the MLV control. The sensitivity of at least three clones, including an infant and a maternal, to neutralization by autologous maternal IgG was determined for each transmission pair. Maternal IgGs achieved an IC₅₀ of 0.5mg/ml or less against 5 of 7 infant and 5 of 6 maternal clones tested (Fig 4.6). The amount of IgG recovered from plasma of mother M1003 allowed a maximum concentration of only 192µg/ml, but this was sufficient to reach an IC₅₀ against 1 of 2 infant and 1 of 2 maternal clones tested. Statistical analysis did not indicate significant within-pair differences between infant and maternal clones.

Entry kinetics in TZMbl cells

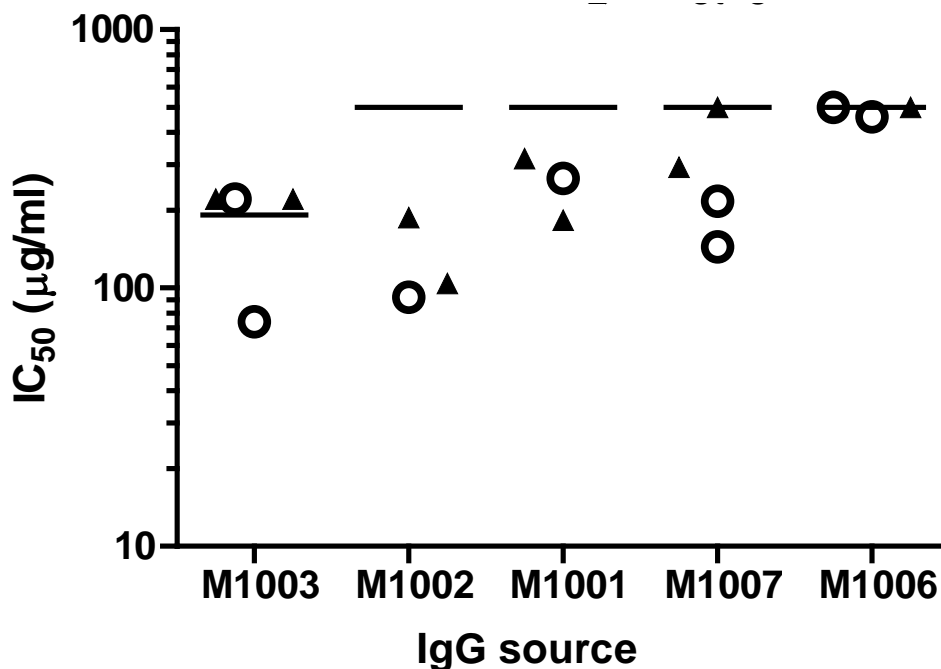


Fig 4.6: No difference in sensitivity to neutralization by autologous maternal IgG between infant and maternal clones. Comparison of neutralization IC_{50} between pseudoviruses expressing *env* clones from infants and mothers within each transmission pair. Infections were carried out in TZMbl cells using 200 sfu as the inoculum dose. Lines indicate maximum concentration of IgG. M1003 plasma achieved an IC_{50} of 221 $\mu\text{g/ml}$ against one of two infant clones tested, just above the 192 $\mu\text{g/ml}$ cutoff. Values are an average of triplicate infections performed in a single assay. Within-pair differences in neutralization sensitivity did not exceed the expected three fold variability of the assay. ▲ = infant, ○ = maternal. All infant clones were assayed except for P1031 where the clone most similar to the consensus of each variant was selected, and P1046 where the clones most similar to, and most distant from, the consensus were chosen. For each mother, the clones most similar to, and most distant from, the infant consensus were assayed. If the amount of IgG was insufficient to assay all clones, the maternal clone most distant from the infant consensus was eliminated.

The entry phenotypes of infant and maternal clones were initially investigated by comparing the differences in titers on TZMbl cells 24 and 48 hours post infection. In 4 of 5 transmission pairs, all infant values were higher than any maternal. In all 5 pairs, the mean infant values were higher than the mean maternal (Fig. 4.7A,B). When pairwise analysis was performed, these differences proved significant ($p < 0.001$). Maternal and infant clones achieved similar titers by 48 hours (Fig. 4.7C) indicating that the observed differences were due to infant clones achieving a greater fraction of their maximum titers by 24 hours rather than to differences between maximum titers.

To further evaluate potential differences in entry phenotype, a 100% inhibitory dose of T20 was added to infected TZMbl cells at various times post infection and the rate of escape from this entry inhibitor determined. When the infant and maternal values were compared within each transmission pair, the infant *env* escaped from inhibition faster than the maternal in 3 of 5 pairs, while in two pairs the rates of escape appeared similar (Fig. 4.8). To analyze T20 escape kinetics, curves characterizing the viral titer as a function of time were developed by fitting second order polynomial regressions using General Linear Mixed Models (121). Pairwise analysis determined that the slopes of infant curves were significantly steeper than the corresponding maternal ($p < 0.001$). Figure 4.8F shows the aggregate infant and maternal curves.

I next investigated if these differences could be replicated in PBL, a physiologically relevant cell type. As these primary cells do not contain readout

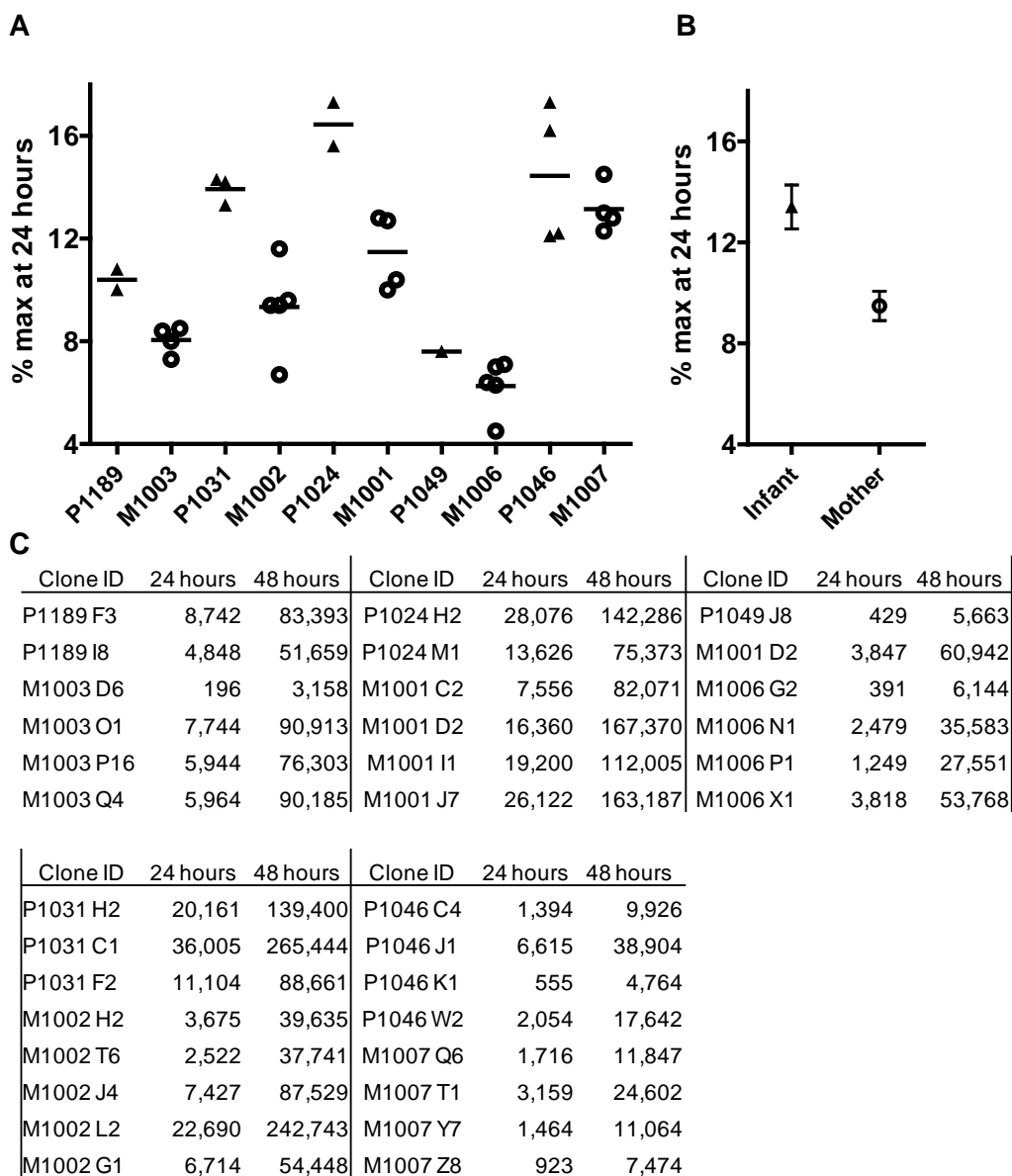


Fig 4.7: Infant *env* clones exhibit more rapid entry than maternal. Pseudovirus titers on TZMbl cells were determined at 24 and 48 hours post infection, and the percent of the max 48 hour titer achieved by 24 hours was plotted. Points are averages from two independent experiments performed in triplicate. **(A)** Data are presented by transmission pair. Solid lines indicate means. **(B)** Aggregate infant and maternal data. Error bars represent one standard error of the mean. **(C)** Average 24 and 48 hour titers in SFU/ml. Mixed Model ANOVA with mother-infant pairing included as a random effect indicated that infant means were significantly higher than the corresponding maternal values ($p < 0.001$). ▲ = infant, ○ = maternal.

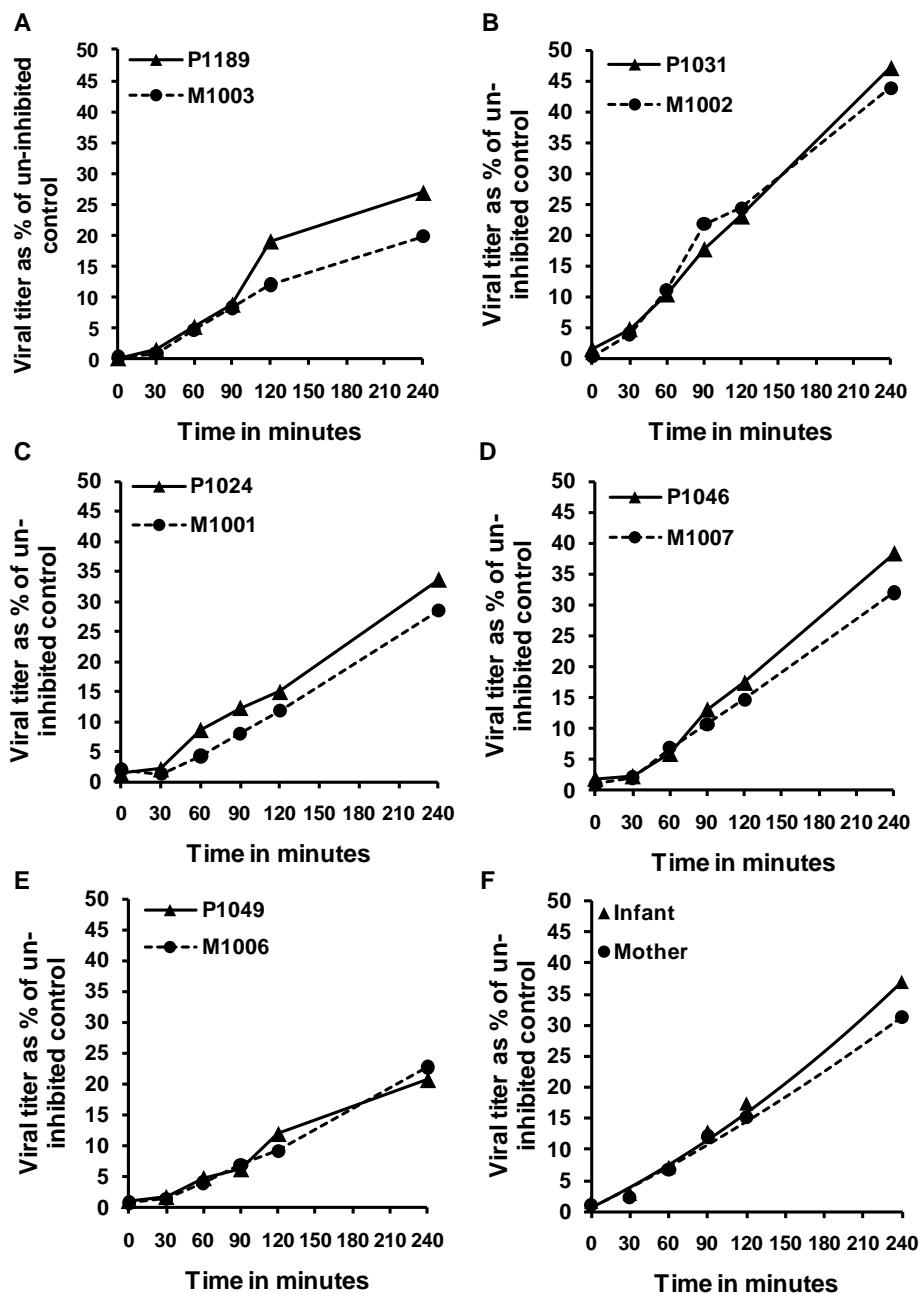


Fig 4.8: Infant *env* clones escape T20 inhibition more rapidly than maternal. Percent of pseudoviruses escaping inhibition by T20 as compared to an un-inhibited control was determined for each time-point for each *env* clone. Infections were carried out in TZMbl cells using 200 sfu as the inoculum dose. (A – E) Mean maternal and infant titers over time plotted by mother-infant pair. All clones were assayed in triplicate in two independent experiments. (F) Infant and maternal kinetic curves were derived using mixed model ANOVA for a polynomial time function with first and second order terms, with mother-infant pairings included as random effects. Infant curves were significantly steeper than the corresponding maternal $p < 0.001$. Plotted are the aggregate infant and maternal curves. ▲ = infant, ● = maternal.

genes, infection was assessed by quantifying a very early HIV-1 reverse transcription product, NSSS, using TaqMan PCR. All infections were performed with the same viral dose. Across all experiments and time-points, on average, cultures infected with infant clones contained more copies of HIV-1 NSSS than those infected with maternal clones (Fig 4.9). Pairwise analysis indicated that in experiments performed on two different donor PBL, from 4 through 8 hours post infection the mean infant signal was significantly higher than the corresponding maternal ($p = 0.046$). Altogether, these data suggest that infant viruses exhibit more rapid entry than maternal.

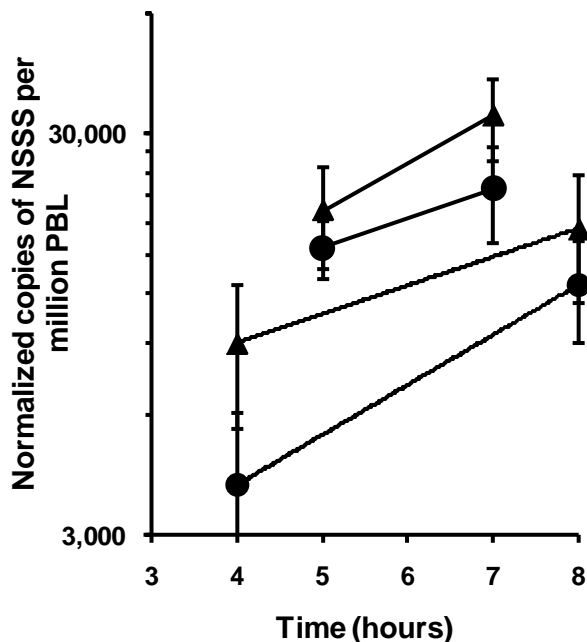


Fig 4.9: Infant *env* clones proceed through reverse transcription faster than maternal. PBL cultures were infected with 100 μ l of media containing 1×10^6 CPM of pseudoviral RT activity, and the number of copies of HIV-1 NSSS in replicate cultures were quantified at several time-points post infection. The copies of NSSS were normalized to the CCR5 housekeeping gene, background from mock-infections was subtracted, and the final value was plotted as copies of NSST per million PBL. Error bars represent one standard error of the mean. Across the four time points examined, mean infant values are significantly higher than maternal ($p = 0.046$). ▲ = infant, ● = maternal. Symbols connected by solid lines represent averages from two independent experiments conducted on the same batch of PBL. Symbols connected by dashed lines represent one experiment conducted on PBLs from a second donor. Clones assayed were selected from mother-infant pairs where transmission occurred in the absence of anti-retroviral therapy (Table 3.1), including all infant clones from P1189 and P1024, and one clone from each variant of P1031 (clones H2 and C1). From each mother, I chose the clones with the fastest and slowest entry (Fig. 4.7). These were M1003 P16 and Q4, M1001 J7 and C2, and M1002 G1 and T6.

Discussion

Efficient HIV-1 infection usually requires the expression of relatively high levels of the CD4 receptor and CCR5 co-receptor on the surface of target cells (3, 151). As the levels of CD4 and CCR5 on mucosal and submucosal cell subsets can be much lower than on CD4⁺ memory T cells (105), the ability of an HIV-1 variant to efficiently infect cells displaying limiting levels of CD4 or CCR5 may be a selective factor in MTCT. Titration on cell lines expressing different levels of CD4 and CCR5 demonstrated the ability of all clones in my panel to infect target cells regardless of the receptor and co-receptor levels displayed. On each cell line tested, maternal and infant clones achieved similar titers both overall and within each transmission pair. Additionally, I did not observe any systematic differences in the sensitivity of maternal and infant *env* to inhibition by sCD4 or the CCR5 binding inhibitor Maraviroc. My findings are consistent with a recent report that sexual transmission of HIV-1 does not appear to select for viruses that can preferentially utilize lower levels of CD4 or CCR5 (3).

CCR5 co-receptor usage has traditionally been equated with macrophage tropism. Peters et al have clarified that not all R5 viruses are macrophage-tropic (147). My data, showing that only 1 of 35 plasma-derived *env* clones achieved greater than 1% of their TZMbl titers on MDM, are in agreement with a study demonstrating that peripheral blood viruses frequently exhibit low levels of macrophage infectivity (148). Inability of all clones tested to replicate in MDM is in agreement with findings that R5 tropic transmitted variants replicate poorly in

macrophages but well in other cell types (80, 169). Finally, these data support recent models which suggest that cell subtypes other than macrophages are the first to encounter HIV-1 during mucosal transmission (34, 169).

The only clone that efficiently infected macrophages, M1002 G1, differs from the rest of the M1002 clones by a 5 amino acid deletion in the V1 loop, which results in the loss of a PNGS, and a T402N substitution which results in the loss of a PNGS in the V4 loop. Loss of PNGS in the V1/V2 and V4 regions of HIV and SIV can enhance macrophage tropism and infection of cells expressing low levels of CD4 (42, 47, 93, 155). In addition to these mutations, M1002 G1 exhibits a further 15 substitutions and four insertions not found in any other *env* selected from this subject. However, none of these mutations occur within CD4 contact residues, the V3 loop, or any other epitope reported to correlate with macrophage tropism.

Enhanced macrophage tropism has been correlated with ability to achieve high titers on CD4 low cell lines such as RC49 (148), and increased sensitivity to reagents that block *env*:CD4 interactions such as sCD4 (146) and b12 (42). My results are in agreement with these findings. Clone M1002 G2 attained the highest titer on the RC49 cell line, was the most sensitive to inhibition by sCD4 and was highly sensitive to neutralization by b12. More efficient CCR5 engagement has also been reported to contribute to enhanced macrophage tropism (60, 65). Compared to other clones, M1002 G2 achieved moderate titers on CCR5 low cells and exhibited average Maraviroc sensitivity. Thus the

enhanced macrophage infectivity of M1002 G2 appears to reflect more efficient utilization of CD4 rather than CCR5.

I adapted the β -galactosidase readout to neutralization assays. Utilizing this method leaves cell monolayers intact and visualizes infected cells directly instead of measuring RLUs in lysed cell supernatant. This facilitates troubleshooting and allows long-term storage and re-reading of plates. X-gal and yellow PBS (the β -galactosidase substrate) are significantly less expensive than luminometer substrates, and the fixed plates can be shipped off-site for counting, circumventing the need to purchase an ELISPOT or Luminescence reader.

I utilized this readout when screening my *env* clones to determine the frequency of resistance to a panel of well-characterized monoclonal NABs. I found that sensitivity to these NABs varied both between and within mother-infant pairs, but the sensitivity of infant clones to neutralization did not appear to correlate with MTCT. Within each transmission pair, the mean infant *env* sensitivity to each NAb generally fell near the center of maternal variation, although this was due both to the transmission of *env* with near mean maternal sensitivity and to the simultaneous transmission of *env* from near both ends of the maternal sensitivity range.

No clone was resistant to 2F5 and only one was resistant to 4E10. Resistance to 50 μ g/ml of 4E10 is very rare across all subtypes of HIV-1 (13), but Aldrovandi and colleagues have detected resistant clones in both mothers and their infants (133). The only clone in my panel resistant to 50 μ g/ml of 4E10 came

from infant P1046 and exhibits the F673L natural polymorphism reported by Aldrovandi and others (63) to provide intrinsic resistance to 4E10. The lack of any clones resistant to 2F5 compares with a large study by Binley et al (13) who found that this NAb neutralized 79% of subtype B isolates. Keele et al (87) has demonstrated significantly higher IC_{50} values for 2F5 and 4E10 among sexually transmitted viruses as compared to the chronic viruses in the donor, although such were not seen by others (164). I did not see such differences in sensitivity to MPER targeted NAb between infant and maternal clones in my panel.

Sequence analysis determined that all instances of increased resistance to 2G12 correlated with loss of one of 5 PNGS that make up the 2G12 epitope. Differences in sensitivity to the monoclonal NAb b12 could not be fully explained by differences in its contact residues (18). However, sensitivity to this NAb correlates with numerous context dependent residues outside the presumed epitope (146). Therefore, uniform genotypic changes were not observed in all clones exhibiting enhanced resistance to b12.

54% and 57% of my *env* clones were neutralized by 20 μ g of 2G12 and b12 respectively, which is slightly less than the 72% of subtype B viruses reported neutralized by these NAb in a study by Binley et al (13). This difference is likely due to the general similarity in neutralization sensitivity of *env* within a transmission pair. Thus instead of screening single clones from each of 32 unrelated subjects, as was done by Binley et al (13), I have only 5 unrelated

clones. With such a small n random variation plays a larger role, making the exact reproduction of results from a much larger cohort unlikely.

I also determined that pooled sero-positive plasma could neutralize all clones to levels at least one (threefold) dilution beyond that of a Murine Leukemia Virus non-specific toxicity control. The sensitivity to heterologous plasma varied both between and within mother-infant pairs, but did not correlate with transmission, implying that infant variants are not inherently resistant to neutralization by heterologous Abs. Infant and maternal clones did not differ significantly in sensitivity to autologous maternal IgG.

The effect of maternal NAbs on MTCT is unclear, with two studies reporting that neutralization escape variants are transmitted (39, 204), while a third found that infant and maternal viruses were similarly sensitive to neutralization by autologous maternal sera (75). Wu et al found that in 9 of 11 transmission pairs infant *env* exhibited lower mean IC_{50} s to their mothers' plasma than the maternal isolates (204), while Dickover et al reported this phenomena in 5 of 7 pairs (39), indicating that infant *env* are not always more resistant than maternal. Further, in both studies, in a number of transmission pairs where lower mean IC_{50} s were reported for infant clones the differences from the maternal mean IC_{50} s were less than three fold. Due to the dilution scheme, my neutralization assay has an inherent 3 fold inter-assay variability, similar to that reported by Binley et al who extensively assessed the reproducibility of this neutralization assay within and between runs (13). As the limiting amounts of

maternal plasma precluded repeat experiments, I may have failed to detect small differences in sensitivity between maternal and infant clones. Together, my results and those reported in the literature indicate that while resistance to maternal NAbs may play a role in viral variant selection during MTCT it is unlikely to be a major selective factor.

CCR5 antagonists are a potent new class of entry inhibitors. As generally only R5 variants are vertically transmitted, CCR5 antagonists may be highly relevant to blocking MTCT; however their effectiveness against infant isolates has not been well characterized. I determined the sensitivity of my infant clones to three entry inhibitors, including the only CCR5 antagonist approved for therapy (Maraviroc). No infant clone was resistant to any inhibitor and I saw no significant differences in sensitivity between maternal and infant *env*. The latter is in contrast to a sexual transmission study by Keele et al (87), who demonstrated significantly higher IC_{50} values for T1249, a fusion inhibitor with a mechanism of action similar to T20, among viruses from acutely infected as compared to chronically infected subjects.

An important finding was that in three different assay systems infant *env* appear to be more efficient in entry than maternal. I developed the first system to rapidly screen pseudoviruses for *env* mediated differences in entry by comparing the fraction of the maximal titer achieved by 24 hours in a single round infection of TZMbl cells. In the second system I compared rates of escape from T20, an inhibitor whose epitope becomes exposed in the final stage of HIV-1 entry.

Experiments in PBL showed that infection with pseudoviruses displaying infant *env* results in a more rapid buildup of an HIV-1 early reverse transcription product.

Escape from membrane impermeable inhibitors of the 6-helix bundle formation such as T20 has previously been interpreted as viral fusion at the plasma membrane (55). It has recently been reported that HIV-1 may enter cells via endocytosis following receptor and co-receptor interactions rather than by fusing at the plasma membrane (30, 125). Virions endocytosed at early stages of entry will escape inhibition by T20. This may explain why the differences between maternal and infant clones observed in the T20 escape experiment, while statistically significant, are less extensive than in those seen in other assays.

My observations of more rapid entry exhibited by infant *env* could reflect differences in viral binding, fusion, or the rate of endocytosis between maternal and infant clones. Studies have reported that chronic and recently transmitted HIV-1 from the same subject (48) and clones from progressors and long-term non-progressors (104) differ in their entry kinetics. It was also reported that the V1-V5 regions of HIV-1 from MTCT viruses confer higher rates of replicative fitness than do maternal *env* (95).

A faster entry phenotype could confer a selective advantage for transmission or early post transmission amplification. Identification of the mechanistic and structural basis of this phenomenon may be useful in the design

of therapies such as targeted vaccines to prevent MTCT. My assays operate across different time windows and may be emphasizing different aspects of entry, making it difficult to directly compare the entry rates of individual *env* clones. Further investigation will be required to identify the stages of entry at which the reported differences occur. It is also important to determine if sexually transmitted viral variants will exhibit a similar enhanced entry phenotype.

In summary, the ability to utilize low receptor and co-receptor levels does not appear to play a major role in the selective bottleneck during vertical transmission of HIV-1 subtype B. Both the maternal and infant viruses infected macrophages poorly. Maternal and infant clones were equally sensitive to four monoclonal NAbs, autologous IgG, and pooled heterologous plasma, implying that inherent neutralization resistance is unlikely to be a major factor controlling the selective bottleneck. All infant clones were sensitive to HIV-1 entry inhibitors, including Maraviroc, in ranges similar to their mothers' suggesting that CCR5 antagonists could be useful additions to the therapies for the prevention of MTCT. Most interestingly, infant clones exhibited faster entry kinetics than maternal clones. Expanding these findings to other cohorts and identifying the mechanistic and structural bases of this phenomenon may be useful in the design of therapies such as targeted vaccines to prevent HIV-1 transmission.

CHAPTER V

Subtype C cohort and genotype analysis

Introduction

In the preceding chapters I investigated the genotypic and phenotypic correlates of viral variant selection during MTCT of HIV-1 subtype B. Historically most infections in Western Europe and North America were with this subtype (74). Therefore, many of the early viral isolates and much of the pathogenesis data were obtained from subjects infected with subtype B. However, worldwide this subtype accounts for approximately 12% of those infected (74). Shortly after the realization that several HIV-1 subtypes exist, it was hypothesized that they may exhibit distinct biological properties. Subsequent investigations have confirmed this, finding inter-subtype differences in transmission rates (14, 161), virulence (9, 85), reverse transcription rates (79), variability at protease cleavage sites (33) and frequency of co-receptor switch over time (23).

It is likely that these differences, together with the up to 35% heterogeneity in genotypes between subtypes (182) will affect vaccine design (59). Historically, subtype B is the best studied and is therefore often used as a model, but may be poorly representative of the pandemic as a whole. For example, in all major non-B subtypes, shorter and less glycosylated *env* are typically passed from the donor to the recipient during mucosal transmission (25, 166, 204), but this correlation is not found during transmission of subtype B (74). It was therefore

important to determine if my novel finding of enhanced entry by infant *env* clones extends to non-B subtypes.

Subtype C is the most rapidly expanding HIV-1 subtype. At least 22 million people are currently infected with this subtype, accounting for almost 60% of all HIV-1 infections (83). Subtype C is most prevalent in Sub-Saharan Africa where the majority of MTCT takes place (83) and thus accounts for the vast majority of new MTCT. I therefore focused on subtype C as the most relevant to further investigation into the correlates of viral variant selection during vertical transmission of HIV-1. To this end, I generated a panel of vertically transmitted and non-transmitted full-length *env* clones from a cohort of subtype C infected mother-infant pairs.

It has been reported that a larger portion of subtype C MTCT may occur *in-utero* than in other subtypes (161). There are indications that viral variant selection during *in-utero* transmission may be influenced by different factors than during *peripartum* transmission (2, 39, 40, 99, 100, 138, 202). I therefore included both *in-utero* and *peripartum* infected infants in my cohort to better represent the routes of transmission leading to the majority of new infant infections.

I generated 126 full-length, viable *env* clones from five subtype C infected mother-infant pairs. Examination of the *env* genotypes confirmed the presence of a selective bottleneck during both *in-utero* and *peripartum* transmission. In contrast to the subtype B findings, I determined infant variants were shorter and

less glycosylated than maternal. I then utilized extensive phylogeny analysis to select a subset of representative *env* clones for in-depth phenotype analysis.

Results

Phylogeny of envelope sequences

Following the scheme developed during clade B panel generation (Fig 3.1) full length *env* genes were amplified from HIV-1 subtype C infected mother and infant pro-viral DNA samples collected within 6 weeks of transmission (Table 5.1). At least seven clones were generated from each subject except CM5. A total of 126 functional clones, 76% of those screened for viability, were obtained. These clones were sequenced from the HXB2 gp160 nucleotide position 31 through 1563. This includes the entire gp120 (with the exception of the N-terminal half of the *env* signal sequence) and the first 30 amino acids of gp41.

These gp120 sequences were aligned and a neighbor-joining tree constructed (Fig 5.1). The tree revealed clear epidemiological linkage within each mother-infant pair, with no evidence of cross-pair or other contamination. Subtype reference sequences included in the tree confirmed that all subjects were infected with subtype C. Maximum likelihood trees and Highlighter alignments of non-gap stripped sequences were used for additional in-depth phylogeny analysis and to select representative clones for phenotype analysis. Utilizing criteria similar to that described for subtype B, two to three *env* clones from each infant and three to four from each mother were selected for in-depth analysis (Table 5.1, Fig 5.1). The exceptions to this were subject CM5 from whom only one sample was successfully amplified, and the pair C4. In this pair all infant *env* and the closely related maternal variants exhibited very low titers

Table 5.1: Subtype C cohort summary

Subject Id ^a	Sample Timing ^b	No. of env clones	No. of pseudo viruses	ART status	Mode of transmission
CM1	0	16	4	SD NVP	<i>In-Utero</i>
CP1	2	7	3	DD NVP	
CM2	0	17	4	SD NVP	<i>In-Utero</i>
CP2	2	11	3	DD NVP	
CM5	0	1	1	SD NVP	<i>Peripartum</i>
CP5	29	12	2	DD NVP	
CM3	0	23	4	SD NVP	<i>Peripartum</i>
CP3	46	11	3	DD NVP	
CM4	0	16	3	SD NVP	<i>Peripartum</i>
CP4	30	12	2	DD NVP	

^aCM, Mother; CP, Infant. ^bDays after delivery.

SD NVP = Single dose nevirapine administered to mother during labor. DD NVP = Nevirapine administered to mothers crossed the placenta and an additional dose was given to the infants in the first day of life.

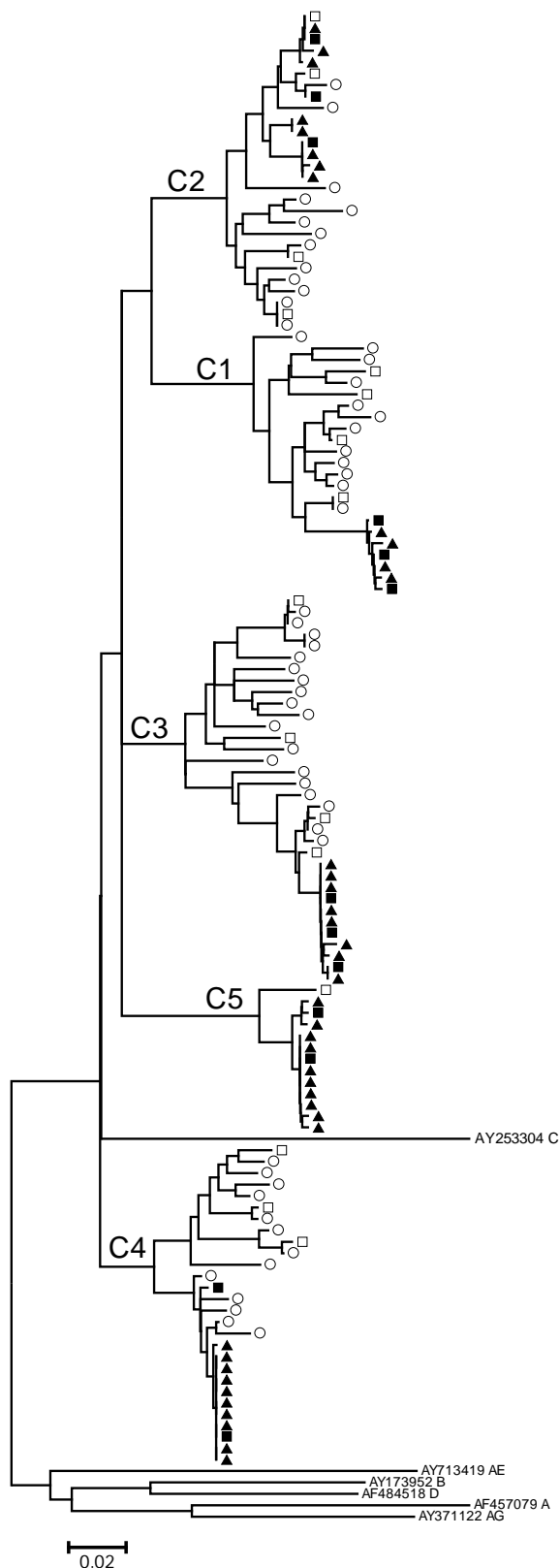


Fig 5.1: Evolutionary relationships of gp120 sequences from *env* clones and subtype reference sequences. Evolutionary history was inferred using the Neighbor-Joining method with 1000 iterations of the bootstrap test. The evolutionary distances were computed using the Kimura 2-parameter method. All positions containing gaps and missing data were eliminated from the dataset. Horizontal scale bar represents 2% genetic distance. Filled symbols represent infant and empty symbols maternal clones. Squares indicate clones selected for further analysis.

when expressed on pseudoviruses, precluding their phenotype analysis.

Therefore three CM4 clones distantly related to infants (Fig 5.1) were used in virological assays. In all 29 clones were selected and sequenced through the entire gp160 (Fig 5.2).

Visual inspection of phylogenetic trees and Highlighter alignments of each mother-infant pair demonstrated probable transmission of a single maternal variant to infants CP1 and CP3, two variants to infants CP5 and CP4, and four to infant CP2. The relationship between maternal and infant gp120 sequences was further analyzed based on the paradigm described by Haaland et al (67) (Table 5.2). A maternal sequence differing from an infant variant by less than five amino acids in the gp120 likely gave rise to that variant. If such sequences represent less than 5% of the maternal quasispecies, a minor maternal variant was likely transmitted to the infant (67). Infants CP1 and CP3 were apparently infected with a single minor variant of the maternal quasispecies, infant CP4 with two minor variants, and infant CP2 with three minor and one major variant (Table 5.2). Infant CP5 was infected with two maternal variants. As only a single clone was amplified from mother CM5, the maternal quasispecies was not sufficiently sampled for the algorithm to be fully reliable in this case. However, stochastically, the amplified CM5 clone likely represents the most prevalent maternal variant and both CP5 clones differ from this sequence by more than 20 amino acids. Therefore it is likely that CP5 was infected by two minor maternal variants.

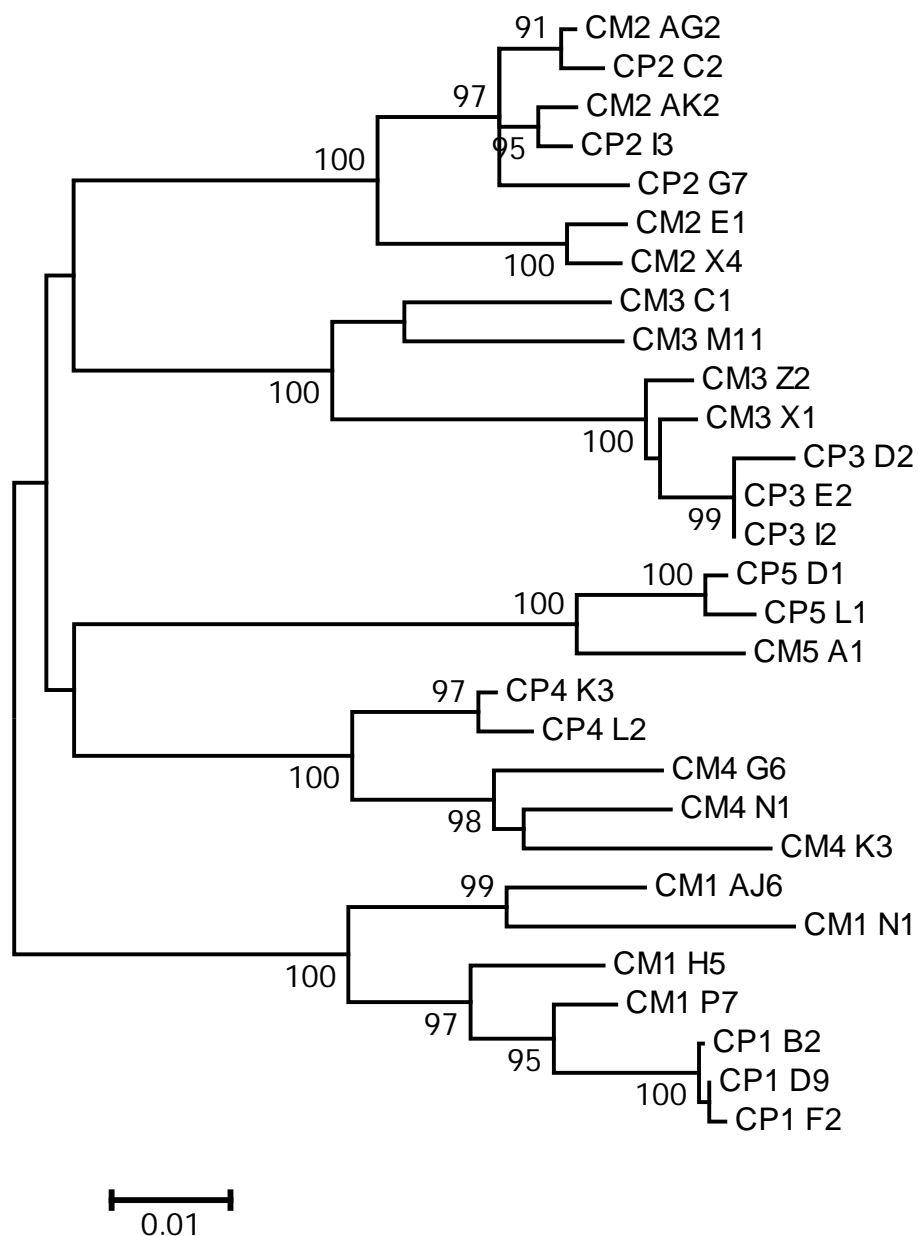


Fig 5.2: Evolutionary relationships of full length HIV-1 gp160 sequences from 29 *env* clones. CM = maternal, CP = infant. Evolutionary history was inferred using the Neighbor-Joining method. The percentage of replicate trees in which the associated sequences clustered together >70% of the time in the bootstrap test (1000 replicates) are shown to the left of branches. The evolutionary distances were computed using the Kimura 2-parameter method. All positions containing gaps and missing data were eliminated from the dataset. The horizontal scale bar represents 1% genetic distance.

Table 5.2: Relationship of maternal and infant gp120 sequences

Infant	Sequences analyzed ^a	Differences ^b	Less than 5 differences ^c	Variant transmitted
CP1	16	>20	0	Minor
CP2	17	15	0	Minor
		0	1	Major
		11	0	Minor
		>20	0	Minor
CP5	1 ^d	>20	0	Minor
		>20	0	Minor
CP3	23	12	0	Minor
CP4	16	7	0	Minor
		12	0	Minor

^aNumber of maternal sequences analyzed. ^bNumber of amino acids that differ between an infant variant consensus sequence and the most closely related maternal sequence.

^cNumber of maternal sequences differing from the infant variant consensus by less than 5 amino acids. ^dOnly a single maternal variant was amplified from CM5.

Infant sequences were more homogeneous than maternal, with the mean diversity in gp120, measured by number of base substitutions per site within each subject, ranging from 0.3-1.7% among *in-utero* infected infants, 0.1-0.4% among *peripartum* infected infants, and 3.5-6.1% among mothers (Fig 5.3). Detailed examination of the infant showing 1.7% sequence diversity (CP2) indicated that its quasispecies was composed of four distinct variants (Fig 5.4A). Diversification within each infant variant was minimal, there was little evidence of recombination between variants and two variants clustered with maternal sequences in a phylogenetic tree (Fig 5.4B). Taken together, these data imply that the infant variants likely arose from the transmission of four distinct maternal variants rather than post-transmission diversification.

I attempted to determine which of the selected maternal viruses could have been transmitted to their infants by comparing the full length maternal gp160 sequences to the consensus sequence of each of their infant's variants. As the most closely related maternal sequences differed from their infants' consensus by at least 10 amino acids, I deemed that none of the selected maternal clones were likely to have been the direct ancestors of the infant variants. These findings are graphically summarized in the gp160 tree (Fig 5.2) where except for the *in-utero* transmission pair C2 all maternal sequences cluster in branches distinct from their infants with bootstrap values > 90%.

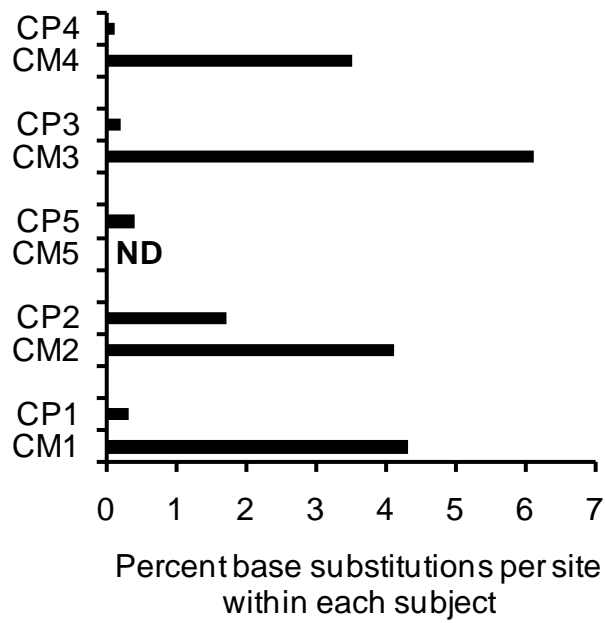


Fig 5.3: Infant quasispecies are more homogeneous than maternal. The percent of base substitutions per site over the gp120 region for each subject were computed using the Kimura 2-parameter method in the MEGA4 software program. ND = not determined.

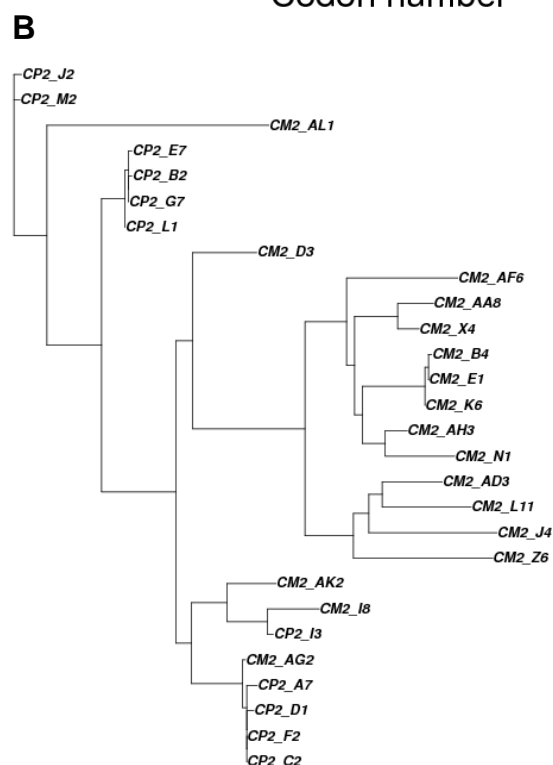
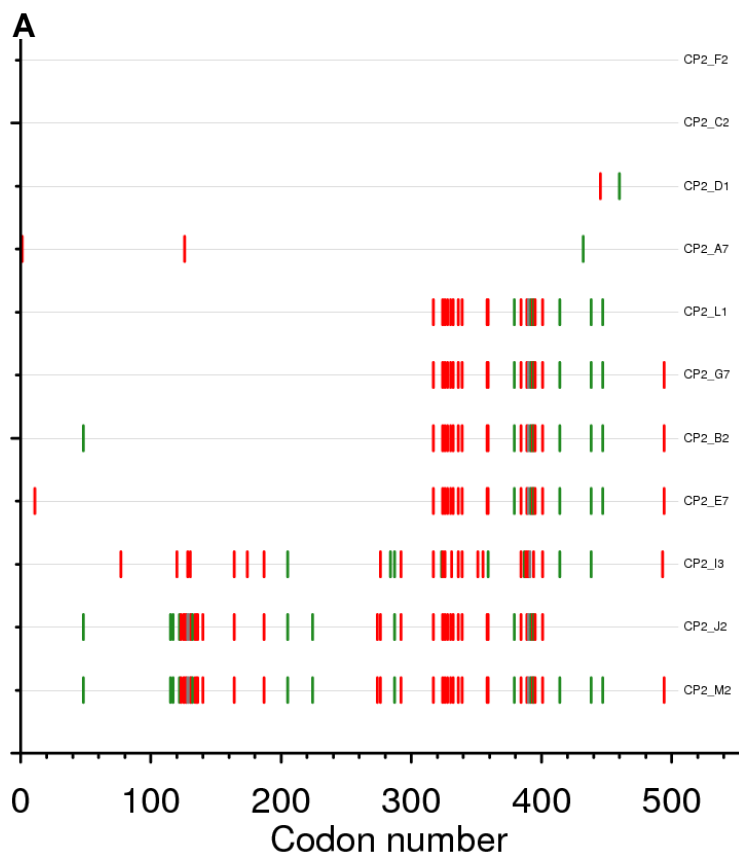


Fig 5.4: Subject CP2 quasispecies consists of four variants. **(A)** Highlighter analysis of infant CP2 gp120. Green bars represent silent and red bars non-silent mutations. Gray bars represent deletions. **(B)** Maximum likelihood tree of all gp120 sequences amplified from the C2 transmission pair.

gp120 length and glycosylation

Changes in *env* length and glycosylation have been reported to correlate with mucosal transmission of HIV-1 (25, 166), including MTCT (204). Shorter *env* that display fewer PNGS appear to be enriched during transmission non-B subtypes. I investigated this correlation in my panel and found that in four mother-infant pairs the infant *env* were both shorter and less glycosylated than the maternal (Fig 5.5). When pairwise comparisons of infant and maternal values were made, these differences proved significant across all pairs ($p < 0.001$). Pair C5 was excluded from the analysis because the single *env* clone amplified from CM5 did not provide sufficient information on the diversity of the maternal quasispecies.

Co-receptor tropism

I established the probable co-receptor usage of the 126 *env* clones *in-silico* by examining the V3 loop charge (12), glycosylation (27) and crown motif (44) (Table 5.3). Charge analysis indicated that 5 of 16 clones from subject CM1 were dual-tropic. However the V3 loops of all these clones exhibited a PNGS in a position that correlates with CCR5 usage (27) and the V3 loop crown motif change from GPGQ to GPGR, which is associated with a shift to X4 tropism (44), was not present in any clone. When tested *in-vitro* no clone from this or any subject exhibited significant utilization of X4 (Table 5.3). Thus all clones in the panel exclusively utilized the CCR5 co-receptor.

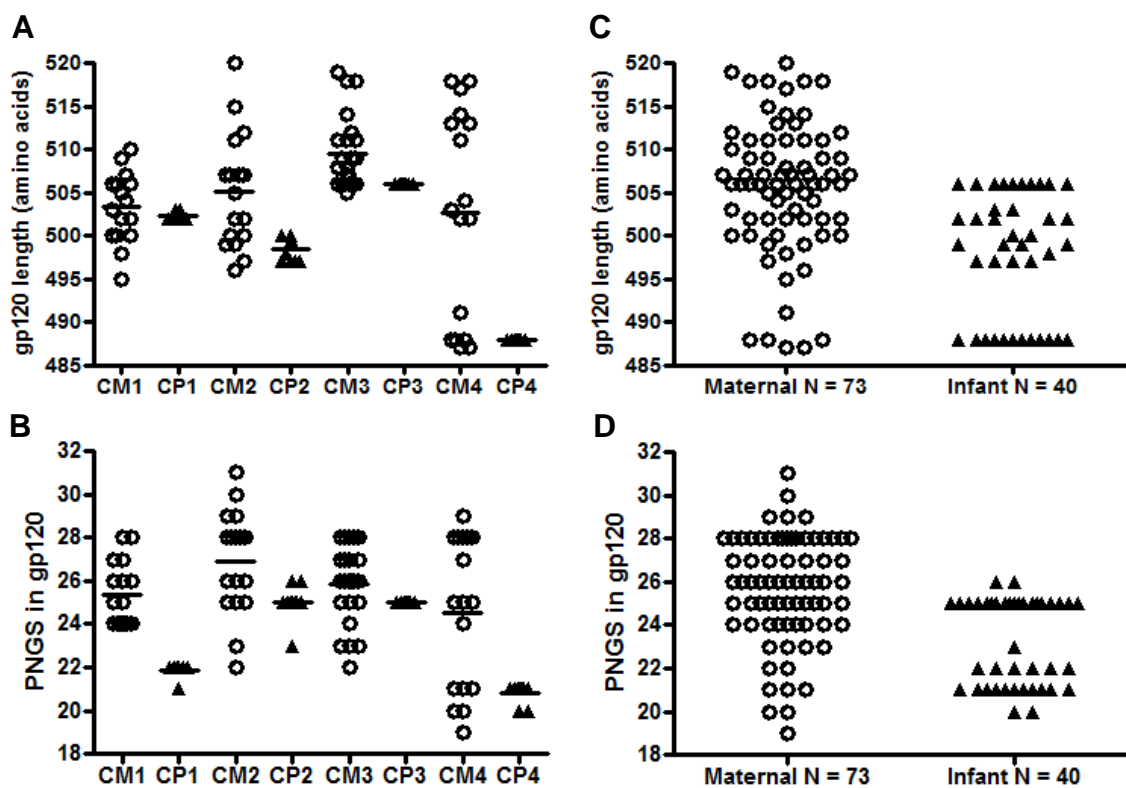


Fig 5.5: Infant *env* are shorter and less glycosylated than maternal clones. **(A)** Length of and **(B)** PNGS in, the gp120 regions of *env* quasispecies in each subject. Horizontal lines indicate mean values within each subject. **(C)** Comparison of aggregate length and **(D)** PNGS, in maternal and infant sequences. Mixed Model ANOVA with mother-infant pairings included as random effects determined that infant clones are shorter and exhibit fewer PNGS than corresponding maternal *env* $p < 0.001$.

Table 5.3: Co-receptor tropism

Subject ID ^a	V3 charge	V3 glycan	V3 crown motif ^b	<i>In-vitro</i> tropism
CM1	+3,+4,+5	Yes	GPGQ	CCR5
CP1	+4	Yes	GPGQ	CCR5
CM2	+3,+4,+5	Yes	GPGQ	CCR5
CP2	+4,+5	Yes	GPGQ	CCR5
CM5	+4	Yes	GPGQ	CCR5
CP5	+4	Yes	GPGQ	CCR5
CM3	+3	Yes	GPGQ	CCR5
CP3	+3	Yes	GPGQ, GLGQ	CCR5
CM4	+3	Yes	GPGQ	CCR5
CM4	+3	Yes	GPGQ	CCR5

^aM, Mother; P, Infant. ^bDominant variant presented first.

Discussion

In this chapter I increased my *env* panel by 126 subtype C clones and confirmed that viral variant selection during MTCT is not random or stochastic, but is driven by viral envelope properties during transmission of the subtype currently responsible for the vast majority of MTCT. The *env* were amplified from pro-viral DNA; as the infants were sampled very shortly post infection, it is likely that the amplified *env* are similar to those found in plasma. Phylogenetic analyses showed that infant *env* sequences were more homogeneous than maternal. The highest sequence diversity seen among four of five infants was 0.4%, which fits well with the expected maximum diversity of 0.6% within an individual shortly after infection with a single virus (87). An *in-utero* infected infant (CP2) exhibited 1.7% diversity which, although still much lower than that exhibited by the corresponding mother, falls beyond the range predicted by the model. However, transmission of multiple variants is more common during *in-utero* MTCT than other forms of mucosal HIV-1 transmission (40, 160). A detailed examination of CP2's quasispecies identified four distinct viral variants. Very little diversification was observed within each variant, there was little evidence of recombination between the variants and two variants clearly had maternal ancestors. This pattern best fits a model of very recent infection with four maternal variants rather than post transmission diversification. This finding is consistent with reports that the majority of *in-utero* transmission occurs very

late in gestation (51, 100) and often results in transmission of multiple maternal variants (40).

Based on the examination of gp120 sequences, of the four variants transmitted to CP2, only one was closely related to a maternal variant. Between them, the remaining four infants in this cohort were infected with a total of six maternal viruses. As the consensus of each of the infant variants differed by at least 7 amino acids from the most closely related sequence amplified from the mothers, the transmitted viruses represent a small fraction of the maternal quasispecies. Together these data support previous findings suggesting a selective bottleneck during MTCT (92, 202), including during *in-utero* transmission (40).

My data show that, unlike the case with the subtype B infected cohort, *env* cloned from infants infected with subtype C are significantly shorter and less glycosylated than the corresponding maternal quasispecies. These results are in agreement with previous reports on subtype C sexual (38) and vertical (207) transmission, and similar patterns are seen during mucosal transmission of other non-B subtypes (25, 166, 204). While the mechanisms underlying this selection are currently unknown, their apparent absence during subtype B transmission implies they are likely not the major factor influencing viral variant selection during MTCT.

When I examined the co-receptor tropism of my *env* clones I determined that all of them were CCR5 tropic, which is consistent with the near exclusive use

of CCR5 by recently mucosally transmitted viruses regardless of subtype (8, 35, 174). The absence of CXCR4 or dual tropic viruses among the mothers is consistent with the co-receptor switch being significantly rarer among subtype C viruses than is the case with other subtypes (23).

Having extensively characterized the genotypes and phylogeny of my subtype C *env*, I selected 29 representative clones for use in virologic assays to determine if the characteristics of infant *env* I reported for subtype B are present in the non-B subtype responsible for the majority mucosal transmission.

CHAPTER VI

Subtype C phenotype analysis

Introduction

In chapter IV I characterized a panel of subtype B *env* clones generated from a paired mother-infant cohort. I observed that infant variants appeared to exhibit a more rapid entry phenotype than the corresponding maternal clones. Two limitations to this novel finding were the small size of the cohort, and that all subjects were infected with subtype B. In addition to extensive sequence heterogeneity, numerous biological differences have been reported between HIV-1 subtypes (9, 14, 23, 33, 79, 85, 161). Therefore, care must be taken when extrapolating findings based on a single subtype to the pandemic as a whole.

As it is primarily found in the developed countries of Western Europe and North America, subtype B MTCT has become very rare. Conversely, while subtype C is most prevalent worldwide, it is primarily found in developing countries of sub-Saharan Africa and is responsible for the majority of MTCT. Therefore, I added this highly relevant subtype in my MTCT cohort. In chapter V I described the generation of the subtype C *env* panel, the analyses I performed to confirm that the infant clones were transmitted across a selective bottleneck, and how I selected 29 representative clones to use in virologic assays.

In this chapter I report the results of the functional analyses. Maternal and infant clones were similarly sensitive to neutralization with heterologous Abs and inhibition with HIV-1 entry inhibitors. However all were resistant to two

monoclonal NAbs that potently neutralized subtype B clones. Most interestingly, I found that the enhanced entry phenotype exhibited by *env* cloned from subtype B *intra-partum* infected infants was also shown by clones obtained from subtype C *peripartum* infected infants.

Results

Sensitivity of *env* to neutralization by monoclonal antibodies

Pseudoviruses expressing the selected *env* were generated and titrated as described in chapter IV (Fig 4.1 and 4.4). Using a standardized assay (117, 128), I tested the neutralization sensitivity profile of my pseudoviruses to a panel of well-characterized human monoclonal NAb to determine the frequency of resistance in naïve subjects. The NAb tested were b12, 2G12, 2F5 and 4E10 (binding epitopes for the four NAb are shown in Fig 1.3A). Due to their low titer, clones from infant CP2 were not used in these assays. The corresponding maternal clones were used only to estimate the variability of the data and are not included in Figures 6.1 – 6.3. All clones (including those from CM2) proved resistant to 20µg/ml of 2F5 and 2G12, while most were also resistant to 20µg/ml of b12 (Fig 6.1). All clones were sensitive to 4E10, with maternal and infant clones in each pair exhibiting similar mean IC₅₀, although maternal IC₅₀ values spanned a greater range.

The PNGS most important for 2G12 binding to subtype B *env* are 295, 332, 339 and 392, with those at 386 and 448 playing an indirect role (170). Most of my clones lacked a PNGS at 295, 332, 392 or a combination of these sites, while several also lacked a site at 386, 339, or 448, consistent with their resistance to this Nab. However, the maternal clone CM1 H5 and all three clones selected from infant CP1 displayed all six of these PNGS but were nevertheless insensitive to 20µg/ml of 2G12. Further analysis determined that all

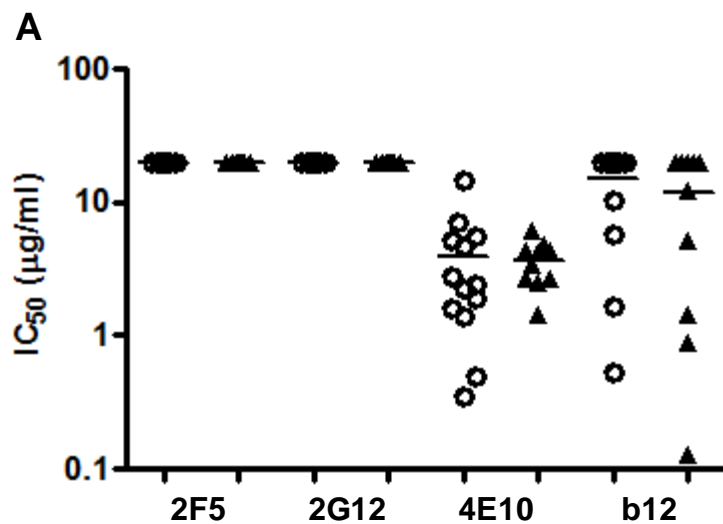


Fig 6.1: Infant and maternal *env* are similarly sensitive to 20 µg/ml of monoclonal neutralizing Abs. 200 sfu of pseudoviruses expressing the cloned *env* were used to infect TZMbl cells in the presence of the indicated inhibitors. Values are an average of triplicate infections performed in a single same experiment. Lines indicate infant and maternal means. ▲ = infant, ○ = maternal.

four clones lacked a PNGS at 442 which is suggested to be part of the 2G12 epitope in subtype C, but not subtype B *env* (64).

The 2F5 epitope is ELDKWA (132), with DKW thought to be the critical recognition determinant (13, 62, 211). The resistance of subtype C viruses to the NAb 2F5 is thought to be due primarily to the substitution K665S in the middle of DKW (13, 62). All clones from four of my mother-infant pairs displayed this substitution, while the transmission pair C2 exhibited the DKW motif. However the full 2F5 epitope sequence in all clones from this pair was ALDKWK explaining their loss of sensitivity.

Sensitivity of *env* clones to pooled seropositive plasma

The neutralization sensitivity profile of the pseudoviruses to pooled heterologous plasma from subtype B infected subjects with high NAb activity was next determined. In 3 of 4 pairs, the mean infant IC₅₀ values in plasma reciprocal dilutions were lower than the corresponding maternal, indicating greater resistance (Fig 6.2). In pair C5, the infant and maternal means were similar, but considering the range of maternal values in other pairs, the single CM5 clone may be poorly representative of this subject's quasispecies. Pairwise differences between infant and maternal clones were not significant ($p = 0.068$).

Sensitivity of *env* clones to HIV-1 entry inhibitors

The sensitivity of the clone panel to three HIV-1 entry inhibitors was next evaluated. The inhibitors used were sCD4, T20 and Maraviroc (the steps of

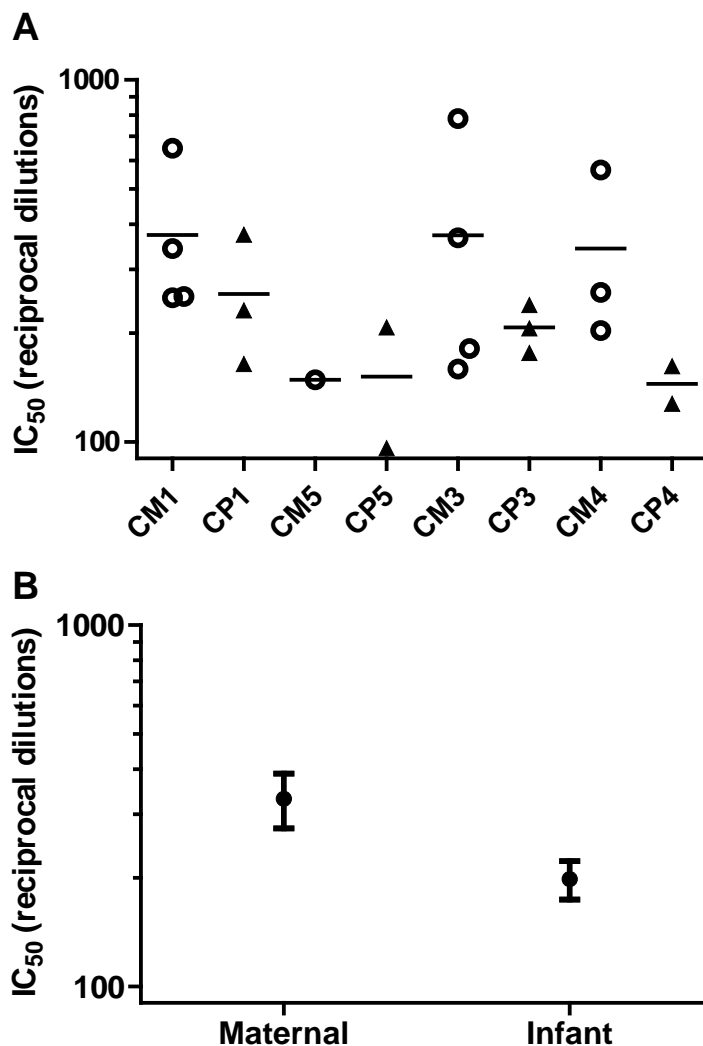


Fig 6.2: Infant *env* may be slightly more resistant to neutralization by pooled seropositive plasma than corresponding maternal clones. **(A)** Data presented by transmission pair. Values are an average of triplicate infections run in the same experiment. 200 sfu of pseudoviruses expressing the cloned *env* were used to infect TZMbl cells. Lines indicate infant and maternal means. ▲ = infant, ○ = maternal. **(B)** Aggregate infant and maternal data. Points indicate means and the error bars represent one standard error of the mean. Mixed Model ANOVA with mother-infant pairing included as a random effect did not detect significant pairwise differences in sensitivity between infant and maternal clones $p = 0.068$.

entry targeted by these inhibitors are summarized in Fig 1.3B). None of the clones proved resistant to any inhibitor. In all 4 pairs examined, the mean infant sensitivity to sCD4 was greater than maternal (Fig 6.3A and B), but these differences did not achieve significance ($p = 0.055$). Infant and maternal T20 IC_{50} values spanned similar ranges, and the mean infant and maternal values did not differ significantly within pairs (Fig 6.3B, $p > 0.1$). Likewise, pairwise differences in infant and maternal sensitivity to Maraviroc did not approach significance (Fig 6.3 B, $p > 0.1$).

Entry kinetics

The entry phenotypes of infant and maternal clones were initially investigated by comparing the percent of the maximum 48 titers achieved on TZMbl cells 48-hours post infection. The titers of all clones from infant CP2 were below the limits of detection of the assay. When pairwise comparisons were made, significant differences in rates of entry between infant and maternal clones were not detected (Fig 6.4A and B). I examined the data further and determined that both infant (Fig 6.4C) and maternal (Fig 6.4D) values appeared to fall into two groups based on the mode of transmission. Clones from *peripartum* infected infants exhibited higher values than any clone transmitted *in-utero*. The mean portion of the maximum titer at 24 hours achieved by *peripartum* transmitted clones was 3.15 fold higher than the mean of *in-utero* transmitted clones, and this difference was significant ($p = 0.0021$). A similar pattern held for maternal clones, with the mean percent of maximum titer achieved by 24 hours by

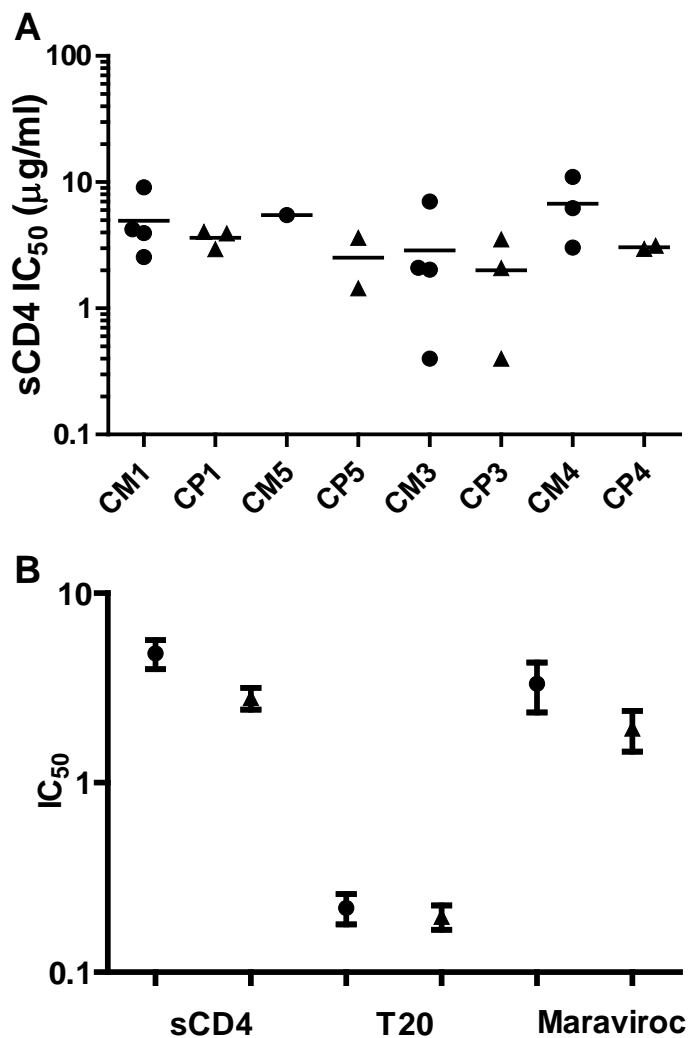


Fig 6.3: Infant *env* may be more sensitive to inhibition by sCD4 than maternal clones. Values are an average of triplicate infections run in the same experiment. 200 sfu of pseudoviruses expressing the cloned *env* were used to infect TZMbl cells. **(A)** Sensitivity of infant and maternal clones to sCD4 by transmission pair. Lines indicate infant and maternal means. **(B)** Aggregate infant and maternal data on sensitivity to HIV-1 entry inhibitors. Points indicate means and the error bars represent one standard error of the mean. Mixed Model ANOVA with mother-infant pairing included as a random effect indicated a trend for greater sensitivity to sCD4 by infant clones than the corresponding maternal *env* $p = 0.055$. Maraviroc IC₅₀ is in ng/ml, sCD4 in µg/ml, and T20 in µg/ml. ▲ = infant, ● = maternal.

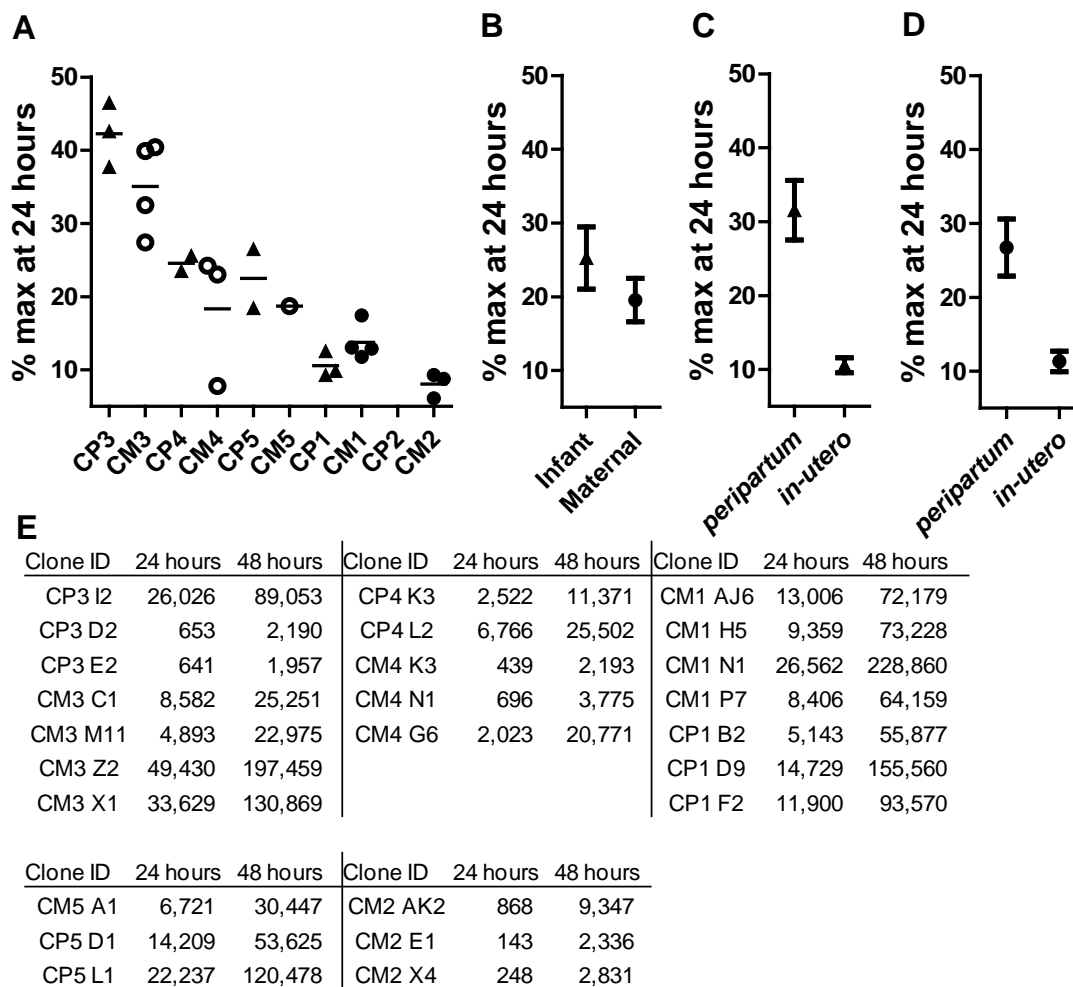


Fig 6.4: *Peripartum* transmitted *env* clones exhibit more rapid entry than *in-utero* transmitted variants. Pseudovirus titers on TZMbl cells were determined at 24 and 48 hours post infection, and the percent of the max 48 hour titers achieved by 24 hours were plotted. Points are averages from triplicate infections in two independent experiments. **(A)** All data presented by transmission pair. Triangles represent infant and circles maternal clones, with *env* from *peripartum* transmission pairs designated by empty symbols; those from *in-utero* pairs are filled. Horizontal lines indicate means. In **(B – D)** triangles indicate infant and circles maternal means. Error bars represent one standard error of the mean. **(B)** Aggregate infant and maternal data. **(C)** *Peripartum* transmitted infant *env* clones exhibit more rapid entry than *in-utero* transmitted infant variants $p = 0.0021$. **(D)** Maternal clones from *peripartum* transmission pairs exhibit more rapid entry than clones from mothers whose infants were infected *in-utero* although the difference does not achieve significance. **(E)** Average 24 and 48 hour titers in SFU/ml.

peripartum transmitters being 1.8 fold higher than the mean for mothers whose infants were infected *in-utero*, although this difference did not achieve significance.

There are indications that viral variant selection during *in-utero* transmission is influenced by different factors than *peripartum* (39). *In-utero* transmission is thought to occur through mother-to-fetus microtransfusions or placental infection, while *peripartum* transmission occurs primarily through exposure of the infant's mucous membranes to maternal blood or secretions (100). During delivery, transmission of a single minor maternal variant is typically observed (2, 40, 202), whereas transmission of single or multiple major maternal is more likely *in-utero* (2, 99, 138).

In light of possible differences in the selective bottleneck during different routes of MTCT, I re-analyzed the entry phenotype data after segregating it by mode of transmission (Fig 6.5). I found that *peripartum* infected infants achieved a significantly higher portion of their maximum titer by 24 hours post infection than the corresponding maternal clones ($p = 0.0177$). When clones from *in-utero* transmission pairs were examined, no significant difference between infant and maternal titers ratios were observed. Regardless of the route of transmission, maternal and infant clones exhibited similar titers at 48 hours, indicating that the observed differences in the portion of the maximum titer achieved by 24 hours were not due to differences between maximum infant and maternal titers (Fig 6.4E).

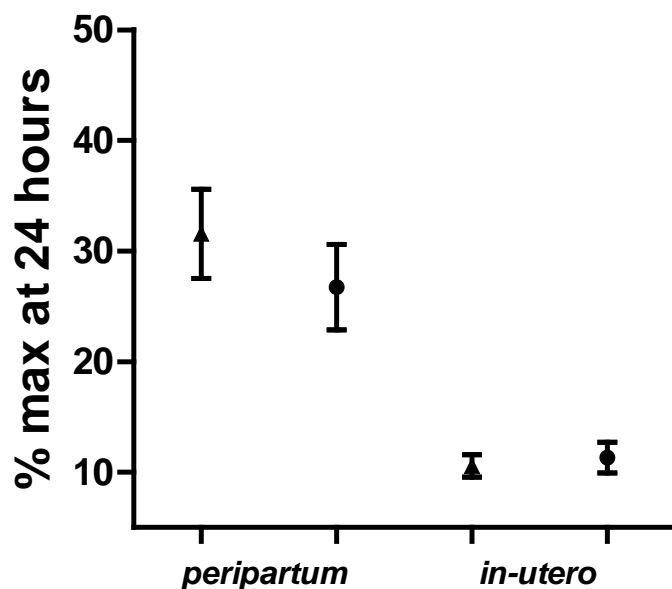


Fig 6.5: *Peripartum* but not *in-utero* transmitted infant *env* exhibit a more rapid entry phenotype than maternal clones. Pseudovirus titers on TZMbl cells were determined at 24 and 48 hours post infection, and the mean percent of the max 48 hour titer achieved by 24 hours was plotted for each category. Higher values indicate that a larger fraction of final titer was achieved by 24 hours. Points indicate means and error bars represent one standard error of the mean. Mixed Model ANOVA with mother-infant pairing included as a random effect indicated that *env* from *peripartum* infected infants exhibited more rapid entry than corresponding maternal clones $p = 0.0177$. ▲ = infant, ● = maternal.

Discussion

In order to extend my previous findings to a non-B cohort, I generated a panel of pseudoviruses expressing subtype C *env*. I screened these clones to determine the frequency resistance to a panel of well-characterized monoclonal NAbs. In agreement with previous reports (13, 62), all subtype C *env* clones were resistant to the NAbs 2F5 and 2G12, and most were resistant to b12. Likewise in agreement with previous reports (13, 62), only the 4E10 NAb exhibited broad and potent activity against subtype C isolates, neutralizing all clones tested at an IC₅₀ of less than 15 µg/ml.

It is speculated that the absence of a PNGS at amino acid position 295 in the gp160 could be responsible for the loss of sensitivity to 2G12 exhibited by subtype C viruses, as 83% of subtype C sequences in the Los Alamos database lacked this PNGS (62, 170). Only 66% of my sequences lacked this PNGS, implying that loss of glycosylation at this position alone is insufficient to explain the near universal resistance of subtype C *env* to 2G12. Consistent with my findings, introduction of a PNGS at 295 into subtype C viruses lacking glycosylation at this position did not render them sensitive to 2G12 (64). In my panel, most of the clones displaying a PNGS at 295 lacked one or more of the five other PNGS implicated in 2G12 binding. However, four clones were resistant to 20µg/ml of 2G12 while exhibiting all six glycans believed to form the 2G12 epitope on subtype B *env*. These clones lacked a PNGS at 442 which is

not part of the subtype B 2G12 epitope, but is suggested by Gray et al (64) to contribute to the formation of the epitope on subtype C viruses.

The prototypical epitope of 2F5, a monoclonal NAb isolated from an HIV-1 subtype B infected subject, is ELDKWA (132). The subtype C consensus for these positions is ALDSWA. As the DKW motif was shown to be critical for 2F5 recognition (13, 62, 211), it is thought that the near universal resistance of subtype C viruses to 2F5 is due primarily to the substitution K66S (13, 62) which occurs in 75% of subtype C clones. Consistent with this proposal, every clone in four of five mother-infant pairs in my subtype C cohort displayed this substitution. Clones from the fifth pair exhibited the ALDKWK sequence demonstrating that mutations in the 2F5 epitope outside of the critical recognition motif are sufficient to render viruses insensitive to 20 μ g/ml of 2F5.

The NAb b12 is reported to neutralize less than 50% of subtype C isolates at 50 μ g/ml (13, 62), which compares with my finding that only 39% of the *env* tested exhibited an IC₅₀ of less than 20 μ g/ml.

The sensitivity of the *env* clones to neutralization by pooled heterologous plasma from subtype B infected subjects varied across a narrow range, with most clones being relatively resistant to this subtype mismatched reagent. Within 3 of 4 transmission pairs infant clones were on average slightly more resistant to heterologous neutralization than maternal but these differences did not achieve significance. Together these data imply that infant variants are likely not

inherently more resistant to neutralization by heterologous Abs than maternal *env*.

CCR5 antagonists such as Maraviroc are a potent new class of entry inhibitors. Unlike HIV-1 subtype B, where following transmission of R5 variants X4 or R5/X4 variants emerge in up to 50% of subjects over the course of an infection (21), subtype C viruses generally continue to exclusively utilize the CCR5 co-receptor (23). As generally only R5 tropic variants are vertically transmitted regardless of subtype, Maraviroc may be highly relevant to blocking MTCT, particularly of subtype C. However, the sensitivity of infant variants to this entry inhibitor has not been well characterized (158). I determined the sensitivity of my *env* clones to three HIV-1 entry inhibitors, including Maraviroc. No clone was resistant to any inhibitor. A trend for increased sensitivity to sCD4 by infant clones was observed across the four transmission pairs tested but did not achieve significance. Sensitivity to T20 and Maraviroc was similar between infant and corresponding maternal *env*.

In agreement with my findings from subtype B *intra-partum* transmission, I observed that *env* clones from infants infected *peripartum* with HIV-1 subtype C exhibited a significantly faster entry phenotype than the corresponding maternal clones.

In summary, infant variants proved insensitive to neutralization by 2F5 and 2G12, and highly resistant to b12, implying that the proposed use of combinations of these NAb as a prophylaxis for blocking MTCT would not be

practical for the subtype responsible for the majority of vertical transmission. The insensitivity of clones displaying the DKW motif to 2F5 implies that mutations in the 2F5 epitope outside of the critical recognition motif are sufficient for resistance. The insensitivity of four of my *env* clones to 2G12 while displaying all the PNGSs implicated in 2G12 epitope formation among subtype B viruses supports the findings of Gray et al (64) that different glycosylation sites are required to form the 2G12 epitope on subtype C viruses and confirms their identification of 442 as one such site.

Maternal and infant clones did not differ significantly in sensitivity to pooled heterologous plasma, implying that inherent neutralization resistance to heterologous Abs is unlikely to be a major factor controlling the selective bottleneck. All infant clones were sensitive to Maraviroc, indicating that this CCR5 antagonist could be a useful addition to the arsenal of inhibitors used to prevent vertical transmission of HIV-1. Most interestingly, *peripartum* transmitted infant *env* clones exhibited a faster entry phenotype than maternal. Identification of the mechanistic and structural basis of this phenomenon may prove useful in the design of therapies for the prevention of MTCT.

CHAPTER VII

Summary of findings and future directions

In the body of this work, I investigated the genotypic and phenotypic properties of infant and maternal *env* clones to identify the correlates of viral variant selection during MTCT of HIV-1. I used the Mother-to-Child model of HIV-1 mucosal transmission because the donor-recipient relationships are unambiguous and samples can be obtained shortly following transmission without the years of monitoring required in some sexual transmission studies. I generated a unique panel consisting of nearly 300 infant and maternal HIV-1 *env* clones from ten vertical transmission pairs infected with HIV-1 subtypes B and C. The former is the best studied subtype of HIV-1 while the later is currently responsible for the vast majority of MTCT. In addition to working with two HIV-1 subtypes I looked at both *peripartum* and *in-utero* routes of vertical transmission.

I first confirmed that MTCT appears to occur across a selective bottleneck regardless of HIV-1 subtype or route of transmission. I then showed that no single genotype appeared to explain this selection. Specifically, I found that enrichment for shorter and less glycosylated *env* occurred during both routes of subtype C MTCT. To date, this is the only genotype linked to viral variant selection during HIV-1 transmission, yet it does not play a selective role during subtype B transmission, as reported both in this work and previous studies. Therefore, enrichment for shorter, less glycosylated infant *env* appears to be just one of several possible adaptations that render *env* variants more transmissible.

I next proceeded to investigate the phenotypic properties of my *env* clones that could play a role in transmission or establishment of infection. I showed that neither the ability to utilize low levels of the HIV-1 receptor and co-receptor, nor enhanced macrophage infectivity plays a major role in this selection. I further demonstrated that most *env* amplified from peripheral blood infect macrophages poorly. Thus, transmitted variants do not appear to be more adapted for infecting mucosal subsets expressing low levels of HIV-1 receptor and co-receptor.

I then investigated if transmitted *env* are more resistant to neutralization than maternal. My failure to find significant differences in sensitivity between maternal and infant clones to four broadly neutralizing monoclonal Abs and autologous and heterologous plasmas suggests that neutralization resistance is unlikely to be a major factor controlling the selective bottleneck during HIV-1 MTCT. Further, these neutralization assays demonstrated that resistance to moderate levels of four monoclonal NAbs derived from subtype B infected patients is common in naïve subjects, particularly those infected with subtype C. Therefore, prophylactic treatment with cocktails of these NAbs is unlikely to be useful in blocking MTCT of the HIV-1 subtype responsible for the majority of vertical transmission.

I subsequently determined the sensitivity of my *env* panel to inhibitors targeting three different stages of HIV-1 entry. The similar sensitivity to sCD4 and Maraviroc exhibited by infant and maternal clones paralleled their use of similar levels of CD4 and CCR5 for efficient entry. Together, these data indicate

that the affinity of Env for the HIV-1 receptor and CCR5 co-receptor are unlikely to play a major role in viral variant selection during MTCT. The sensitivity to ng/ml amounts of Maraviroc exhibited by infant clones implies that this CCR5 antagonist will make a useful addition to the arsenal of HIV-1 MTCT prevention therapies. Maternal and infant clones exhibited similar sensitivity to T20. Guided by the prevalent models of HIV-1 entry and lack of resistance to this inhibitor, I utilized T20 to investigate the entry kinetics of my *env* clones (Fig. 4.8).

Most intriguingly, in both HIV-1 subtypes tested, *peripartum* transmitted infant *env* clones exhibited a faster entry phenotype than maternal. Studies of Simian and Simian-Human Immunodeficiency Virus infection in non-human primates have shed light on the events immediately following exposure through the first days before viremia, a critical spatial and temporal window that is difficult to study in humans. They report that virus crosses the mucosa in a matter of hours (78) to establish a small founder population of infected cells in the submucosa (123, 208). There, low levels of viral propagation proceed over the first week of infection, until this local expansion produces sufficient progeny for systemic dissemination and establishment of a self propagating infection in secondary lymphoid organs (123). Immediately following systemic dissemination, numerous lymphatic tissues become permanent viral reservoirs (68, 159) and largely irreversible CD4 T-cell depletion occurs.

The faster entry phenotype of infant *env* reported in this work could confer a selective advantage during this local propagation phase of infection. HIV-1

susceptible cells are relatively rare in the submucosal, with the initial rounds of viral replication thought to occur in resting CD4⁺ T cells lacking conventional markers of activation, which includes low levels of CCR5 expression (208). HIV-1 infected cells down regulate their CD4 expression, and in this work I demonstrated that low levels of CD4 and CCR5 on target cells greatly reduce HIV-1 infectivity. Co-infection of previously infected resting CD4⁺ T cells may therefore be infrequent. Thus, if viruses with distinct entry rates are initially transmitted, over several rounds of infection the more rapidly entering viruses may out-compete the others for the relatively rare target cells in the submucosa and be the only ones to proceed past the local propagation stage to establish viremia. Identification of the mechanistic and structural basis of enhanced entry may therefore be useful in the design of therapies and vaccines to either prevent MTCT, or to better target the transmitted virus during the first days of infection before systemic dissemination and irreversible CD4⁺ T-cell depletion can occur.

In light of a recent report that HIV-1 entry may be endocytosis dependent (30, 125, 126), determining if differences in the rates of endocytic uptake of maternal and infant clones could underlie the enhanced entry phenotype is an interesting avenue to explore. In Appendix II, I demonstrate that my envelope clones exhibit a dose-response curve to an endocytosis inhibitor. Distinguishing possible differences in endocytic uptake between maternal and infant clones will require a more robust assay system, likely utilizing single particle tracking.

An interesting preliminary observation is that all *env* cloned from subtype B infected subjects and from subtype C *in-utero* transmission pairs exhibit similar entry phenotypes while all *env* cloned from subtype C peripartum transmitted pairs appears to mediate more rapid entry (Fig 7.1). Further, the more rapid entry exhibited by subtype C *peripartum* transmitted infant *env* was not observed in the *in-utero* transmission pair. While the size of the cohort and lack of subtype B *in-utero* transmitters precludes definitive interpretation of these data, the results highlight the importance of taking both the HIV-1 subtype and route of transmission into account when generalizing the findings from a given model system to the pandemic as a whole.

Genetic and functional differences between subtypes B and C transmitted *env* variants indicate multiple mechanisms of selection. For example, while subtype C *env* adapted for transmission or early post-transmission diversification at least in part by modulating their length and glycosylation, other, not yet identified, genetic mechanisms must underlie subtype B selection. Therefore, while one end result of selection in both HIV-1 subtypes is the generation of *env* variants exhibiting enhanced entry kinetics, it is probable that distinct genotypic changes underlie this phenotype in each subtype.

Further investigation in a larger cohort, preferably including additional HIV-1 subtypes, is necessary to confirm the novel report of enhanced entry exhibited by recently transmitted *env* clones and to extend these findings to other routes of mucosal transmission. If similar selection for more rapid entry occurs during

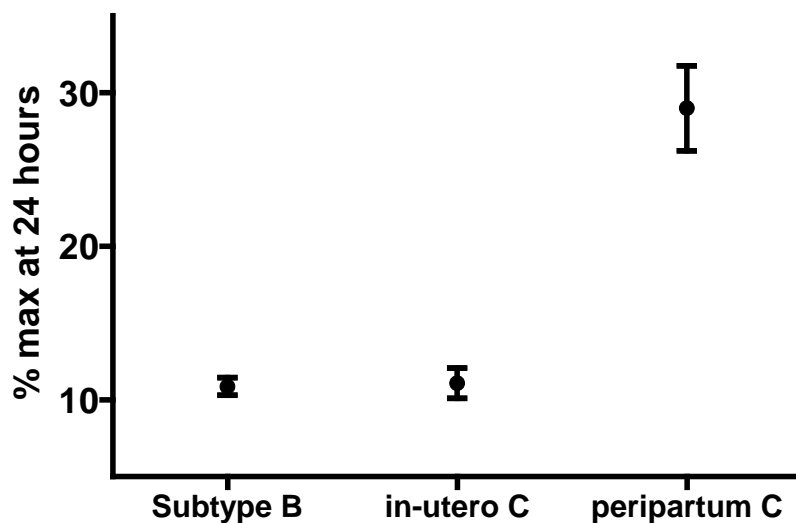


Fig 7.1: Pseudoviruses expressing *env* cloned from subtype C infected *peripartum* transmission pairs exhibit a more rapid entry phenotype than those from subtype C *in-utero* transmission pairs or subtype B infected subjects. Pseudovirus titers on TZMbl cells were determined at 24 and 48 hours post infection, and the percent of the max 48 hour titers achieved by 24 hours were plotted. Points indicate means and error bars represent one standard error of the mean.

sexual transmission, understanding the mechanisms underlying this phenotype could inform the design of therapies for blocking HIV-1 infection.

APPENDIX I

Antigenicity of maternal and infant envelope proteins

Introduction

The high incidence of MTCT of HIV-1 in resource-limited countries (83) emphasizes the urgent need for effective preventative strategies (113). While in developed countries HAART combined with formula feeding have decreased the incidence of MTCT to less than 2% (29, 83, 127), the most effective and widely available intervention for blocking MTCT in the developing world is a single dose of nevirapine administered to the mother at the start of labor and to the baby at birth. This treatment decrease rates of MTCT by up to half, through blocking the majority of *intra-partum* transmission (66, 136), but does not prevent transmission through breastfeeding.

The majority of MTCT takes place in sub-Saharan Africa where abstinence from breast feeding is frequently not a viable option. In addition to numerous cultural and financial factors and the lack of clean water, the infants require maternal milk-borne antibodies for protection from numerous endemic diseases (53). Therefore, while prolonged breastfeeding by HIV-1 positive mothers doubles the risk of MTCT as compared to formula fed infants (106, 124, 134), the mortality rates are similar between the two groups due to a higher frequency of diarrheal diseases in the formula fed infants (134). In many areas of the world, reducing vertical HIV-1 transmission during breastfeeding without further jeopardizing infant health is one of the most urgent healthcare dilemmas.

The most efficient solution to preventing MTCT is a prophylactic vaccine regimen started at birth (113), possibly combined with a short course of antiretroviral drugs to provide protection until the vaccine induced immune response attains protective levels. This strategy may also result in long-term protection, preventing the children from acquiring HIV-1 when they become sexually active as adults.

HIV-1 is a retrovirus that integrates into the genome of the host's cells. In order to be fully protective, a putative vaccine would likely need to effect sterilizing immunity by inducing an antibody response capable of neutralizing the virus before it enters cells (20, 118, 122, 130). The failure of Merck's STEP clinical trial (www.HVTN.org) indicates that induction of cell-mediated immunity alone, while beneficial (7, 10, 173), is insufficient for full protection. To date, only one HIV-1 human vaccine trial has shown any protective efficacy (162). While the exact correlates of protection in this study are unknown, the vaccine combined antigens from two previous trials, both of which induced neutralizing antibody responses (149, 165).

The unprecedented diversity, mutation rate and immune escape mechanisms of HIV-1 have contributed to the failure of vaccine candidates to generate broad and effective neutralizing antibody responses in human trials (19, 52, 111). Additionally, the rare, broadly neutralizing, monoclonal Abs isolated from infected subjects and utilized in successful passive immunization trials could not be induced by vaccines (71).

One approach to overcoming HIV-1's diversity is identification of common neutralization epitopes on the *env* of many different primary isolates (28, 81, 131). However, these efforts have failed to produce a vaccine capable of eliciting a potent neutralizing response against multiple heterologous primary HIV-1 isolates. Another approach is to use a polyvalent vaccine consisting of multiple primary *env* antigens to induce a broad antibody response (24). While this usually results in a broader response than that generated against a single epitope, in humans the levels of the response are generally too low to afford protection. To increase the potency of polyvalent vaccines, the heterologous prime-boost method was developed (89, 157). The only human trial of an HIV-1 vaccine that showed protective efficacy utilized the polyvalent, heterologous prime-boost approach (162).

Despite the increased breadth of neutralization commonly induced by polyvalent the approach, identification of relevant antigens is vital to the design of effective vaccines. MTCT occurs in the presence of maternal NABs. Infant viruses isolated shortly after transmission are reportedly more resistant to neutralization by autologous maternal plasma than the concurrent maternal viruses (39, 204). Maternal antibodies cross the placenta, peaking at delivery. In the infant they may act as the sort of NAb prophylaxis shown to be protective in macaque vertical transmission models (50, 77). Thus, escape from autologous maternal NABs may be one of the factors underlying the selective bottleneck observed during MTCT.

The body of my dissertation describes and summarizes numerous additional differences between infant and maternal clones. Therefore, infant rather than maternal HIV-1 *env* antigens may be most relevant to the design of vaccines for blocking MTCT. However, the antigenicity of infant isolates has not been examined in detail nor compared with that of maternal *env*.

To address this deficiency, we set up collaboration with Dr. Shan Lu, an expert in the field of HIV-1 vaccine development. Dr. Lu's lab has established a simple and effective implementation of the heterologous prime-boost strategy, the DNA prime-protein boost. In this approach, immunizations with a DNA plasmid encoding antigenic genes are followed by immunizations with the purified proteins products of the antigenic genes (190, 193). This approach is amiable to both single antigen (190) and polyvalent vaccines (193). Utilizing this methodology the Lu lab has demonstrated protection against primary HIV-1 isolates in macaques (141) and elicited broad neutralizing antibody responses in a human clinical trial (192).

Together, we assessed the antigenicity and immunogenicity of select infant and maternal *env* clones from my cohort.

Results

Antigen selection

Utilizing previously determined sequence, neutralization and inhibition information, two pairs of maternal and infant *env* clones were selected from my clade B *env* panel to serve as immunogens in a DNA prime-protein boost vaccine regimen (Table A1.1). All selected *env* expressed the GPGR V3 crown motif (Table 3.3) and exhibited well-conserved CD4 binding sites and neutralization domains (Table A1.1). To investigate the effects of resistance on immunogenicity, clones that were relatively sensitive (P1031 H2 and M1002 T6) or resistant (P1046 C4 and M1007 Q6) to the monoclonal NAbs b12 and 2G12, and to sCD4 were selected (Table A1.1).

Production of vaccine components and rabbit immunization

In the Lu lab, gp120 subunits were PCR amplified from the selected *env*, cloned into a vaccine vector and the ability of the resultant constructs to properly express gp120 proteins was determined as previously described (191). To investigate the immunogenicity of the selected gp120 clones, the Lu lab immunized four groups of New Zealand White rabbits using a DNA prime-protein boost regimen. Each rabbit received three biweekly DNA immunizations and a protein boost one and two months following the last DNA prime (Table A1.2). Serum samples were obtained from the rabbits prior to the start of the regimen and on the day of, and two weeks following, each immunization.

Table A1.1: Neutralization and inhibition sensitivity of selected *env*

Clone ID	NAb IC ₅₀ (µg/ml)				Plasma IC ₅₀ ^a	sCD4 IC ₅₀ (µg/ml)
	2F5	2G12	4E10	B12		
P1031 H2	6.9	0.5	0.6	<0.01	116	4.05
M1002 T6	1.1	0.9	3.1	0.5	663	2.98
P1046 C4	4.1	>20	4.8	>20	938	13.07
M1007 Q6	5.5	>20	7.4	>20	311	15.92

^aIC₅₀ in reciprocal dilutions of pooled heterologous plasma from HIV-1 positive donors

Table A1.2: Rabbit immunization groups

Group	No. of Rabbits	gp120 Immunogen	DNA prime			Protein boost		
			Route	Dose	No.	Route	Dose	No.
A	2	M1002-T6	Gene gun	36 µg	3	IM	100 µg	2
B	2	P1046-C4	Gene gun	36 µg	3	IM	100 µg	2
C	2	P1031-H2	Gene gun	36 µg	3	IM	100 µg	2
D	2	M1007-Q6	Gene gun	36 µg	3	IM	100 µg	2

IM, Intra Muscular. Rabbit immunizations were performed by the Lu lab.

Antigenicity and immunogenicity assessment

To determine if the vaccine constructs expressing the selected gp120 clones could function as effective antigens, the induction of gp120-specific binding antibody responses in the immunized rabbits was assessed. Following the DNA prime, high titers of gp120-specific antibodies against the autologous antigens were detected by ELISA in all immunized rabbits (Fig A1.1A). Across all immunization groups, these titers were enhanced by the protein boost (Fig A1.1A). The gp120-specific antibody responses in immunized rabbit sera were also assessed by Western blot analysis using the sera as the detection antibody against gp120 in the cell lysate and culture supernatant from 293T cell cultures transiently transfected by each of the four vaccine constructs. Sera from each immunization group were able to bind the gp120 proteins. Sera from rabbit R679 (immunized with the M1007-Q6 construct), which recognized gp120 generated by each of the four vaccine constructs (Fig A1.1B), is representative of all 4 immunization groups.

We next assessed the breadth and potency of the vaccine induced gp120-specific neutralizing antibody responses. Sera collected two weeks after the final protein injection were used by both our labs to neutralize panels of HIV-1 clade B *env* pseudotyped viruses. The panel used by the Lu lab included *env* from two relatively neutralization sensitive viruses, each of the four clones used as immunogens and five unrelated primary isolates (Table A1.3). Sera obtained prior to the start of the immunization regimen did not exhibit any gp120-specific

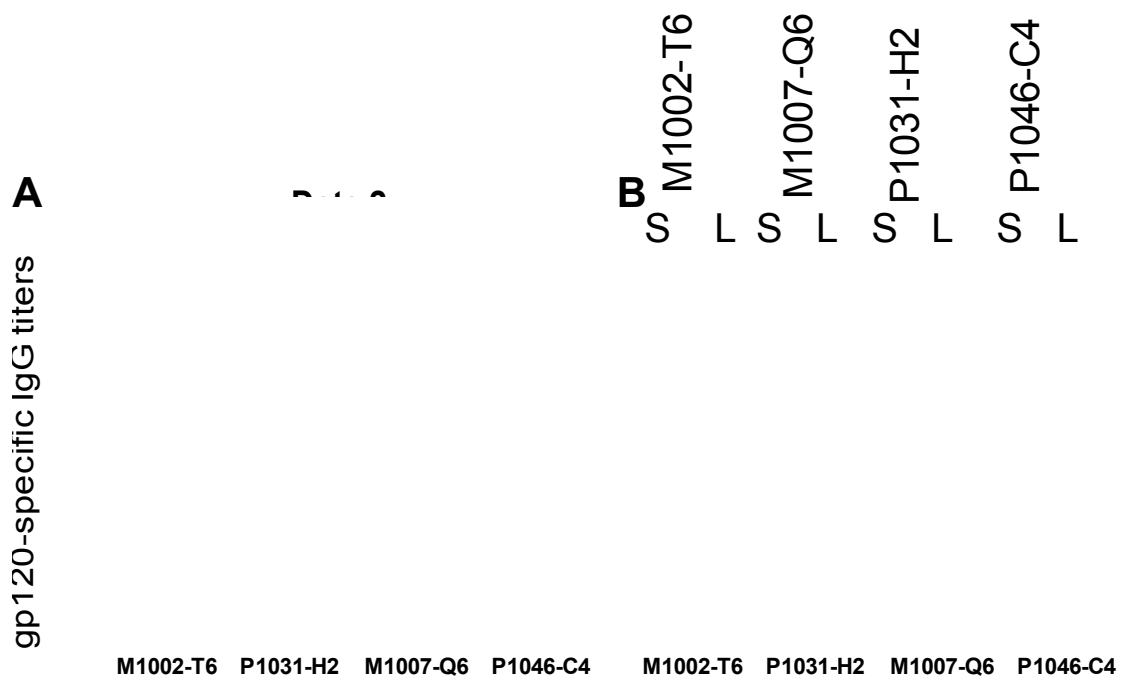


Fig A1.1: Induction of gp120 specific binding antibody responses. **(A)** gp120-specific antibody titers in sera of immunized rabbits measured by ELISA against the autologous gp120 antigens. Samples were obtained two weeks after the last of three DNA immunizations (grey) or the final protein boost (black). Values shown are means of titers from each pair of rabbits with one standard deviation error bars. **(B)** Western blot of culture supernatants (S) and cell lysates (L) from 293T cells transiently transfected with the vaccine constructs. Sera obtained from a rabbit (R679) immunized with the M1007-Q6 construct two weeks after completion of the immunization regimen was used as the detection antibody and is representative of all four immunization groups. This work was performed in the Lu lab.

Table A1.3: Induction of NAb by the immunization regimens

		Immunogens relatively sensitive to b12, 2G12 and sCD4				Immunogens relatively resistant to b12, 2G12 and sCD4			
		M1002-T6		P1031-H2		M1007-Q6		P1046-C4	
		R663	R664	R670	R671	R678	R679	R668	R669
Sensitive viruses	SF162	1132	340	2764	514	172	1112	622	172
	NL4-3					21	61	63	21
Vaccine constructs	M1007-Q6				11	20		12	
	P1046-C4					55	11	27	
	M1002-T6					25			
	P1031-H2					17			
Other primary isolates	SS1196.1	49	51	49		49	135	257	
	6535.3			11		15	21	13	
	QH0692.42	74	52	10		46	50	120	
	p6B33	20							
	p6LN40			12		21	12	14	
Murine Leukemia Virus									
NAb titers		> 1000		101 to 1000		10 to 100		< 10	

Data presented was generated by the Lu lab and is consistent with the results from our lab.

neutralization and none of the post immunization sera neutralized an MLV pseudotyped virus used as a non-specific toxicity control (Table A1.3). Sera from each immunized rabbit exhibited neutralizing responses against the highly sensitive SF162 virus. Neutralization activity against other viruses varied considerably both within and between immunization groups, but the responses from rabbits immunized with the M1007-Q6 and P1046-C4 constructs were markedly broader than those immunized with P1031-H2 and M1002-T6 (Table A1.3). When the frequencies of the positive and negative NAb responses in rabbits immunized by each pair of constructs were compared, positive responses proved twice as frequent in those immunized with the resistant clones ($p = 0.005$) (Table A1.4).

Table A1.4: Frequencies of NAb responses in paired immunization groups

Rabbits vaccinated with:	Positive responses	Negative responses
Immunogens relatively sensitive to b12, 2G12 and sCD4	14 (32%)	30 (68%)
Immunogens relatively resistant to b12, 2G12 and sCD4	27 (61%)	17 (39%)

Data is presented as number of positive or negative responses (percent total).
Chi square test: $p = 0.005$. Table was generated by the Lu lab.

Discussion

In collaboration with the Lu lab, we selected two pairs of maternal and infant *env* clones from my clade B panel to serve as immunogens in a DNA prime-protein boost vaccine regimen. One pair of selected maternal and infant *env* was relatively more resistant than the other to the monoclonal Nabs b12 and 2G12 and to sCD4. All clones exhibited well-conserved CD4 binding sites and the prototypical clade B V3 crown motif.

We initially assessed the induction of binding antibody responses in the immunized rabbits by ELISA and found that all produced high titers of gp120-specific antibodies against the autologous antigens by the end of the DNA prime stage. The levels achieved by the four groups differed by less than one log, indicating that the four clones were similarly antigenic. Protein boost increased these titers by approximately a log, in agreement with previous heterologous prime-boost studies (190, 193). We confirmed these findings using a Western-blot assay, detecting gp120-specific antibodies in sera from each immunization group. In addition to autologous responses, rabbit sera contained antibodies capable of recognizing heterologous *env*. Sera from a representative rabbit recognized *env* antigens encoded by each of the four vaccine constructs, validating the ability of the polyvalent vaccine approach to induce a broad Ab response against heterologous primary HIV-1 isolates.

While binding antibodies can play a protective role through induction of mechanisms such as Antibody-Dependent Cell-Mediated Cytotoxicity (98, 144,

185), neutralizing antibodies are essential to provide the sterilizing protection required for a fully effective vaccine. Apparently successful induction of binding antibodies to a well characterized neutralization epitope may fail to show any neutralization activity (112). We therefore assessed the breadth and potency of the gp120-specific neutralizing antibody responses induced by our vaccine regimen against a panel of HIV-1 clade B *env* pseudotyped viruses. By the end of the immunization regimen, all rabbit sera could neutralize the highly sensitive SF162 virus and at least one other heterologous virus. Further, each of the 11 viruses in the panel could be neutralized by sera from at least one rabbit. Vaccine constructs consisting of several *env* clones have been shown to generate a broader response than each subunit alone (193). Presumably a vaccine consisting of all four antigens used in this study would reliably neutralize all viruses in this panel.

Interestingly, we observed significantly broader and more potent neutralization responses from rabbits immunized with the more b12, 2G12 and sCD4 resistant *env* clones. Conversely, major differences in antigenicity and immunogenicity between maternal and infant clones were not detected within or between the two groups.

Together, this preliminary data confirms the ability of the polyvalent vaccine approach, implemented via a heterologous prime-boost regimen, to induce broad and potent neutralizing antibody responses, and hints that the neutralization sensitivity of the *env* immunogens may affect the quality of the

response. To further investigate this relationship we are collaborating with the Lu lab to immunize rabbits with vaccine constructs expressing immunogens from my clade C *env* panel.

Appendix II

Role of endocytosis in HIV-1 entry

Introduction

In order for mammalian viruses to initiate infection, they must penetrate the plasma membrane of the target cell. For enveloped viruses this requires the fusion of the viral and cell membranes. Endocytosis is an obligatory part of the entry process for pH dependent viruses, such as influenza (142) and vesicular stomatitis virus (119), whose fusion proteins are activated by the acidic pH of endosomes (119, 179). Conversely, pH independent viruses, which undergo fusion upon receptor binding without the need for an acidic activation step, are generally thought to fuse at the plasma membrane (101).

HIV-1 is a pH independent (120, 180) enveloped virus. Its entry process begins with the binding of the gp120 subunit of the envelope protein (Env) to the CD4 receptor on the target cell. This results in a conformation change which exposes the hereto masked co-receptor binding site and allows Env binding to one of a number of chemokine receptors. Co-receptor binding results in major conformational changes in the gp41 subunit of the Env, exposing an N-terminal hydrophobic peptide which inserts into the membrane of the target cell. Subsequent conformational changes in the gp41 subunit pull the cell and viral membranes together, resulting in the formation of a fusion pore, its expansion, and viral entry. An overview of this model of the entry is shown in Figure 1.3B.

Since the HIV-1 Env does not require acidification for activation (120, 180), unlike the case with pH dependent viruses, no clear requirement for endocytosis was apparent for HIV-1 entry. Therefore, HIV-1 was thought to undergo fusion at the plasma membrane (116). While endocytosis of HIV-1 has been observed, this was generally not considered to be a functional route of entry. Based on experiments where the inhibition of endosomal, lysosomal and proteasomal function increased the infectivity of HIV-1, the internalized virions were believed to be trapped in the endocytic vesicles and degraded by the lysosome (54, 194). In contrast to these findings, a study which used cells transfected with inducible dominant negative dynamin, a molecule essential for a clathrin-mediated endocytosis (31, 76), reported that endocytosis contributes to the productive entry of HIV-1 (30).

The role of endocytosis in HIV-1 entry was recently re-visited in an elegant study utilizing real-time single particle tracking of labeled viruses (125). The authors reported that complete HIV-1 fusion occurred only in endosomes while fusion at the membrane did not proceed past the lipid mixing step. They further reported that, in concurrence with a previous study (30), this endocytosis was dynamin dependent. These findings, which imply that pH independence does not necessarily remove the need for endocytosis, parallel reports of endocytosis utilization for entry by other pH independent viruses (86, 94).

Understanding the mechanism of HIV-1 entry is basic to the rational design of therapies for preventing transmission. For example, HIV-1 fusion

inhibitors such as T20 and C34 are not membrane permeable. If HIV-1 fuses in endosomes rather than at the plasma membrane their potency would likely be attenuated. Likewise, elucidation of the mechanisms underlying the enhanced entry kinetics of infant *env* clones reported in this manuscript requires the understanding of HIV-1 entry. Additional work is required to interpret the seemingly contradictory data and determine the significance of endocytosis for HIV-1 entry. To this end, I designed a system to test the effect of inhibition of dynamin-dependent endocytosis on the infectivity of primary isolates of HIV-1 *env*.

Results

As a pilot study into the requirement of dynamin-dependent endocytosis for HIV-1 entry, I investigated the effect of Dynasore, a well characterized reversible inhibitor of dynamin-dependent endocytosis (115), on HIV-1 infectivity. Oligomerization of dynamin is essential for clathrin-dependent coated vesicle budding during endocytosis (31, 76). This self-assembly of dynamin structures utilizes GTP hydrolysis (46) and Dynasore, which is a membrane-permeable small molecule, inhibits dynamin oligomerization by interfering with its GTPase activity (115). Treatment of cells with Dynasore reduces transferrin uptake, a commonly used monitor of endocytosis, in a dose dependent manner (115). Treatment with 80 μ M Dynasore blocks endocytosis at levels similar to that obtained by the over-expression of dominant-negative dynamin (31), which reduces transferrin uptake into HeLa cells by over 90% percent (115).

I determined the effect of Dynasore on HIV-1 infectivity by pre-treating TZMbl cell monolayers with serial dilutions of Dynasore and infecting them with pseudoviruses expressing the clade B HIV-1 *env* described in the body of this work. Parallel infections with pseudoviruses expressing the Vesicular Stomatitis Virus glycoprotein (VSV-G) served as a positive control for dynamin-dependent endocytosis (125, 183). As prolonged inhibition of endocytosis is toxic to cells, 150 minutes following infection the monolayers were washed and the media replaced. To prevent further infection with virus that had not yet been endocytosed, the fresh media was supplemented with a 100% inhibitory dose of

the T20 fusion inhibitor. Following a 48 hour incubation, the monolayers were fixed and infected cells visualized using the β -galactosidase readout. For every clone tested, a parallel control infection was performed in the absence of Dynasore.

All HIV-1 *env* clones tested (n = 24) exhibited dose-response curves and IC_{50} values to Dynasore similar to those shown by the VSV-G pseudotyped control (Fig A2.1A). Treatment with 80 μ M Dynasore on average reduced HIV-1 infectivity by 88% as compared to un-inhibited controls; pseudoviruses displaying VSV-G were similarly inhibited (Fig A2.1B).

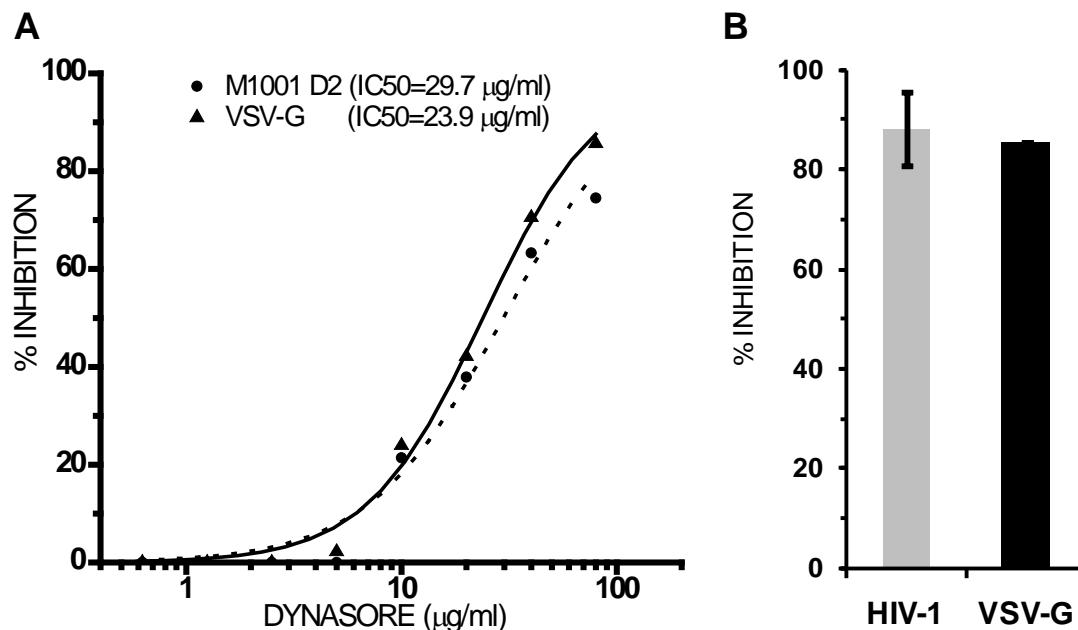


Fig A2.1: Viruses pseudotyped with HIV-1 *env* and VSV-G exhibit similar sensitivity to Dynasore. **(A)** Dose-response curves to Dynasore exhibited by VSV-G and a representative HIV-1 *env* clone. IC₅₀ values are included in the legend. Solid line = VSV-G, dashed = HIV-1 *env*. **(B)** Reduction in pseudoviral titers by 80 μM Dynasore as a percentage of un-inhibited control. Error bar represents one standard deviation from the mean. Data is pooled from three independent assays performed in duplicate (n = 24). The VSV-G control was run in duplicate in a single assay. Infections were performed in TZMbl cells.

Discussion

The finding that pH independent HIV-1 requires dynamin-dependent endocytosis for entry (125) may be paradigm changing, but the mechanisms underlying this phenomena and its *in-vivo* significance are unclear. A recent study did not find dose-dependent inhibition of HIV-1 by Dynasore and failed to observe significant inhibition even at the 80 μ M concentration during infection of human T cells (205), highlighting the urgent need to revisit the HIV-1 entry process.

I designed a system to investigate the dependence of pseudoviruses displaying primary HIV-1 *env* on dynamin-dependent endocytosis for infectivity. I utilized Dynasore to inhibit dynamin-dependent endocytosis and found that primary HIV-1 *env* exhibited dose-response relationships similar to those of pseudoviruses expressing the endocytosis dependent VSV-G. At 80 μ M of Dynasore, which reduces endocytosis by over 90% (115), the infectivity of HIV-1 *env* pseudotyped viruses decreased by an average of 88%. This preliminary data suggests that primary HIV-1 isolates may utilize dynamin-dependent endocytosis for entry. While further work is necessary to determine the mechanisms underlying this observation, the well characterized *env* panels described in this work may prove useful tools in this regard.

BIBLIOGRAPHY

1. Ahmad, N. 2005. The vertical transmission of human immunodeficiency virus type 1: molecular and biological properties of the virus. *Crit. Rev. Clin. Lab. Sci.* 42:1-34.
2. Ahmad, N., B. M. Baroudy, R. C. Baker, and C. Chappay. 1995. Genetic analysis of human immunodeficiency virus type 1 envelope V3 region isolates from mothers and infants after perinatal transmission. *J. Virol.* 69:1001-1012.
3. Alexander, M., R. Lynch, J. Mulenga, S. Allen, C. A. Derdeyn, and E. Hunter. 2010. Donor and recipient envs from heterosexual human immunodeficiency virus subtype C transmission pairs require high receptor levels for entry. *J. Virol.* 84:4100-4104.
4. Alkhatib, G., C. Combadiere, C. C. Broder, Y. Feng, P. E. Kennedy, P. M. Murphy, and E. A. Berger. 1996. CC CKR5: a RANTES, MIP-1alpha, MIP-1beta receptor as a fusion cofactor for macrophage-tropic HIV-1. *Science.* 272:1955-1958.
5. Allen, T. M., and M. Altfeld. 2003. HIV-1 superinfection. *J. Allergy Clin. Immunol.* 112:829-35; quiz 836.
6. Altfeld, M., T. M. Allen, X. G. Yu, M. N. Johnston, D. Agrawal, B. T. Korber, D. C. Montefiori, D. H. O'Connor, B. T. Davis, P. K. Lee, E. L. Maier, J. Harlow, P. J. Goulder, C. Brander, E. S. Rosenberg, and B. D. Walker. 2002. HIV-1 superinfection despite broad CD8+ T-cell responses containing replication of the primary virus. *Nature.* 420:434-439.
7. Amara, R. R., F. Villinger, J. D. Altman, S. L. Lydy, S. P. O'Neil, S. I. Staprans, D. C. Montefiori, Y. Xu, J. G. Herndon, L. S. Wyatt, M. A. Candido, N. L. Kozyr, P. L. Earl, J. M. Smith, H. L. Ma, B. D. Grimm, M. L. Hulse, J. Miller, H. M. McClure, J. M. McNicholl, B. Moss, and H. L. Robinson. 2001. Control of a mucosal challenge and prevention of AIDS by a multiprotein DNA/MVA vaccine. *Science.* 292:69-74.
8. Asjo, B., L. Morfeldt-Manson, J. Albert, G. Biberfeld, A. Karlsson, K. Lidman, and E. M. Fenyo. 1986. Replicative capacity of human immunodeficiency virus from patients with varying severity of HIV infection. *Lancet.* 2:660-662.
9. Baeten, J. M., B. Chohan, L. Lavreys, V. Chohan, R. S. McClelland, L. Certain, K. Mandaliya, W. Jaoko, and J. Overbaugh. 2007. HIV-1 subtype D infection is

associated with faster disease progression than subtype A in spite of similar plasma HIV-1 loads. *J. Infect. Dis.* 195:1177-1180.

10. Barouch, D. H., S. Santra, J. E. Schmitz, M. J. Kuroda, T. M. Fu, W. Wagner, M. Bilska, A. Craiu, X. X. Zheng, G. R. Krivulka, K. Beaudry, M. A. Lifton, C. E. Nickerson, W. L. Trigona, K. Punt, D. C. Freed, L. Guan, S. Dubey, D. Casimiro, A. Simon, M. E. Davies, M. Chastain, T. B. Strom, R. S. Gelman, D. C. Montefiori, M. G. Lewis, E. A. Emini, J. W. Shiver, and N. L. Letvin. 2000. Control of viremia and prevention of clinical AIDS in rhesus monkeys by cytokine-augmented DNA vaccination. *Science.* 290:486-492.

11. Barre-Sinoussi, F., J. C. Chermann, F. Rey, M. T. Nugeyre, S. Chamaret, J. Gruest, C. Dauguet, C. Axler-Blin, F. Vezinet-Brun, C. Rouzioux, W. Rozenbaum, and L. Montagnier. 1983. Isolation of a T-lymphotropic retrovirus from a patient at risk for acquired immune deficiency syndrome (AIDS). *Science.* 220:868-871.

12. Bhattacharyya, D., B. R. Brooks, and L. Callahan. 1996. Positioning of positively charged residues in the V3 loop correlates with HIV type 1 syncytium-inducing phenotype. *AIDS Res. Hum. Retroviruses.* 12:83-90.

13. Binley, J. M., T. Wrin, B. Korber, M. B. Zwick, M. Wang, C. Chappey, G. Stiegler, R. Kunert, S. Zolla-Pazner, H. Katinger, C. J. Petropoulos, and D. R. Burton. 2004. Comprehensive cross-clade neutralization analysis of a panel of anti-human immunodeficiency virus type 1 monoclonal antibodies. *J. Virol.* 78:13232-13252.

14. Blackard, J. T., B. Renjifo, W. Fawzi, E. Hertzmark, G. Msamanga, D. Mwakagile, D. Hunter, D. Spiegelman, N. Sharghi, C. Kagoma, and M. Essex. 2001. HIV-1 LTR subtype and perinatal transmission. *Virology.* 287:261-265.

15. Boussif, O., F. Lezoualc'h, M. A. Zanta, M. D. Mergny, D. Scherman, B. Demeneix, and J. P. Behr. 1995. A versatile vector for gene and oligonucleotide transfer into cells in culture and in vivo: polyethylenimine. *Proc. Natl. Acad. Sci. U. S. A.* 92:7297-7301.

16. Brander, C., N. Frahm, and B. D. Walker. 2006. The challenges of host and viral diversity in HIV vaccine design. *Curr. Opin. Immunol.* 18:430-437.

17. Bryson, Y. J., K. Luzuriaga, J. L. Sullivan, and D. W. Wara. 1992. Proposed definitions for in utero versus intrapartum transmission of HIV-1. *N. Engl. J. Med.* 327:1246-1247.

18. Bublil, E. M., S. Yeger-Azuz, and J. M. Gershoni. 2006. Computational prediction of the cross-reactive neutralizing epitope corresponding to the

[corrected] monoclonal [corrected] antibody b12 specific for HIV-1 gp120. *FASEB J.* 20:1762-1774.

19. Bures, R., A. Gaitan, T. Zhu, C. Graziosi, K. M. McGrath, J. Tartaglia, P. Caudrelier, R. El Habib, M. Klein, A. Lazzarin, D. M. Stablein, M. Deers, L. Corey, M. L. Greenberg, D. H. Schwartz, and D. C. Montefiori. 2000. Immunization with recombinant canarypox vectors expressing membrane-anchored glycoprotein 120 followed by glycoprotein 160 boosting fails to generate antibodies that neutralize R5 primary isolates of human immunodeficiency virus type 1. *AIDS Res. Hum. Retroviruses.* 16:2019-2035.
20. Burton, D. R., R. C. Desrosiers, R. W. Doms, W. C. Koff, P. D. Kwong, J. P. Moore, G. J. Nabel, J. Sodroski, I. A. Wilson, and R. T. Wyatt. 2004. HIV vaccine design and the neutralizing antibody problem. *Nat. Immunol.* 5:233-236.
21. Callaway, D. S., R. M. Ribeiro, and M. A. Nowak. 1999. Virus phenotype switching and disease progression in HIV-1 infection. *Proc. Biol. Sci.* 266:2523-2530.
22. Ceballos, A., G. Andreani, C. Ripamonti, D. Dilernia, R. Mendez, R. D. Rabinovich, P. C. Cardenas, C. Zala, P. Cahn, G. Scarlatti, and L. Martinez Peralta. 2008. Lack of viral selection in human immunodeficiency virus type 1 mother-to-child transmission with primary infection during late pregnancy and/or breastfeeding. *J. Gen. Virol.* 89:2773-2782. doi: 10.1099/vir.0.83697-0.
23. Cecilia, D., S. S. Kulkarni, S. P. Tripathy, R. R. Gangakhedkar, R. S. Paranjape, and D. A. Gadkari. 2000. Absence of coreceptor switch with disease progression in human immunodeficiency virus infections in India. *Virology.* 271:253-258.
24. Cho, M. W., Y. B. Kim, M. K. Lee, K. C. Gupta, W. Ross, R. Plishka, A. Buckler-White, T. Igarashi, T. Theodore, R. Byrum, C. Kemp, D. C. Montefiori, and M. A. Martin. 2001. Polyvalent envelope glycoprotein vaccine elicits a broader neutralizing antibody response but is unable to provide sterilizing protection against heterologous Simian/human immunodeficiency virus infection in pigtailed macaques. *J. Virol.* 75:2224-2234.
25. Chohan, B., D. Lang, M. Sagar, B. Korber, L. Lavreys, B. Richardson, and J. Overbaugh. 2005. Selection for human immunodeficiency virus type 1 envelope glycosylation variants with shorter V1-V2 loop sequences occurs during transmission of certain genetic subtypes and may impact viral RNA levels. *J. Virol.* 79:6528-6531.

26. Clavel, F., and A. J. Hance. 2004. HIV drug resistance. *N. Engl. J. Med.* 350:1023-1035.
27. Clevestig, P., L. Pramanik, T. Leitner, and A. Ehrnst. 2006. CCR5 use by human immunodeficiency virus type 1 is associated closely with the gp120 V3 loop N-linked glycosylation site. *J. Gen. Virol.* 87:607-612. doi: 10.1099/vir.0.81510-0.
28. Conley, A. J., J. A. Kessler 2nd, L. J. Boots, J. S. Tung, B. A. Arnold, P. M. Keller, A. R. Shaw, and E. A. Emini. 1994. Neutralization of divergent human immunodeficiency virus type 1 variants and primary isolates by IAM-41-2F5, an anti-gp41 human monoclonal antibody. *Proc. Natl. Acad. Sci. U. S. A.* 91:3348-3352.
29. Cooper, E. R., M. Charurat, L. Mofenson, I. C. Hanson, J. Pitt, C. Diaz, K. Hayani, E. Handelsman, V. Smeriglio, R. Hoff, W. Blattner, and Women and Infants' Transmission Study Group. 2002. Combination antiretroviral strategies for the treatment of pregnant HIV-1-infected women and prevention of perinatal HIV-1 transmission. *J. Acquir. Immune Defic. Syndr.* 29:484-494.
30. Daecke, J., O. T. Fackler, M. T. Dittmar, and H. G. Krausslich. 2005. Involvement of clathrin-mediated endocytosis in human immunodeficiency virus type 1 entry. *J. Virol.* 79:1581-1594.
31. Damke, H., T. Baba, D. E. Warnock, and S. L. Schmid. 1994. Induction of mutant dynamin specifically blocks endocytic coated vesicle formation. *J. Cell Biol.* 127:915-934.
32. Daniel, W. W. 1990. *Applied Nonparametric Statistics*. Pacific Grove, Duxbury, CA.
33. de Oliveira, T., S. Engelbrecht, E. Janse van Rensburg, M. Gordon, K. Bishop, J. zur Megede, S. W. Barnett, and S. Cassol. 2003. Variability at human immunodeficiency virus type 1 subtype C protease cleavage sites: an indication of viral fitness? *J. Virol.* 77:9422-9430.
34. de Witte, L., A. Nabatov, and T. B. Geijtenbeek. 2008. Distinct roles for DC-SIGN+-dendritic cells and Langerhans cells in HIV-1 transmission. *Trends Mol. Med.* 14:12-19.
35. Deng, H., R. Liu, W. Ellmeier, S. Choe, D. Unutmaz, M. Burkhart, P. Di Marzio, S. Marmon, R. E. Sutton, C. M. Hill, C. B. Davis, S. C. Peiper, T. J. Schall, D. R. Littman, and N. R. Landau. 1996. Identification of a major co-receptor for primary isolates of HIV-1. *Nature.* 381:661-666.

36. Derdeyn, C. A., J. M. Decker, F. Bibollet-Ruche, J. L. Mokili, M. Muldoon, S. A. Denham, M. L. Heil, F. Kasolo, R. Musonda, B. H. Hahn, G. M. Shaw, B. T. Korber, S. Allen, and E. Hunter. 2004. Envelope-constrained neutralization-sensitive HIV-1 after heterosexual transmission. *Science*. 303:2019-2022.
37. Derdeyn, C. A., J. M. Decker, J. N. Sfakianos, X. Wu, W. A. O'Brien, L. Ratner, J. C. Kappes, G. M. Shaw, and E. Hunter. 2000. Sensitivity of human immunodeficiency virus type 1 to the fusion inhibitor T-20 is modulated by coreceptor specificity defined by the V3 loop of gp120. *J. Virol.* 74:8358-8367.
38. Derdeyn, C. A., and E. Hunter. 2008. Viral characteristics of transmitted HIV. *Curr. Opin. HIV. AIDS*. 3:16-21.
39. Dickover, R., E. Garratty, K. Yusim, C. Miller, B. Korber, and Y. Bryson. 2006. Role of maternal autologous neutralizing antibody in selective perinatal transmission of human immunodeficiency virus type 1 escape variants. *J. Virol.* 80:6525-6533.
40. Dickover, R. E., E. M. Garratty, S. Plaeger, and Y. J. Bryson. 2001. Perinatal transmission of major, minor, and multiple maternal human immunodeficiency virus type 1 variants in utero and intrapartum. *J. Virol.* 75:2194-2203.
41. Duenas-Decamp, M. J., P. Peters, D. Burton, and P. R. Clapham. 2009. Determinants flanking the CD4 binding loop modulate macrophage-tropism of HIV-1 R5 envelopes. *J. Virol.*
42. Dunfee, R. L., E. R. Thomas, and D. Gabuzda. 2009. Enhanced macrophage tropism of HIV in brain and lymphoid tissues is associated with sensitivity to the broadly neutralizing CD4 binding site antibody b12. *Retrovirology*. 6:69.
43. Dunfee, R. L., E. R. Thomas, P. R. Gorry, J. Wang, J. Taylor, K. Kunstman, S. M. Wolinsky, and D. Gabuzda. 2006. The HIV Env variant N283 enhances macrophage tropism and is associated with brain infection and dementia. *Proc. Natl. Acad. Sci. U. S. A.* 103:15160-15165.
44. Duri, K., W. Soko, F. Gumbo, K. Kristiansen, M. Mapingure, B. Stray-Pedersen, F. Muller, and the BHAMC Group. 2010. Genotypic Analysis of Human Immunodeficiency Virus Type 1 (HIV-1) env V3 Loop Sequences: Bioinformatics Prediction of Coreceptor Usage among 28 Infected Mother-Infant Pairs in a Drug-Naive Population. *AIDS Res. Hum. Retroviruses*.
45. Earl, P. L., R. W. Doms, and B. Moss. 1990. Oligomeric structure of the human immunodeficiency virus type 1 envelope glycoprotein. *Proc. Natl. Acad. Sci. U. S. A.* 87:648-652.

46. Eccleston, J. F., D. D. Binns, C. T. Davis, J. P. Albanesi, and D. M. Jameson. 2002. Oligomerization and kinetic mechanism of the dynamin GTPase. *Eur. Biophys. J.* 31:275-282.
47. Edwards, T. G., T. L. Hoffman, F. Baribaud, S. Wyss, C. C. LaBranche, J. Romano, J. Adkinson, M. Sharron, J. A. Hoxie, and R. W. Doms. 2001. Relationships between CD4 independence, neutralization sensitivity, and exposure of a CD4-induced epitope in a human immunodeficiency virus type 1 envelope protein. *J. Virol.* 75:5230-5239.
48. Etemad, B., A. Fellows, B. Kwambana, A. Kamat, Y. Feng, S. Lee, and M. Sagar. 2009. Human immunodeficiency virus type 1 V1-to-V5 envelope variants from the chronic phase of infection use CCR5 and fuse more efficiently than those from early after infection. *J. Virol.* 83:9694-9708.
49. Feng, Y., C. C. Broder, P. E. Kennedy, and E. A. Berger. 1996. HIV-1 entry cofactor: functional cDNA cloning of a seven-transmembrane, G protein-coupled receptor. *Science.* 272:872-877.
50. Ferrantelli, F., R. A. Rasmussen, K. A. Buckley, P. L. Li, T. Wang, D. C. Montefiori, H. Katinger, G. Stiegler, D. C. Anderson, H. M. McClure, and R. M. Ruprecht. 2004. Complete protection of neonatal rhesus macaques against oral exposure to pathogenic simian-human immunodeficiency virus by human anti-HIV monoclonal antibodies. *J. Infect. Dis.* 189:2167-2173.
51. Fischetti, L., K. Danso, A. Dompok, V. Addo, L. Haaheim, and J. P. Allain. 2005. Vertical transmission of HIV in Ghanaian women diagnosed in cord blood and post-natal samples. *J. Med. Virol.* 77:351-359. doi: 10.1002/jmv.20463.
52. Flynn, N. M., D. N. Forthal, C. D. Harro, F. N. Judson, K. H. Mayer, M. F. Para, and rgp120 HIV Vaccine Study Group. 2005. Placebo-controlled phase 3 trial of a recombinant glycoprotein 120 vaccine to prevent HIV-1 infection. *J. Infect. Dis.* 191:654-665.
53. Fowler, M. G., and M. L. Newell. 2002. Breast-feeding and HIV-1 transmission in resource-limited settings. *J. Acquir. Immune Defic. Syndr.* 30:230-239.
54. Fredericksen, B. L., B. L. Wei, J. Yao, T. Luo, and J. V. Garcia. 2002. Inhibition of endosomal/lysosomal degradation increases the infectivity of human immunodeficiency virus. *J. Virol.* 76:11440-11446.

55. Gallo, S. A., C. M. Finnegan, M. Viard, Y. Raviv, A. Dimitrov, S. S. Rawat, A. Puri, S. Durell, and R. Blumenthal. 2003. The HIV Env-mediated fusion reaction. *Biochim. Biophys. Acta.* 1614:36-50.
56. Gao, F., S. G. Morrison, D. L. Robertson, C. L. Thornton, S. Craig, G. Karlsson, J. Sodroski, M. Morgado, B. Galvao-Castro, H. von Briesen, S. Beddows, J. Weber, P. M. Sharp, G. M. Shaw, and B. H. Hahn. 1996. Molecular cloning and analysis of functional envelope genes from human immunodeficiency virus type 1 sequence subtypes A through G. The WHO and NIAID Networks for HIV Isolation and Characterization. *J. Virol.* 70:1651-1667.
57. Gaschen, B., J. Taylor, K. Yusim, B. Foley, F. Gao, D. Lang, V. Novitsky, B. Haynes, B. H. Hahn, T. Bhattacharya, and B. Korber. 2002. Diversity considerations in HIV-1 vaccine selection. *Science.* 296:2354-2360.
58. Goonetilleke, N., M. K. Liu, J. F. Salazar-Gonzalez, G. Ferrari, E. Giorgi, V. V. Ganusov, B. F. Keele, G. H. Learn, E. L. Turnbull, M. G. Salazar, K. J. Weinhold, S. Moore, CHAVI Clinical Core B, N. Letvin, B. F. Haynes, M. S. Cohen, P. Hraber, T. Bhattacharya, P. Borrow, A. S. Perelson, B. H. Hahn, G. M. Shaw, B. T. Korber, and A. J. McMichael. 2009. The first T cell response to transmitted/founder virus contributes to the control of acute viremia in HIV-1 infection. *J. Exp. Med.*
59. Gorry, P. R., R. L. Dunfee, M. E. Mefford, K. Kunstman, T. Morgan, J. P. Moore, J. R. Mascola, K. Agopian, G. H. Holm, A. Mehle, J. Taylor, M. Farzan, H. Wang, P. Ellery, S. J. Willey, P. R. Clapham, S. M. Wolinsky, S. M. Crowe, and D. Gabuzda. 2007. Changes in the V3 region of gp120 contribute to unusually broad coreceptor usage of an HIV-1 isolate from a CCR5 Delta32 heterozygote. *Virology.* 362:163-178.
60. Gorry, P. R., J. Taylor, G. H. Holm, A. Mehle, T. Morgan, M. Cayabyab, M. Farzan, H. Wang, J. E. Bell, K. Kunstman, J. P. Moore, S. M. Wolinsky, and D. Gabuzda. 2002. Increased CCR5 affinity and reduced CCR5/CD4 dependence of a neurovirulent primary human immunodeficiency virus type 1 isolate. *J. Virol.* 76:6277-6292.
61. Graham, F. L., J. Smiley, W. C. Russell, and R. Nairn. 1977. Characteristics of a human cell line transformed by DNA from human adenovirus type 5. *J. Gen. Virol.* 36:59-74.
62. Gray, E. S., T. Meyers, G. Gray, D. C. Montefiori, and L. Morris. 2006. Insensitivity of paediatric HIV-1 subtype C viruses to broadly neutralising monoclonal antibodies raised against subtype B. *PLoS Med.* 3:e255.

63. Gray, E. S., P. L. Moore, F. Bibollet-Ruche, H. Li, J. M. Decker, T. Meyers, G. M. Shaw, and L. Morris. 2008. 4E10-resistant variants in a human immunodeficiency virus type 1 subtype C-infected individual with an anti-membrane-proximal external region-neutralizing antibody response. *J. Virol.* 82:2367-2375.
64. Gray, E. S., P. L. Moore, R. A. Pantophlet, and L. Morris. 2007. N-Linked Glycan Modifications in gp120 of Human Immunodeficiency Virus Type 1 Subtype C Render Partial Sensitivity to 2G12 Antibody Neutralization. *J. Virol.* 81:10769-10776.
65. Gray, L., J. Sterjovski, M. Churchill, P. Ellery, N. Nasr, S. R. Lewin, S. M. Crowe, S. L. Wesselingh, A. L. Cunningham, and P. R. Gorry. 2005. Uncoupling coreceptor usage of human immunodeficiency virus type 1 (HIV-1) from macrophage tropism reveals biological properties of CCR5-restricted HIV-1 isolates from patients with acquired immunodeficiency syndrome. *Virology.* 337:384-398.
66. Guay, L. A., P. Musoke, T. Fleming, D. Bagenda, M. Allen, C. Nakabiito, J. Sherman, P. Bakaki, C. Ducar, M. Deseyve, L. Emel, M. Mirochnick, M. G. Fowler, L. Mofenson, P. Miotti, K. Dransfield, D. Bray, F. Mmiro, and J. B. Jackson. 1999. Intrapartum and neonatal single-dose nevirapine compared with zidovudine for prevention of mother-to-child transmission of HIV-1 in Kampala, Uganda: HIVNET 012 randomised trial. *Lancet.* 354:795-802.
67. Haaland, R. E., P. A. Hawkins, J. Salazar-Gonzalez, A. Johnson, A. Tichacek, E. Karita, O. Manigart, J. Mulenga, B. F. Keele, G. M. Shaw, B. H. Hahn, S. A. Allen, C. A. Derdeyn, and E. Hunter. 2009. Inflammatory genital infections mitigate a severe genetic bottleneck in heterosexual transmission of subtype A and C HIV-1. *PLoS Pathog.* 5:e1000274.
68. Haase, A. T. 1999. Population biology of HIV-1 infection: viral and CD4+ T cell demographics and dynamics in lymphatic tissues. *Annu. Rev. Immunol.* 17:625-656.
69. Hahn, B. H., G. M. Shaw, K. M. De Cock, and P. M. Sharp. 2000. AIDS as a zoonosis: scientific and public health implications. *Science.* 287:607-614.
70. Hammer, S. M., J. J. Eron Jr, P. Reiss, R. T. Schooley, M. A. Thompson, S. Walmsley, P. Cahn, M. A. Fischl, J. M. Gatell, M. S. Hirsch, D. M. Jacobsen, J. S. Montaner, D. D. Richman, P. G. Yeni, P. A. Volberding, and International AIDS Society-USA. 2008. Antiretroviral treatment of adult HIV infection: 2008 recommendations of the International AIDS Society-USA panel. *JAMA.* 300:555-570.

71. Haynes, B. F., and D. C. Montefiori. 2006. Aiming to induce broadly reactive neutralizing antibody responses with HIV-1 vaccine candidates. *Expert Rev. Vaccines*. 5:579-595.
72. Hel, Z., D. Venzon, M. Poudyal, W. P. Tsai, L. Giuliani, R. Woodward, C. Chougnet, G. Shearer, J. D. Altman, D. Watkins, N. Bischofberger, A. Abimiku, P. Markham, J. Tartaglia, and G. Franchini. 2000. Viremia control following antiretroviral treatment and therapeutic immunization during primary SIV251 infection of macaques. *Nat. Med.* 6:1140-1146.
73. Helseth, E., U. Olshevsky, C. Furman, and J. Sodroski. 1991. Human immunodeficiency virus type 1 gp120 envelope glycoprotein regions important for association with the gp41 transmembrane glycoprotein. *J. Virol.* 65:2119-2123.
74. Hemelaar, J., E. Gouws, P. D. Ghys, and S. Osmanov. 2006. Global and regional distribution of HIV-1 genetic subtypes and recombinants in 2004. *AIDS*. 20:W13-23.
75. Hengel, R. L., M. S. Kennedy, R. W. Steketee, D. M. Thea, E. J. Abrams, G. Lambert, and J. S. McDougal. 1998. Neutralizing antibody and perinatal transmission of human immunodeficiency virus type 1. New York City Perinatal HIV Transmission Collaborative Study Group. *AIDS Res. Hum. Retroviruses*. 14:475-481.
76. Hill, E., J. van Der Kaay, C. P. Downes, and E. Smythe. 2001. The role of dynamin and its binding partners in coated pit invagination and scission. *J. Cell Biol.* 152:309-323.
77. Hofmann-Lehmann, R., J. Vlasak, R. A. Rasmussen, B. A. Smith, T. W. Baba, V. Liska, F. Ferrantelli, D. C. Montefiori, H. M. McClure, D. C. Anderson, B. J. Bernacky, T. A. Rizvi, R. Schmidt, L. R. Hill, M. E. Keeling, H. Katinger, G. Stiegler, L. A. Cavacini, M. R. Posner, T. C. Chou, J. Andersen, and R. M. Ruprecht. 2001. Postnatal passive immunization of neonatal macaques with a triple combination of human monoclonal antibodies against oral simian-human immunodeficiency virus challenge. *J. Virol.* 75:7470-7480.
78. Hu, J., M. B. Gardner, and C. J. Miller. 2000. Simian immunodeficiency virus rapidly penetrates the cervicovaginal mucosa after intravaginal inoculation and infects intraepithelial dendritic cells. *J. Virol.* 74:6087-6095.
79. Iordanskiy, S., M. Waltke, Y. Feng, and C. Wood. 2010. Subtype-associated differences in HIV-1 reverse transcription affect the viral replication. *Retrovirology*. 7:85.

80. Isaacman-Beck, J., E. A. Hermann, Y. Yi, S. J. Ratcliffe, J. Mulenga, S. Allen, E. Hunter, C. A. Derdeyn, and R. G. Collman. 2009. Heterosexual transmission of human immunodeficiency virus type 1 subtype C: Macrophage tropism, alternative coreceptor use, and the molecular anatomy of CCR5 utilization. *J. Virol.* 83:8208-8220.
81. Javaherian, K., A. J. Langlois, C. McDanal, K. L. Ross, L. I. Eckler, C. L. Jellis, A. T. Profy, J. R. Rusche, D. P. Bolognesi, and S. D. Putney. 1989. Principal neutralizing domain of the human immunodeficiency virus type 1 envelope protein. *Proc. Natl. Acad. Sci. U. S. A.* 86:6768-6772.
82. Johnson, J. A., J. F. Li, X. Wei, J. Lipscomb, D. Irlbeck, C. Craig, A. Smith, D. E. Bennett, M. Monsour, P. Sandstrom, E. R. Lanier, and W. Heneine. 2008. Minority HIV-1 drug resistance mutations are present in antiretroviral treatment-naive populations and associate with reduced treatment efficacy. *PLoS Med.* 5:e158.
83. Joint United Nations Programme on HIV/AIDS (UNAIDS). 2010. UNAIDS report on the global AIDS epidemic 2010. .
84. Jordan, M. R., M. Kearney, S. Palmer, W. Shao, F. Maldarelli, E. P. Coakley, C. Chappey, C. Wanke, and J. M. Coffin. 2010. Comparison of standard PCR/cloning to single genome sequencing for analysis of HIV-1 populations. *J. Virol. Methods.*
85. Kanki, P. J., D. J. Hamel, J. L. Sankale, C. Hsieh, I. Thior, F. Barin, S. A. Woodcock, A. Gueye-Ndiaye, E. Zhang, M. Montano, T. Siby, R. Marlink, I. NDoye, M. E. Essex, and S. MBoup. 1999. Human immunodeficiency virus type 1 subtypes differ in disease progression. *J. Infect. Dis.* 179:68-73.
86. Katen, L. J., M. M. Januszski, W. F. Anderson, K. J. Hasenkrug, and L. H. Evans. 2001. Infectious entry by amphotropic as well as ecotropic murine leukemia viruses occurs through an endocytic pathway. *J. Virol.* 75:5018-5026.
87. Keele, B. F., E. E. Giorgi, J. F. Salazar-Gonzalez, J. M. Decker, K. T. Pham, M. G. Salazar, C. Sun, T. Grayson, S. Wang, H. Li, X. Wei, C. Jiang, J. L. Kirchherr, F. Gao, J. A. Anderson, L. H. Ping, R. Swanstrom, G. D. Tomaras, W. A. Blattner, P. A. Goepfert, J. M. Kilby, M. S. Saag, E. L. Delwart, M. P. Busch, M. S. Cohen, D. C. Montefiori, B. F. Haynes, B. Gaschen, G. S. Athreya, H. Y. Lee, N. Wood, C. Seoighe, A. S. Perelson, T. Bhattacharya, B. T. Korber, B. H. Hahn, and G. M. Shaw. 2008. Identification and characterization of transmitted and early founder virus envelopes in primary HIV-1 infection. *Proc. Natl. Acad. Sci. U. S. A.*

88. Keele, B. F., F. Van Heuverswyn, Y. Li, E. Bailes, J. Takehisa, M. L. Santiago, F. Bibollet-Ruche, Y. Chen, L. V. Wain, F. Liegeois, S. Loul, E. M. Ngole, Y. Bienvenue, E. Delaporte, J. F. Brookfield, P. M. Sharp, G. M. Shaw, M. Peeters, and B. H. Hahn. 2006. Chimpanzee reservoirs of pandemic and nonpandemic HIV-1. *Science*. 313:523-526.
89. Kent, S. J., A. Zhao, S. J. Best, J. D. Chandler, D. B. Boyle, and I. A. Ramshaw. 1998. Enhanced T-cell immunogenicity and protective efficacy of a human immunodeficiency virus type 1 vaccine regimen consisting of consecutive priming with DNA and boosting with recombinant fowlpox virus. *J. Virol.* 72:10180-10188.
90. Kimura, M. 1980. A simple method for estimating evolutionary rates of base substitutions through comparative studies of nucleotide sequences. *J. Mol. Evol.* 16:111-120.
91. Klatzmann, D., E. Champagne, S. Chamaret, J. Gruest, D. Guetard, T. Hercend, J. C. Gluckman, and L. Montagnier. 1984. T-lymphocyte T4 molecule behaves as the receptor for human retrovirus LAV. *Nature*. 312:767-768.
92. Kliks, S., C. H. Contag, H. Corliss, G. Learn, A. Rodrigo, D. Wara, J. I. Mullins, and J. A. Levy. 2000. Genetic analysis of viral variants selected in transmission of human immunodeficiency viruses to newborns. *AIDS Res. Hum. Retroviruses*. 16:1223-1233.
93. Kolchinsky, P., E. Kiprilov, P. Bartley, R. Rubinstein, and J. Sodroski. 2001. Loss of a single N-linked glycan allows CD4-independent human immunodeficiency virus type 1 infection by altering the position of the gp120 V1/V2 variable loops. *J. Virol.* 75:3435-3443.
94. Kolokoltsov, A. A., D. Deniger, E. H. Fleming, N. J. Roberts Jr, J. M. Karpilow, and R. A. Davey. 2007. Small interfering RNA profiling reveals key role of clathrin-mediated endocytosis and early endosome formation for infection by respiratory syncytial virus. *J. Virol.* 81:7786-7800.
95. Kong, X., J. T. West, H. Zhang, D. M. Shea, T. J. M'soka, and C. Wood. 2008. The human immunodeficiency virus type 1 envelope confers higher rates of replicative fitness to perinatally transmitted viruses than to nontransmitted viruses. *J. Virol.* 82:11609-11618.
96. Korber, B., B. Gaschen, K. Yusim, R. Thakallapally, C. Kesmir, and V. Detours. 2001. Evolutionary and immunological implications of contemporary HIV-1 variation. *Br. Med. Bull.* 58:19-42.

97. Korber, B., M. Muldoon, J. Theiler, F. Gao, R. Gupta, A. Lapedes, B. H. Hahn, S. Wolinsky, and T. Bhattacharya. 2000. Timing the ancestor of the HIV-1 pandemic strains. *Science*. 288:1789-1796.
98. Koup, R. A., J. E. Robinson, Q. V. Nguyen, C. A. Pikora, B. Blais, A. Roskey, D. Panicali, and J. L. Sullivan. 1991. Antibody-dependent cell-mediated cytotoxicity directed by a human monoclonal antibody reactive with gp120 of HIV-1. *AIDS*. 5:1309-1314.
99. Kourtis, A. P., A. M. Amedee, M. Bulterys, S. Danner, R. Van Dyke, M. J. O'Sullivan, R. Maupin, and D. J. Jamieson. 2010. Various Viral Compartments in HIV-1-Infected Mothers Contribute to In Utero Transmission of HIV-1. *AIDS Res. Hum. Retroviruses*.
100. Kourtis, A. P., M. Bulterys, S. R. Nesheim, and F. K. Lee. 2001. Understanding the timing of HIV transmission from mother to infant. *JAMA*. 285:709-712.
101. Koyama, A. H., and T. Uchida. 1987. The mode of entry of herpes simplex virus type 1 into Vero cells. *Microbiol. Immunol.* 31:123-130.
102. Kwong, P. D., M. L. Doyle, D. J. Casper, C. Cicala, S. A. Leavitt, S. Majeed, T. D. Steenbeke, M. Venturi, I. Chaiken, M. Fung, H. Katinger, P. W. Parren, J. Robinson, D. Van Ryk, L. Wang, D. R. Burton, E. Freire, R. Wyatt, J. Sodroski, W. A. Hendrickson, and J. Arthos. 2002. HIV-1 evades antibody-mediated neutralization through conformational masking of receptor-binding sites. *Nature*. 420:678-682.
103. Lallemand, M., G. Jourdain, S. Le Coeur, J. Y. Mary, N. Ngo-Giang-Huong, S. Koetsawang, S. Kanshana, K. McIntosh, V. Thaineua, and Perinatal HIV Prevention Trial (Thailand) Investigators. 2004. Single-dose perinatal nevirapine plus standard zidovudine to prevent mother-to-child transmission of HIV-1 in Thailand. *N. Engl. J. Med.* 351:217-228.
104. Lassen, K. G., M. A. Lobritz, J. R. Bailey, S. Johnston, S. Nguyen, B. Lee, T. Chou, R. F. Siliciano, M. Markowitz, and E. J. Arts. 2009. Elite suppressor-derived HIV-1 envelope glycoproteins exhibit reduced entry efficiency and kinetics. *PLoS Pathog.* 5:e1000377.
105. Lee, B., M. Sharron, L. J. Montaner, D. Weissman, and R. W. Doms. 1999. Quantification of CD4, CCR5, and CXCR4 levels on lymphocyte subsets, dendritic cells, and differentially conditioned monocyte-derived macrophages. *Proc. Natl. Acad. Sci. U. S. A.* 96:5215-5220.

106. Leroy, V., M. L. Newell, F. Dabis, C. Peckham, P. Van de Perre, M. Bulterys, C. Kind, R. J. Simonds, S. Wiktor, and P. Msellati. 1998. International multicentre pooled analysis of late postnatal mother-to-child transmission of HIV-1 infection. Ghent International Working Group on Mother-to-Child Transmission of HIV. *Lancet*. 352:597-600.
107. Letvin, N. L. 2006. Progress and obstacles in the development of an AIDS vaccine. *Nat. Rev. Immunol.* 6:930-939.
108. Letvin, N. L., D. H. Barouch, and D. C. Montefiori. 2002. Prospects for vaccine protection against HIV-1 infection and AIDS. *Annu. Rev. Immunol.* 20:73-99.
109. Li, M., F. Gao, J. R. Mascola, L. Stamatatos, V. R. Polonis, M. Koutsoukos, G. Voss, P. Goepfert, P. Gilbert, K. M. Greene, M. Bilska, D. L. Kothe, J. F. Salazar-Gonzalez, X. Wei, J. M. Decker, B. H. Hahn, and D. C. Montefiori. 2005. Human immunodeficiency virus type 1 env clones from acute and early subtype B infections for standardized assessments of vaccine-elicited neutralizing antibodies. *J. Virol.* 79:10108-10125.
110. Li, M., J. F. Salazar-Gonzalez, C. A. Derdeyn, L. Morris, C. Williamson, J. E. Robinson, J. M. Decker, Y. Li, M. G. Salazar, V. R. Polonis, K. Mlisana, S. A. Karim, K. Hong, K. M. Greene, M. Bilska, J. Zhou, S. Allen, E. Chomba, J. Mulenga, C. Vwalika, F. Gao, M. Zhang, B. T. Korber, E. Hunter, B. H. Hahn, and D. C. Montefiori. 2006. Genetic and neutralization properties of subtype C human immunodeficiency virus type 1 molecular env clones from acute and early heterosexually acquired infections in Southern Africa. *J. Virol.* 80:11776-11790.
111. Lu, S. 2006. Combination DNA plus protein HIV vaccines. *Springer Semin. Immunopathol.* 28:255-265.
112. Luallen, R. J., J. Lin, H. Fu, K. K. Cai, C. Agrawal, I. Mboudjeka, F. H. Lee, D. Montefiori, D. F. Smith, R. W. Doms, and Y. Geng. 2008. An engineered *Saccharomyces cerevisiae* strain binds the broadly neutralizing human immunodeficiency virus type 1 antibody 2G12 and elicits mannose-specific gp120-binding antibodies. *J. Virol.* 82:6447-6457.
113. Luzuriaga, K., M. L. Newell, F. Dabis, J. L. Excler, and J. L. Sullivan. 2006. Vaccines to prevent transmission of HIV-1 via breastmilk: scientific and logistical priorities. *Lancet.* 368:511-521.
114. Luzuriaga, K., and J. L. Sullivan. 2002. Pediatric HIV-1 infection: advances and remaining challenges. *AIDS. Rev.* 4:21-26.

115. Macia, E., M. Ehrlich, R. Massol, E. Boucrot, C. Brunner, and T. Kirchhausen. 2006. Dynasore, a cell-permeable inhibitor of dynamin. *Dev. Cell.* 10:839-850.
116. Maddon, P. J., J. S. McDougal, P. R. Clapham, A. G. Dalgleish, S. Jamal, R. A. Weiss, and R. Axel. 1988. HIV infection does not require endocytosis of its receptor, CD4. *Cell.* 54:865-874.
117. Mascola, J. R., P. D'Souza, P. Gilbert, B. H. Hahn, N. L. Haigwood, L. Morris, C. J. Petropoulos, V. R. Polonis, M. Sarzotti, and D. C. Montefiori. 2005. Recommendations for the design and use of standard virus panels to assess neutralizing antibody responses elicited by candidate human immunodeficiency virus type 1 vaccines. *J. Virol.* 79:10103-10107.
118. Mascola, J. R., and D. C. Montefiori. 2003. HIV-1: nature's master of disguise. *Nat. Med.* 9:393-394.
119. Matlin, K. S., H. Reggio, A. Helenius, and K. Simons. 1982. Pathway of vesicular stomatitis virus entry leading to infection. *J. Mol. Biol.* 156:609-631.
120. McClure, M. O., M. Marsh, and R. A. Weiss. 1988. Human immunodeficiency virus infection of CD4-bearing cells occurs by a pH-independent mechanism. *EMBO J.* 7:513-518.
121. McLean, R. A., W. L. Sanders, and W. W. Stroup. 1991. A unified approach to mixed linear models. *American Statistician.* 45:54.
122. McMichael, A. J. 2006. HIV vaccines. *Annu. Rev. Immunol.* 24:227-255.
123. Miller, C. J., Q. Li, K. Abel, E. Y. Kim, Z. M. Ma, S. Wietgreffe, L. La Franco-Scheuch, L. Compton, L. Duan, M. D. Shore, M. Zupancic, M. Busch, J. Carlis, S. Wolinsky, and A. T. Haase. 2005. Propagation and dissemination of infection after vaginal transmission of simian immunodeficiency virus. *J. Virol.* 79:9217-9227.
124. Miotti, P. G., T. E. Taha, N. I. Kumwenda, R. Broadhead, L. A. Mtimavalye, L. Van der Hoeven, J. D. Chipangwi, G. Liomba, and R. J. Biggar. 1999. HIV transmission through breastfeeding: a study in Malawi. *JAMA.* 282:744-749.
125. Miyauchi, K., Y. Kim, O. Latinovic, V. Morozov, and G. B. Melikyan. 2009. HIV enters cells via endocytosis and dynamin-dependent fusion with endosomes. *Cell.* 137:433-444.

126. Miyauchi, K., M. M. Kozlov, and G. B. Melikyan. 2009. Early steps of HIV-1 fusion define the sensitivity to inhibitory peptides that block 6-helix bundle formation. *PLoS Pathog.* 5:e1000585.
127. Mofenson, L. M., and J. A. McIntyre. 2000. Advances and research directions in the prevention of mother-to-child HIV-1 transmission. *Lancet.* 355:2237-2244.
128. Montefiori, D. 2004. Evaluating neutralizing antibodies against HIV, SIV and SHIV in luciferase reporter gene assays, p. 12.11.1-12.11.15. *In* J. E. Coligan, D. H. Kruisbeek, E. M. Margulies, W. Strober, and R. Coico (eds.), *Current Protocols in Immunology*. John Wiley & Sons, Inc.
129. Moore, C. B., M. John, I. R. James, F. T. Christiansen, C. S. Witt, and S. A. Mallal. 2002. Evidence of HIV-1 adaptation to HLA-restricted immune responses at a population level. *Science.* 296:1439-1443.
130. Morris, L. 2002. Neutralizing antibody responses to HIV-1 infection. *IUBMB Life.* 53:197-199.
131. Moulard, M., S. K. Phogat, Y. Shu, A. F. Labrijn, X. Xiao, J. M. Binley, M. Y. Zhang, I. A. Sidorov, C. C. Broder, J. Robinson, P. W. Parren, D. R. Burton, and D. S. Dimitrov. 2002. Broadly cross-reactive HIV-1-neutralizing human monoclonal Fab selected for binding to gp120-CD4-CCR5 complexes. *Proc. Natl. Acad. Sci. U. S. A.* 99:6913-6918.
132. Muster, T., F. Steindl, M. Purtscher, A. Trkola, A. Klima, G. Himmler, F. Ruker, and H. Katinger. 1993. A conserved neutralizing epitope on gp41 of human immunodeficiency virus type 1. *J. Virol.* 67:6642-6647.
133. Nakamura, K. J., J. S. Gach, L. Jones, K. Semrau, J. Walter, F. Bibollet-Ruche, J. M. Decker, L. Heath, W. D. Decker, M. Sinkala, C. Kankasa, D. Thea, J. Mullins, L. Kuhn, M. B. Zwick, and G. M. Aldrovandi. 2010. 4E10-resistant HIV-1 isolated from four subjects with rare membrane-proximal external region polymorphisms. *PLoS One.* 5:e9786.
134. Nduati, R., G. John, D. Mbori-Ngacha, B. Richardson, J. Overbaugh, A. Mwatha, J. Ndinya-Achola, J. Bwayo, F. E. Onyango, J. Hughes, and J. Kreiss. 2000. Effect of breastfeeding and formula feeding on transmission of HIV-1: a randomized clinical trial. *JAMA.* 283:1167-1174.
135. Neumann, T., I. Hagmann, S. Lohrengel, M. L. Heil, C. A. Derdeyn, H. G. Krausslich, and M. T. Dittmar. 2005. T20-insensitive HIV-1 from naive patients

exhibits high viral fitness in a novel dual-color competition assay on primary cells. *Virology*. 333:251-262.

136. Newell, M. L. 2006. Current issues in the prevention of mother-to-child transmission of HIV-1 infection. *Trans. R. Soc. Trop. Med. Hyg.* 100:1-5.

137. Newell, M. L., H. Coovadia, M. Cortina-Borja, N. Rollins, P. Gaillard, F. Dabis, and Ghent International AIDS Society (IAS) Working Group on HIV Infection in Women and Children. 2004. Mortality of infected and uninfected infants born to HIV-infected mothers in Africa: a pooled analysis. *Lancet*. 364:1236-1243.

138. Nowak, P., A. C. Karlsson, L. Naver, A. B. Bohlin, A. Piasek, and A. Sonnerborg. 2002. The selection and evolution of viral quasispecies in HIV-1 infected children. *HIV. Med.* 3:1-11.

139. OriginLab Corporation. 2003. Origin Scientific Graphing and Analysis Software. , Northampton, MA.

140. Over, M., and P. Piot. 1996. Human immunodeficiency virus infection and other sexually transmitted diseases in developing countries: public health importance and priorities for resource allocation. *J. Infect. Dis.* 174:S162-75.

141. Pal, R., V. S. Kalyanaraman, B. C. Nair, S. Whitney, T. Keen, L. Hocker, L. Hudacik, N. Rose, I. Mboudjeka, S. Shen, T. H. Wu-Chou, D. Montefiori, J. Mascola, P. Markham, and S. Lu. 2006. Immunization of rhesus macaques with a polyvalent DNA prime/protein boost human immunodeficiency virus type 1 vaccine elicits protective antibody response against simian human immunodeficiency virus of R5 phenotype. *Virology*. 348:341-353.

142. Patterson, S., J. S. Oxford, and R. R. Dourmashkin. 1979. Studies on the mechanism of influenza virus entry into cells. *J. Gen. Virol.* 43:223-229.

143. Perelson, A. S., A. U. Neumann, M. Markowitz, J. M. Leonard, and D. D. Ho. 1996. HIV-1 dynamics in vivo: virion clearance rate, infected cell life-span, and viral generation time. *Science*. 271:1582-1586.

144. Peressin, M., V. Holl, S. Schmidt, T. Decoville, D. Mirisky, A. Lederle, M. Delaporte, K. Xu, A. M. Aubertin, and C. Moog. 2011. HIV-1 Replication in Langerhans and Interstitial Dendritic Cells Is Inhibited by Neutralizing and Fc-Mediated Inhibitory Antibodies. *J. Virol.* 85:1077-1085.

145. Peters, P. J., J. Bhattacharya, S. Hibbitts, M. T. Dittmar, G. Simmons, J. Bell, P. Simmonds, and P. R. Clapham. 2004. Biological analysis of human

immunodeficiency virus type 1 R5 envelopes amplified from brain and lymph node tissues of AIDS patients with neuropathology reveals two distinct tropism phenotypes and identifies envelopes in the brain that confer an enhanced tropism and fusogenicity for macrophages. *J. Virol.* 78:6915-6926.

146. Peters, P. J., M. J. Duenas-Decamp, W. M. Sullivan, R. Brown, C. Ankghuambom, K. Luzuriaga, J. Robinson, D. R. Burton, J. Bell, P. Simmonds, J. Ball, and P. Clapham. 2008. Variation in HIV-1 R5 macrophage-tropism correlates with sensitivity to reagents that block envelope: CD4 interactions but not with sensitivity to other entry inhibitors. *Retrovirology.* 5:5.

147. Peters, P. J., M. J. Duenas-Decamp, W. M. Sullivan, and P. R. Clapham. 2007. Variation of macrophage tropism among HIV-1 R5 envelopes in brain and other tissues. *J. Neuroimmune Pharmacol.* 2:32-41. 148. Peters, P. J., W. M. Sullivan, M. J. Duenas-Decamp, J. Bhattacharya, C. Ankghuambom, R. Brown, K. Luzuriaga, J. Bell, P. Simmonds, J. Ball, and P. R. Clapham. 2006. Non-macrophage-tropic human immunodeficiency virus type 1 R5 envelopes predominate in blood, lymph nodes, and semen: implications for transmission and pathogenesis. *J. Virol.* 80:6324-6332.

149. Pitisuttithum, P., P. Gilbert, M. Gurwith, W. Heyward, M. Martin, F. van Griensven, D. Hu, J. W. Tappero, K. Choopanya, and Bangkok Vaccine Evaluation Group. 2006. Randomized, double-blind, placebo-controlled efficacy trial of a bivalent recombinant glycoprotein 120 HIV-1 vaccine among injection drug users in Bangkok, Thailand. *J. Infect. Dis.* 194:1661-1671.

150. Plantier, J. C., M. Leoz, J. E. Dickerson, F. De Oliveira, F. Cordonnier, V. Leme, F. Damond, D. L. Robertson, and F. Simon. 2009. A new human immunodeficiency virus derived from gorillas. *Nat. Med.* 15:871-872.

151. Platt, E. J., K. Wehrly, S. E. Kuhmann, B. Chesebro, and D. Kabat. 1998. Effects of CCR5 and CD4 cell surface concentrations on infections by macrophagetropic isolates of human immunodeficiency virus type 1. *J. Virol.* 72:2855-2864.

152. Powell, R. L., T. Kinge, and P. N. Nyambi. 2010. Infection by discordant strains of HIV-1 markedly enhances the neutralizing antibody response against heterologous virus. *J. Virol.* 84:9415-9426.

153. Preston, B. D., B. J. Poiesz, and L. A. Loeb. 1988. Fidelity of HIV-1 reverse transcriptase. *Science.* 242:1168-1171.

154. Price, D. A., P. J. Goulder, P. Klenerman, A. K. Sewell, P. J. Easterbrook, M. Troop, C. R. Bangham, and R. E. Phillips. 1997. Positive selection of HIV-1

cytotoxic T lymphocyte escape variants during primary infection. *Proc. Natl. Acad. Sci. U. S. A.* 94:1890-1895.

155. Puffer, B. A., S. Pohlmann, A. L. Edinger, D. Carlin, M. D. Sanchez, J. Reitter, D. D. Watry, H. S. Fox, R. C. Desrosiers, and R. W. Doms. 2002. CD4 independence of simian immunodeficiency virus Envs is associated with macrophage tropism, neutralization sensitivity, and attenuated pathogenicity. *J. Virol.* 76:2595-2605.

156. Quinn, T. C., and J. Overbaugh. 2005. HIV/AIDS in women: an expanding epidemic. *Science.* 308:1582-1583..

157. Ramsay, A. J., K. H. Leong, and I. A. Ramshaw. 1997. DNA vaccination against virus infection and enhancement of antiviral immunity following consecutive immunization with DNA and viral vectors. *Immunol. Cell Biol.* 75:382-388.

158. Read, J. S. 2010. Prevention of Mother-to-Child Transmission of HIV: Antiretroviral Strategies. *Clin. Perinatol.* 37:765-776. doi: 10.1016/j.clp.2010.08.007.

159. Reinhart, T. A., M. J. Rogan, D. Huddleston, D. M. Rausch, L. E. Eiden, and A. T. Haase. 1997. Simian immunodeficiency virus burden in tissues and cellular compartments during clinical latency and AIDS. *J. Infect. Dis.* 176:1198-1208.

160. Renjifo, B., M. Chung, P. Gilbert, D. Mwakagile, G. Msamanga, W. Fawzi, and M. Essex. 2003. In-utero transmission of quasispecies among human immunodeficiency virus type 1 genotypes. *Virology.* 307:278-282.

161. Renjifo, B., P. Gilbert, B. Chaplin, G. Msamanga, D. Mwakagile, W. Fawzi, M. Essex, and Tanzanian Vitamin and HIV Study Group. 2004. Preferential in-utero transmission of HIV-1 subtype C as compared to HIV-1 subtype A or D. *AIDS.* 18:1629-1636.

162. Rerks-Ngarm, S., P. Pitisuttithum, S. Nitayaphan, J. Kaewkungwal, J. Chiu, R. Paris, N. Prensri, C. Namwat, M. de Souza, E. Adams, M. Benenson, S. Gurunathan, J. Tartaglia, J. G. McNeil, D. P. Francis, D. Stablein, D. L. Bix, S. Chunsuttiwat, C. Khamboonruang, P. Thongcharoen, M. L. Robb, N. L. Michael, P. Kunasol, J. H. Kim, and MOPH-TAVEG Investigators. 2009. Vaccination with ALVAC and AIDSVAX to prevent HIV-1 infection in Thailand. *N. Engl. J. Med.* 361:2209-2220.

163. Rosenberg, E. S., and B. D. Walker. 1998. HIV type 1-specific helper T cells: a critical host defense. *AIDS Res. Hum. Retroviruses.* 14 Suppl 2:S143-7.

164. Rusert, P., H. Kuster, B. Joos, B. Misselwitz, C. Gujer, C. Leemann, M. Fischer, G. Stiegler, H. Katinger, W. C. Olson, R. Weber, L. Aceto, H. F. Gunthard, and A. Trkola. 2005. Virus isolates during acute and chronic human immunodeficiency virus type 1 infection show distinct patterns of sensitivity to entry inhibitors. *J. Virol.* 79:8454-8469.
165. Russell, N. D., B. S. Graham, M. C. Keefer, M. J. McElrath, S. G. Self, K. J. Weinhold, D. C. Montefiori, G. Ferrari, H. Horton, G. D. Tomaras, S. Gurunathan, L. Baglyos, S. E. Frey, M. J. Mulligan, C. D. Harro, S. P. Buchbinder, L. R. Baden, W. A. Blattner, B. A. Koblin, L. Corey, and National Institute of Allergy and Infectious Diseases HIV Vaccine Trials Network. 2007. Phase 2 study of an HIV-1 canarypox vaccine (vCP1452) alone and in combination with rgp120: negative results fail to trigger a phase 3 correlates trial. *J. Acquir. Immune Defic. Syndr.* 44:203-212.
166. Sagar, M., X. Wu, S. Lee, and J. Overbaugh. 2006. Human immunodeficiency virus type 1 V1-V2 envelope loop sequences expand and add glycosylation sites over the course of infection, and these modifications affect antibody neutralization sensitivity. *J. Virol.* 80:9586-9598.
167. Saitou, N., and M. Nei. 1987. The neighbor-joining method: a new method for reconstructing phylogenetic trees. *Mol. Biol. Evol.* 4:406-425.
168. Salazar-Gonzalez, J. F., E. Bailes, K. T. Pham, M. G. Salazar, M. B. Guffey, B. F. Keele, C. A. Derdeyn, P. Farmer, E. Hunter, S. Allen, O. Manigart, J. Mulenga, J. A. Anderson, R. Swanstrom, B. F. Haynes, G. S. Athreya, B. T. Korber, P. M. Sharp, G. M. Shaw, and B. H. Hahn. 2008. Deciphering human immunodeficiency virus type 1 transmission and early envelope diversification by single-genome amplification and sequencing. *J. Virol.* 82:3952-3970.
169. Salazar-Gonzalez, J. F., M. G. Salazar, B. F. Keele, G. H. Learn, E. E. Giorgi, H. Li, J. M. Decker, S. Wang, J. Baalwa, M. H. Kraus, N. F. Parrish, K. S. Shaw, M. B. Guffey, K. J. Bar, K. L. Davis, C. Ochsenbauer-Jambor, J. C. Kappes, M. S. Saag, M. S. Cohen, J. Mulenga, C. A. Derdeyn, S. Allen, E. Hunter, M. Markowitz, P. Hraber, A. S. Perelson, T. Bhattacharya, B. F. Haynes, B. T. Korber, B. H. Hahn, and G. M. Shaw. 2009. Genetic identity, biological phenotype, and evolutionary pathways of transmitted/founder viruses in acute and early HIV-1 infection. *J. Exp. Med.*
170. Sanders, R. W., M. Venturi, L. Schiffner, R. Kalyanaraman, H. Katinger, K. O. Lloyd, P. D. Kwong, and J. P. Moore. 2002. The mannose-dependent epitope for neutralizing antibody 2G12 on human immunodeficiency virus type 1 glycoprotein gp120. *J. Virol.* 76:7293-7305.

171. SAS Institute Inc. 1997. The MIXED Procedure. SAS Institute, Inc.
172. Sattentau, Q. J., and J. P. Moore. 1991. Conformational changes induced in the human immunodeficiency virus envelope glycoprotein by soluble CD4 binding. *J. Exp. Med.* 174:407-415.
173. Schmitz, J. E., M. J. Kuroda, S. Santra, V. G. Sasseville, M. A. Simon, M. A. Lifton, P. Racz, K. Tenner-Racz, M. Dalesandro, B. J. Scallon, J. Ghayeb, M. A. Forman, D. C. Montefiori, E. P. Rieber, N. L. Letvin, and K. A. Reimann. 1999. Control of viremia in simian immunodeficiency virus infection by CD8+ lymphocytes. *Science.* 283:857-860.
174. Schuitemaker, H., M. Koot, N. A. Kootstra, M. W. Dercksen, R. E. de Goede, R. P. van Steenwijk, J. M. Lange, J. K. Schattenkerk, F. Miedema, and M. Tersmette. 1992. Biological phenotype of human immunodeficiency virus type 1 clones at different stages of infection: progression of disease is associated with a shift from monocytoprotropic to T-cell-tropic virus population. *J. Virol.* 66:1354-1360.
175. Shankarappa, R., J. B. Margolick, S. J. Gange, A. G. Rodrigo, D. Upchurch, H. Farzadegan, P. Gupta, C. R. Rinaldo, G. H. Learn, X. He, X. L. Huang, and J. I. Mullins. 1999. Consistent viral evolutionary changes associated with the progression of human immunodeficiency virus type 1 infection. *J. Virol.* 73:10489-10502.
176. Shiu, C., C. K. Cunningham, T. Greenough, P. Muresan, V. Sanchez-Merino, V. Carey, J. B. Jackson, C. Ziemniak, L. Fox, M. Belzer, S. C. Ray, K. Luzuriaga, D. Persaud, and Pediatric AIDS Clinical Trials Group P1059 Team. 2009. Identification of ongoing human immunodeficiency virus type 1 (HIV-1) replication in residual viremia during recombinant HIV-1 poxvirus immunizations in patients with clinically undetectable viral loads on durable suppressive highly active antiretroviral therapy. *J. Virol.* 83:9731-9742.
177. Siegel, S. 1956. *Nonparametric Statistics for the Behavioral Sciences.* McGraw-Hill Book Company, New York.
178. Simen, B. B., J. F. Simons, K. H. Hullsiek, R. M. Novak, R. D. Macarthur, J. D. Baxter, C. Huang, C. Lubeski, G. S. Turenchalk, M. S. Braverman, B. Desany, J. M. Rothberg, M. Egholm, M. J. Kozal, and Terry Bein Community Programs for Clinical Research on AIDS. 2009. Low-abundance drug-resistant viral variants in chronically HIV-infected, antiretroviral treatment-naive patients significantly impact treatment outcomes. *J. Infect. Dis.* 199:693-701.

179. Skehel, J. J., P. M. Bayley, E. B. Brown, S. R. Martin, M. D. Waterfield, J. M. White, I. A. Wilson, and D. C. Wiley. 1982. Changes in the conformation of influenza virus hemagglutinin at the pH optimum of virus-mediated membrane fusion. *Proc. Natl. Acad. Sci. U. S. A.* 79:968-972.
180. Stein, B. S., S. D. Gowda, J. D. Lifson, R. C. Penhallow, K. G. Bensch, and E. G. Engleman. 1987. pH-independent HIV entry into CD4-positive T cells via virus envelope fusion to the plasma membrane. *Cell.* 49:659-668.
181. Streeck, H., M. Lichterfeld, G. Alter, A. Meier, N. Teigen, B. Yassine-Diab, H. K. Sidhu, S. Little, A. Kelleher, J. P. Routy, E. S. Rosenberg, R. P. Sekaly, B. D. Walker, and M. Altfeld. 2007. Recognition of a defined region within p24 gag by CD8+ T cells during primary human immunodeficiency virus type 1 infection in individuals expressing protective HLA class I alleles. *J. Virol.* 81:7725-7731.
182. Subbarao, S., and G. Schochetman. 1996. Genetic variability of HIV-1. *AIDS.* 10 Suppl A:S13-23.
183. Sun, X., V. K. Yau, B. J. Briggs, and G. R. Whittaker. 2005. Role of clathrin-mediated endocytosis during vesicular stomatitis virus entry into host cells. *Virology.* 338:53-60.
184. Trkola, A., T. Dragic, J. Arthos, J. M. Binley, W. C. Olson, G. P. Allaway, C. Cheng-Mayer, J. Robinson, P. J. Maddon, and J. P. Moore. 1996. CD4-dependent, antibody-sensitive interactions between HIV-1 and its co-receptor CCR-5. *Nature.* 384:184-187.
185. Tyler, D. S., S. D. Stanley, S. Zolla-Pazner, M. K. Gorny, P. P. Shadduck, A. J. Langlois, T. J. Matthews, D. P. Bolognesi, T. J. Palker, and K. J. Weinhold. 1990. Identification of sites within gp41 that serve as targets for antibody-dependent cellular cytotoxicity by using human monoclonal antibodies. *J. Immunol.* 145:3276-3282.
186. Vaine, M., S. Wang, E. T. Crooks, P. Jiang, D. C. Montefiori, J. Binley, and S. Lu. 2008. Improved induction of antibodies against key neutralizing epitopes by human immunodeficiency virus type 1 gp120 DNA prime-protein boost vaccination compared to gp120 protein-only vaccination. *J. Virol.* 82:7369-7378.
187. Verhofstede, C., E. Demecheleer, N. De Cabooter, P. Gaillard, F. Mwanjumba, P. Claeys, V. Chohan, K. Mandaliya, M. Temmerman, and J. Plum. 2003. Diversity of the human immunodeficiency virus type 1 (HIV-1) env sequence after vertical transmission in mother-child pairs infected with HIV-1 subtype A. *J. Virol.* 77:3050-3057.

188. Walker, B. D., and D. R. Burton. 2008. Toward an AIDS vaccine. *Science*. 320:760-764.
189. Walter, J., L. Kuhn, and G. M. Aldrovandi. 2008. Advances in basic science understanding of mother-to-child HIV-1 transmission. *Curr. Opin. HIV. AIDS*. 3:146-150.
190. Wang, S., J. Arthos, J. M. Lawrence, D. Van Ryk, I. Mboudjeka, S. Shen, T. H. Chou, D. C. Montefiori, and S. Lu. 2005. Enhanced immunogenicity of gp120 protein when combined with recombinant DNA priming to generate antibodies that neutralize the JR-FL primary isolate of human immunodeficiency virus type 1. *J. Virol.* 79:7933-7937.
191. Wang, S., D. J. Farfan-Arribas, S. Shen, T. H. Chou, A. Hirsch, F. He, and S. Lu. 2006. Relative contributions of codon usage, promoter efficiency and leader sequence to the antigen expression and immunogenicity of HIV-1 Env DNA vaccine. *Vaccine*. 24:4531-4540.
192. Wang, S., J. S. Kennedy, K. West, D. C. Montefiori, S. Coley, J. Lawrence, S. Shen, S. Green, A. L. Rothman, F. A. Ennis, J. Arthos, R. Pal, P. Markham, and S. Lu. 2008. Cross-subtype antibody and cellular immune responses induced by a polyvalent DNA prime-protein boost HIV-1 vaccine in healthy human volunteers. *Vaccine*. 26:3947-3957.
193. Wang, S., R. Pal, J. R. Mascola, T. H. Chou, I. Mboudjeka, S. Shen, Q. Liu, S. Whitney, T. Keen, B. C. Nair, V. S. Kalyanaraman, P. Markham, and S. Lu. 2006. Polyvalent HIV-1 Env vaccine formulations delivered by the DNA priming plus protein boosting approach are effective in generating neutralizing antibodies against primary human immunodeficiency virus type 1 isolates from subtypes A, B, C, D and E. *Virology*. 350:34-47.
194. Wei, B. L., P. W. Denton, E. O'Neill, T. Luo, J. L. Foster, and J. V. Garcia. 2005. Inhibition of lysosome and proteasome function enhances human immunodeficiency virus type 1 infection. *J. Virol.* 79:5705-5712.
195. Wei, X., J. M. Decker, H. Liu, Z. Zhang, R. B. Arani, J. M. Kilby, M. S. Saag, X. Wu, G. M. Shaw, and J. C. Kappes. 2002. Emergence of resistant human immunodeficiency virus type 1 in patients receiving fusion inhibitor (T-20) monotherapy. *Antimicrob. Agents Chemother.* 46:1896-1905.
196. Wei, X., J. M. Decker, S. Wang, H. Hui, J. C. Kappes, X. Wu, J. F. Salazar-Gonzalez, M. G. Salazar, J. M. Kilby, M. S. Saag, N. L. Komarova, M. A. Nowak, B. H. Hahn, P. D. Kwong, and G. M. Shaw. 2003. Antibody neutralization and escape by HIV-1. *Nature*. 422:307-312.

197. Weidle, P. J., and S. Nesheim. 2010. HIV Drug Resistance and Mother-to-Child Transmission of HIV. *Clin. Perinatol.* 37:825-842.
198. Weiss, C. D., J. A. Levy, and J. M. White. 1990. Oligomeric organization of gp120 on infectious human immunodeficiency virus type 1 particles. *J. Virol.* 64:5674-5677.
199. Weissenhorn, W., A. Dessen, S. C. Harrison, J. J. Skehel, and D. C. Wiley. 1997. Atomic structure of the ectodomain from HIV-1 gp41. *Nature.* 387:426-430.
200. Weissenhorn, W., S. A. Wharton, L. J. Calder, P. L. Earl, B. Moss, E. Aliprandis, J. J. Skehel, and D. C. Wiley. 1996. The ectodomain of HIV-1 env subunit gp41 forms a soluble, alpha-helical, rod-like oligomer in the absence of gp120 and the N-terminal fusion peptide. *EMBO J.* 15:1507-1514.
201. Wolinsky, S. M., B. T. Korber, A. U. Neumann, M. Daniels, K. J. Kunstman, A. J. Whetsell, M. R. Furtado, Y. Cao, D. D. Ho, and J. T. Safrit. 1996. Adaptive evolution of human immunodeficiency virus-type 1 during the natural course of infection. *Science.* 272:537-542.
202. Wolinsky, S. M., C. M. Wike, B. T. Korber, C. Hutto, W. P. Parks, L. L. Rosenblum, K. J. Kunstman, M. R. Furtado, and J. L. Munoz. 1992. Selective transmission of human immunodeficiency virus type-1 variants from mothers to infants. *Science.* 255:1134-1137.
203. Worobey, M., M. Gemmel, D. E. Teuwen, T. Haselkorn, K. Kunstman, M. Bunce, J. J. Muyembe, J. M. Kabongo, R. M. Kalengayi, E. Van Marck, M. T. Gilbert, and S. M. Wolinsky. 2008. Direct evidence of extensive diversity of HIV-1 in Kinshasa by 1960. *Nature.* 455:661-664.
204. Wu, X., A. B. Parast, B. A. Richardson, R. Nduati, G. John-Stewart, D. Mbori-Ngacha, S. M. Rainwater, and J. Overbaugh. 2006. Neutralization escape variants of human immunodeficiency virus type 1 are transmitted from mother to infant. *J. Virol.* 80:835-844.
205. Yu, D., W. Wang, A. Yoder, M. Spear, and Y. Wu. 2009. The HIV envelope but not VSV glycoprotein is capable of mediating HIV latent infection of resting CD4 T cells. *PLoS Pathog.* 5:e1000633.
206. Zhang, H., F. Hoffmann, J. He, X. He, C. Kankasa, J. T. West, C. D. Mitchell, R. M. Ruprecht, G. Orti, and C. Wood. 2006. Characterization of HIV-1 subtype C envelope glycoproteins from perinatally infected children with different courses of disease. *Retrovirology.* 3:73.

207. Zhang, H., D. C. Tully, F. G. Hoffmann, J. He, C. Kankasa, and C. Wood. 2010. Restricted genetic diversity of HIV-1 subtype C envelope glycoprotein from perinatally infected Zambian infants. *PLoS One*. 5:e9294.
208. Zhang, Z., T. Schuler, M. Zupancic, S. Wietgreffe, K. A. Staskus, K. A. Reimann, T. A. Reinhart, M. Rogan, W. Cavert, C. J. Miller, R. S. Veazey, D. Notermans, S. Little, S. A. Danner, D. D. Richman, D. Havlir, J. Wong, H. L. Jordan, T. W. Schacker, P. Racz, K. Tenner-Racz, N. L. Letvin, S. Wolinsky, and A. T. Haase. 1999. Sexual transmission and propagation of SIV and HIV in resting and activated CD4+ T cells. *Science*. 286:1353-1357.
209. Zhou, T., L. Xu, B. Dey, A. J. Hessel, D. Van Ryk, S. H. Xiang, X. Yang, M. Y. Zhang, M. B. Zwick, J. Arthos, D. R. Burton, D. S. Dimitrov, J. Sodroski, R. Wyatt, G. J. Nabel, and P. D. Kwong. 2007. Structural definition of a conserved neutralization epitope on HIV-1 gp120. *Nature*. 445:732-737.
210. Zhuang, J., A. E. Jetzt, G. Sun, H. Yu, G. Klarmann, Y. Ron, B. D. Preston, and J. P. Dougherty. 2002. Human immunodeficiency virus type 1 recombination: rate, fidelity, and putative hot spots. *J. Virol*. 76:11273-11282.
211. Zwick, M. B., R. Kelleher, R. Jensen, A. F. Labrijn, M. Wang, G. V. Quinnan Jr, P. W. Parren, and D. R. Burton. 2003. A novel human antibody against human immunodeficiency virus type 1 gp120 is V1, V2, and V3 loop dependent and helps delimit the epitope of the broadly neutralizing antibody immunoglobulin G1 b12. *J. Virol*. 77:6965-6978.